AD NUMBER
AD875902
LIMITATION CHANGES

TO:

Approved for public release; distribution is unlimited.

FROM:

Distribution authorized to U.S. Gov't. agencies and their contractors; Administrative/Operational Use; SEP 1970. Other requests shall be referred to Army Aviation Materiel Labs., Fort Eustis, VA.

AUTHORITY

USAAVLABS ltr 30 Mar 1976

THIS REPORT HAS BEEN DELIMITED
AND CLEARED FOR PUBLIC RELEASE
UNDER DOD DIRECTIVE 5200.20 AND
NO RESTRICTIONS ARE IMPOSED UPON
ITS USE AND DISCLOSURE.

DISTRIBUTION STATEMENT A

APPROVED FOR PUBLIC RELEASE;
DISTRIBUTION UNLIMITED.

AD8759O2

USAAVLABS TECHNICAL REPORT 70-40

RADIAL OUTFLOW COMPRESSOR COMPONENT DEVELOPMENT PHASE IV TEST RESULTS

By

D. E. Morrison

September 1970

U. S. ARMY AVIATION MATERIEL LABORATORIES
FORT EUSTIS, VIRGINIA

DISCLAIMERS

The objective of this contractual effort was to acquire and present
high-speed performance data in order to define the capability of
the current radial outflow compressor.

This report was prepared by General Electric Company under the terms
of Contract DAAJ02-69-C-0070. It describes the modifications to the
existing radial outflow compressor, the tests performed, and the
results of those tests.

The modifications to the compressor resulted in the capability to
operate the compressor continuously at all design speeds. The
compressor performed essentially the same as during the basic program
previously reported.

This report has been reviewed by technical personnel of this Command,
and the conclusions contained herein are concurred in by this Command.
The U.S. Army Project Engineer for this effort was Mr. Robert A.
Langworthy.

Task 1G162203D14413
Contract DAAJ02-69-C-0070
USAAVLABS Technical Report 70-40
September 1970

RADIAL OUTFLOW COMPRESSOR COMPONENT DEVELOPMENT

PHASE IV TEST RESULTS

By
D. E. Morrison

Prepared by

General Electric Company
Cincinnati, Ohio

for

U.S. ARMY AVIATION MATERIEL LABORATORIES
FORT EUSITIS, VIRGINIA

SUMMARY

The Radial Outflow Compressor (ROC) Phase IV configuration tested was identical to the Phase III configuration except for a change made in the rotating diffuser flowpath area distribution. Sustained test operations at 90- and 100-percent corrected speeds were accomplished for the first time on the ROC program.

The circular inlet vane position had little effect on rotor performance in the testing limited to the range of corrected speeds from 50 through 80 percent.

Rotor operation, with the recontoured disc reproducing No. 2 (Phase II) diffuser area distribution, was characterized by slightly higher rotor total pressure ratios and efficiencies relative to those produced by the Phase III configuration. Rotor outlet Mach numbers were lower than those obtained with the Phase III configuration but substantially higher than the estimated values. Maximum rotor performance was obtained with the 83.4-degree supersonic stator setting. The maximum measured rotor total pressure ratio was 7.2 with a rotor efficiency of 80 percent (the peak efficiency) at 100-percent corrected speed.

The stator system with the supersonic stator settings of 82 or 79 degrees demonstrated the capability of operating with overall loss levels approaching those obtained in the cascade tests.

The maximum measured stage total pressure ratio was 6.1 at the maximum stage efficiency of 66 percent. These values were obtained at 100-percent corrected speed with the 82-degree supersonic stator setting and the 76-degree subsonic stator settings.

FOREWORD

The Phase IV Radial Outflow Compressor program was carried out under United States Army Contract DAAJ02-69-C-0070 by the Advanced Technology Programs Department, Aircraft Engine Technical Division, Aircraft Engine Group, General Electric Company, Cincinnati, Ohio. The United States Army Project Engineer was Mr. R. A. Langworthy. The General Electric Project Engineer was Mr. J. W. Blanton. The program was initiated in May 1969 and was completed in March 1970.

TABLE OF CONTENTS

LIST OF ILLUSTRATIONS

INTRODUCTION

The objectives of the Phase IV Radial Outflow Compressor (ROC) program were to set the circular inlet vane at the optimum position for the rotor performance and to generate a compressor map of 6 speed lines with the supersonic stators and the subsonic stators set at the most suitable position. The basic output of the Phase IV ROC program was to be reduced test data to determine rotor performance, stage performance, and the operating match between the rotor and the stator. The analyses and evaluation of the test data were to be held to specified minimal limits. Based on the test results, recommendations were to be made relative to future investigations of the Radial Outflow Compressor.

PERFORMANCE ESTIMATES

As an aid in evaluating the Radial Outflow Compressor (ROC) Phase IV
test results, estimated performance data were compiled which represent
reasonable performance expectations for a developed compressor with
zero inlet whirl. These data, given in Table I, were based on rotor
performance estimates as contained in the report on the Phase II work[1]
and extended to account for the performance of the tandem (supersonic-
subsonic) stator vanes and the outlet scroll ducting. The extension
of the rotor performance provided estimates of stage (overall) total
pressure ratio and stage (overall) adiabatic efficiency for the ROC.
Use was made of earlier tandem cascade test data in terms of total
pressure loss coefficient as a function of inlet Mach number and as
contained in the report on the Phase I work[2]. These pressure loss
data were adjusted upward, allowing to some extent for the effects of
unsteady and nonuniform flow out of the rotor at the supersonic stator
inlet, in estimating a reasonable pressure loss coefficient character-
istic as a function of supersonic stator inlet Mach number. The
envelope of the tandem cascade test data, together with the estimated
pressure loss characteristic for the tandem stator system, is shown
in Figure 1. The total pressure loss characteristic, as shown in
Figure 2, from the discharge of the subsonic stator to the measuring
plane in the scroll outlet collector arms, was derived from test data
acquired in the Phase IV testing.

2

TABLE I. SUMMARY, ROC ESTIMATED PERFORMANCE, ZERO PRESWIRL

% η/√θ	W√θ/δ (Lbs/Sec)	Rotor				Total Temperature Ratio	Overall Stage	
		Total Pressure Ratio	Static Pressure Ratio	Mach Number	Efficiency (%)		Total Pressure Ratio	Efficiency (%)
100	3.20	5.33	3.23	0.878	81.82	1.753	4.81	75.3
	3.60	5.93	3.57	0.883	87.37	1.758	5.30	80.7
	3.96	6.40	3.80	0.896	90.83	1.769	5.74	84.3
	4.08	6.53	3.85	0.903	91.38	1.775	5.84	84.7
	4.08	8.43	3.73	1.145	83.12	2.008	7.22	75.4
90	2.93	4.31	2.75	0.827	83.99	1.616	3.91	77.3
	3.31	4.73	2.97	0.841	88.97	1.627	4.26	82.0
	3.68	5.08	3.12	0.863	91.67	1.643	4.53	84.1
	3.73	5.12	3.14	0.867	91.89	1.647	4.57	84.1
	3.73	6.41	2.97	1.110	82.68	1.846	5.53	74.6
80	2.65	3.46	2.34	0.770	86.28	1.493	3.15	78.8
	3.01	3.74	2.47	0.792	90.18	1.506	3.36	81.9
	3.36	3.98	2.56	0.819	92.29	1.524	3.54	83.2
	3.45	4.04	2.58	0.828	92.51	1.529	3.58	83.2
	3.45	4.89	2.37	1.071	82.02	1.699	4.18	72.3
70	2.35	2.74	1.97	0.707	87.27	1.382	2.51	78.7
	2.68	2.94	2.06	0.732	90.91	1.396	2.64	80.9
	3.01	3.11	2.11	0.763	92.66	1.412	2.75	81.4
	3.17	3.18	2.12	0.781	92.77	1.422	2.79	80.8
	3.17	3.71	1.89	1.033	80.13	1.567	3.13	68.1
60	2.04	2.18	1.66	0.636	87.59	1.285	2.00	77.0
	2.34	2.31	1.72	0.662	91.11	1.296	2.08	78.7
	2.64	2.42	1.76	0.693	92.70	1.309	2.13	78.3
	2.93	2.52	1.76	0.732	92.27	1.326	2.17	75.8
	2.93	2.81	1.50	0.991	76.61	1.448	2.32	60.7
50	1.72	1.76	1.43	0.552	87.69	1.20	1.64	75.7
	1.97	1.84	1.47	0.578	91.12	1.208	1.67	76.1
	2.24	1.91	1.49	0.608	92.62	1.218	1.70	74.6
	2.50	1.96	1.49	0.643	92.13	1.230	1.69	70.3
	2.73	2.00	1.47	0.683	89.98	1.243	1.66	64.0
	2.73	2.14	1.20	0.946	70.83	1.341	1.67	46.5
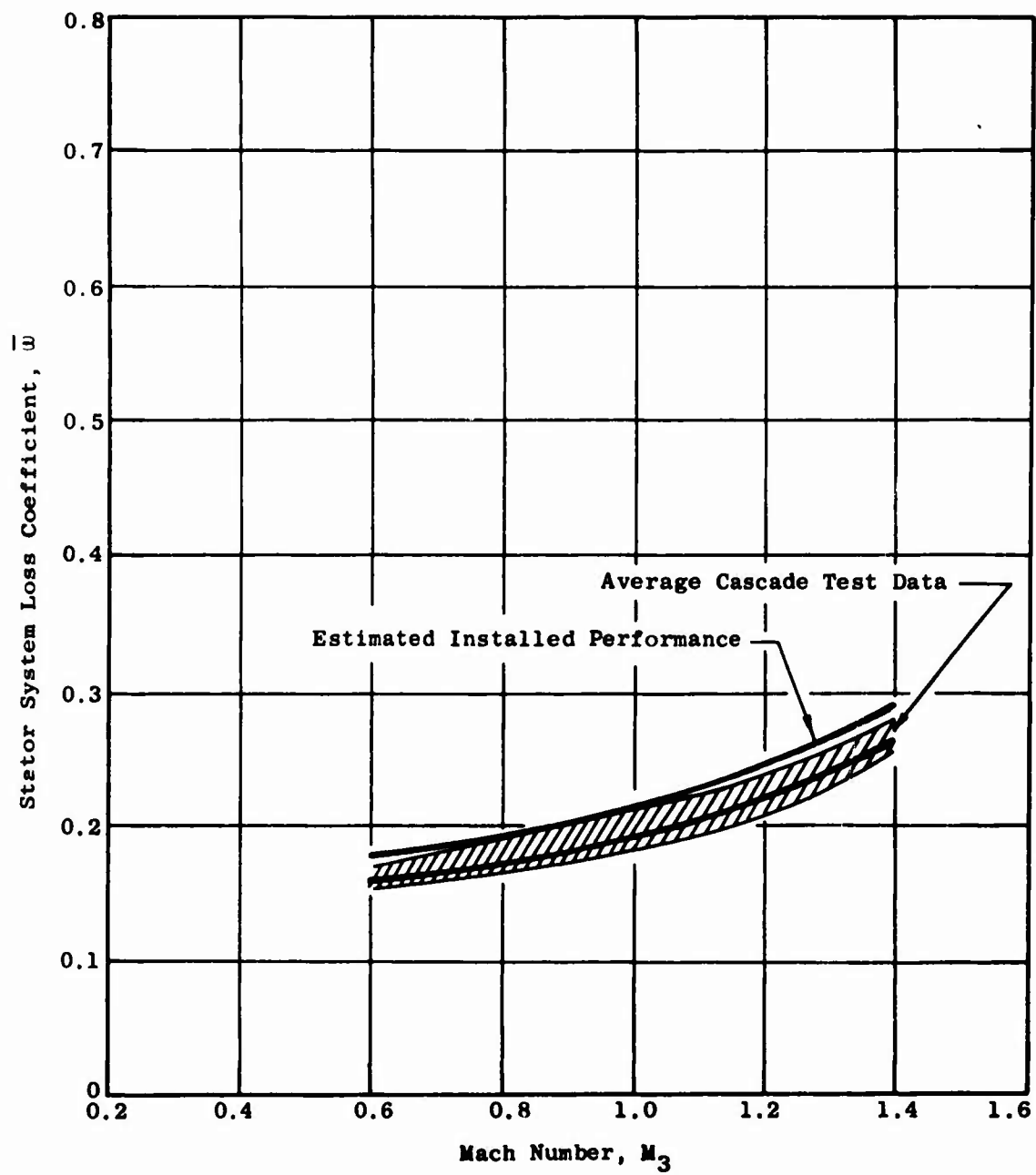
Figure 1. Radial Outflow Compressor Tandem Stator System Loss Coefficient
Vs Stator Inlet Mach Number.
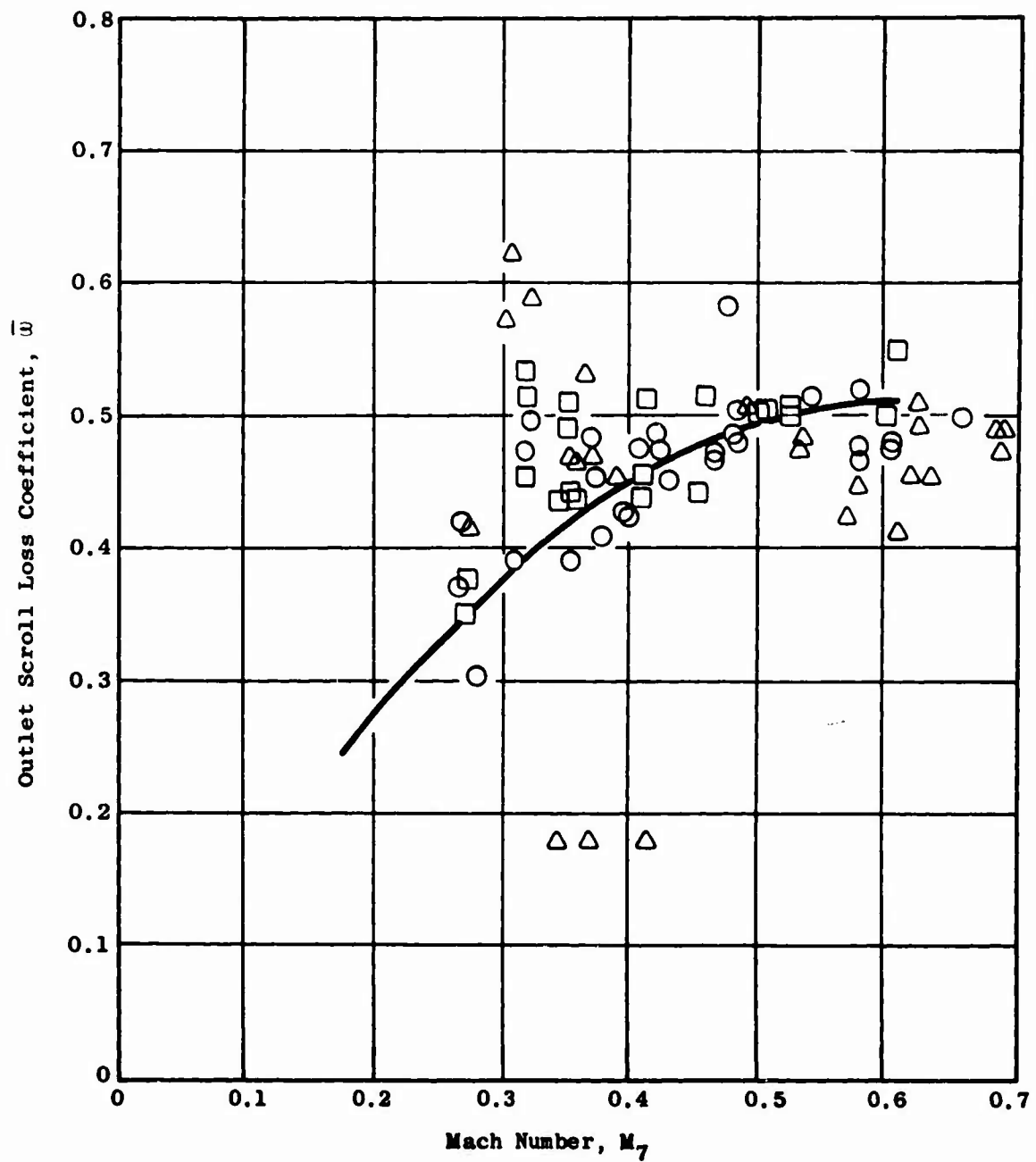
Figure 2. Radial Outflow Compressor Scroll Loss Coefficient Vs Average
Mach Number at Stator System Discharge.

TEST CONFIGURATION

REDESIGNED ROTOR

The Phase IV rotor was a redesign of the Phase III rotor to reproduce
the rotating diffuser area distribution used in the Phase II work. The
resulting Phase IV configuration was analyzed to evaluate safe operation
at full speed.

Phase IV Diffuser Contour

A modification of the rotor disc was designed to change the flow area
distribution of the vaneless diffuser for the Phase IV configuration
from the schedule used in Phase III back to the Phase II schedule used
in Buildup F[1]. The corresponding width schedules for Phase IV and
Phase III diffusers are compared in Figure 3. The physical change made
to the Phase III disc contour is represented in Figure 4. Growths re-
sulting from stress and thermal conditions were considered along with
the original Phase II hot flowpath shape and dimensions in the process
of determining the profile for the modified disc. The rotor disc, with
blades attached, after test, in the Phase III configuration, and before
machining to the Phase IV configuration, is shown in Figure 5.

A view of the Phase IV disc after completion of the contour machining
operations is shown in Figure 6. A circumferential step (increasing
the passage width) 0.020 inch deep was left on the disc on the flow-
path surface on which the blade roots butt. The step was blended back
approximately one-sixteenth of an inch into the upstream surface, re-
ducing the step to 0.005 inch. Complete elimination of the step would
have given unacceptable clearance between the blade trailing edges and
the rotor disc. The assembly drawing of the Phase III vehicle, Figure 7,
describes the Phase IV configuration with the exception of the rotor
disc contour change, which is illustrated in Figure 4.

Mechanical Analysis of the Phase IV Configuration

In addition to the differential growth of the rotor disc and shroud,
indicating a mismatch between the front and rear blade fixing radii,
the analysis also indicated that the shroud tip deflects axially (for-
ward), relative to the casing, under load. Although consideration was
given to several methods for controlling the deflection of the shroud
rim, including winding on it a high-modulus composite hoop to preload
and deflect the shroud, none of these appeared to be practical. The
differential growth between the shroud and the disc, loading the blades
in bending, appeared to be tolerable at speeds up to 82 percent. Above
this speed, it would be expected that the blade stems would bend, re-
sulting in some compromise in blade life. Combined with the experi-
ence gained in the high-speed operation on the Phase III work, the

6
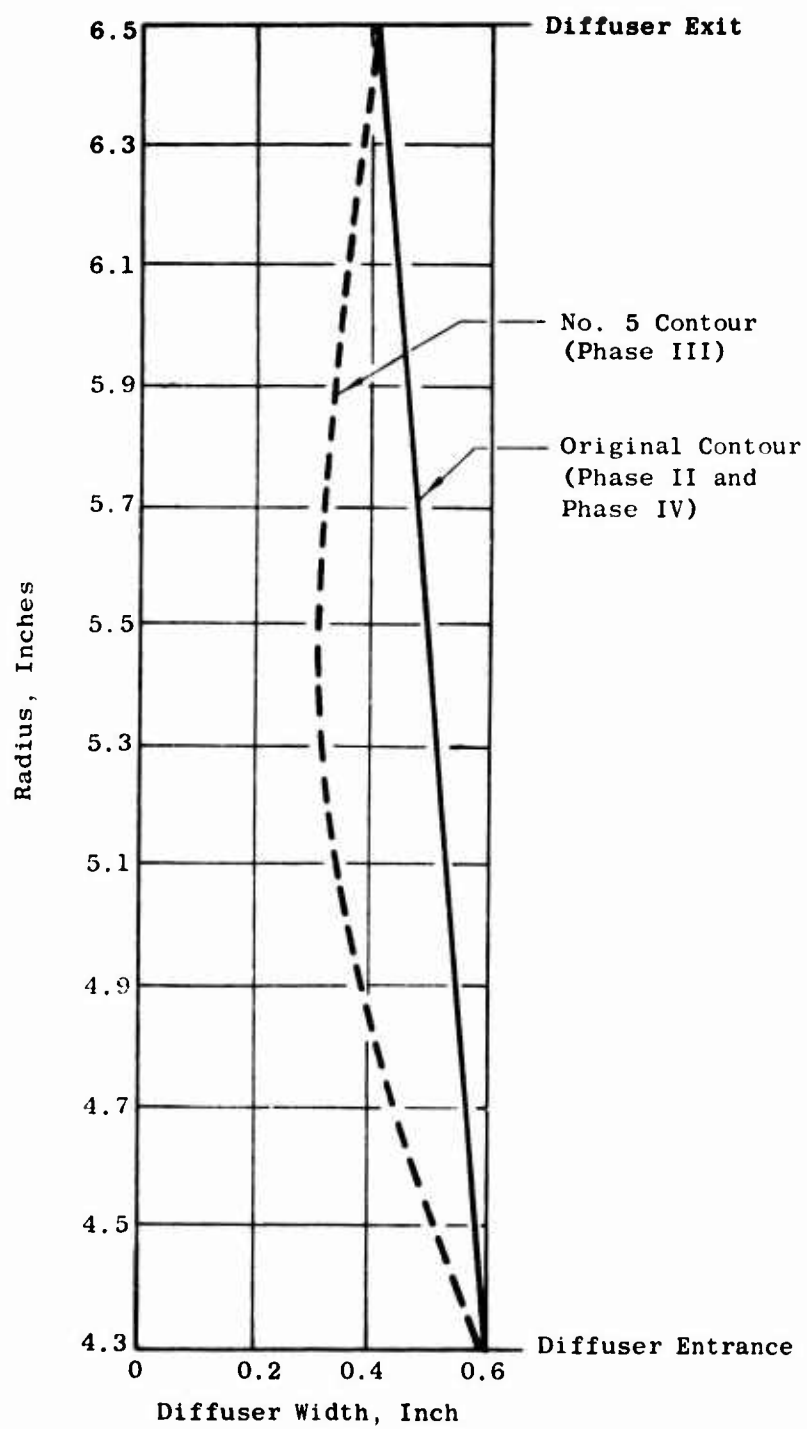
Figure 3. Comparison of Contours of Rotating Vaneless
Diffuser Passage for Phase III and Phase IV.
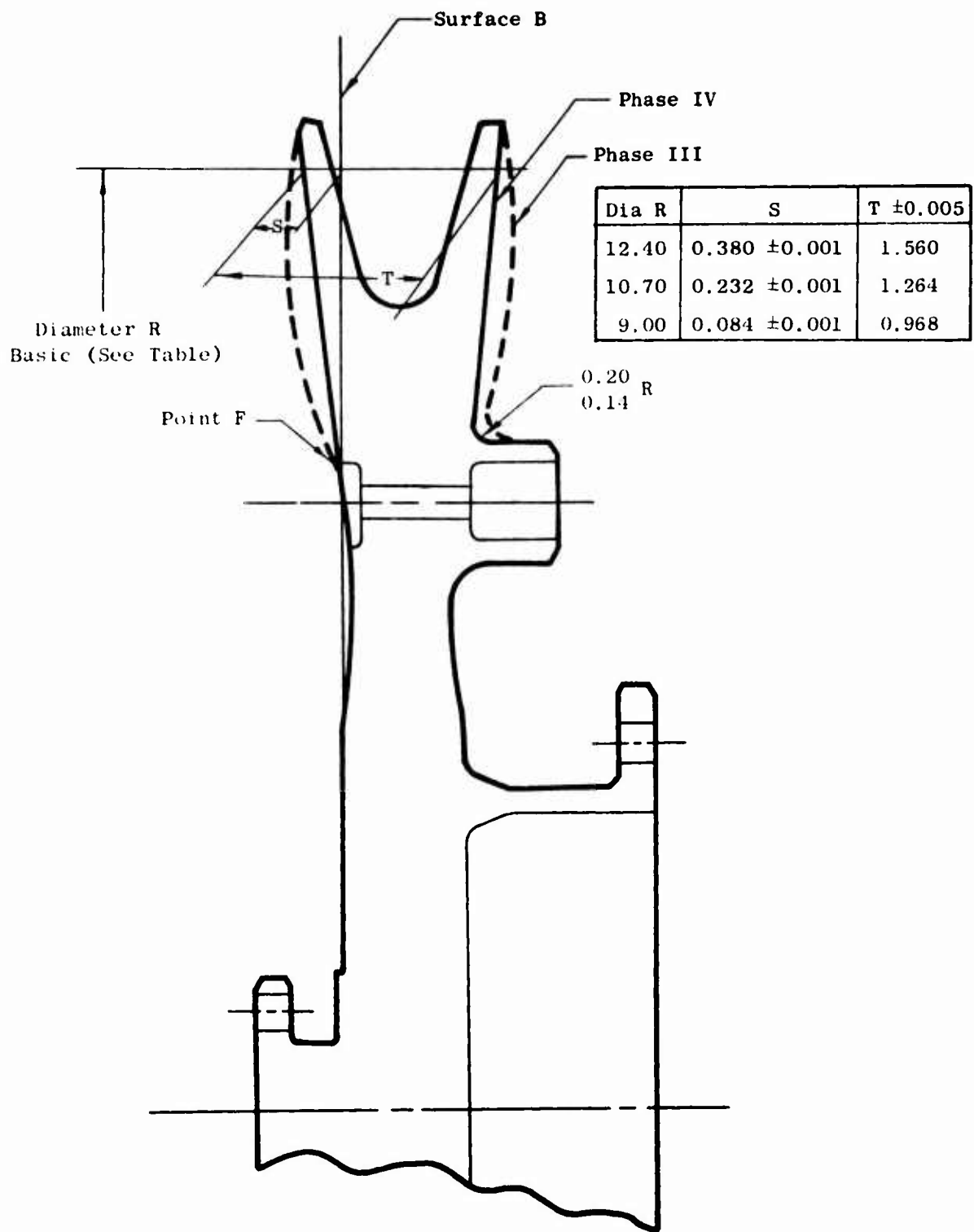
Figure 4. Phase IV ROC Disc Modification.

The table in the figure:

Dia R	S	T ±0.005
12.40	0.380 ±0.001	1.560
10.70	0.232 ±0.001	1.264
9.00	0.084 ±0.001	0.968
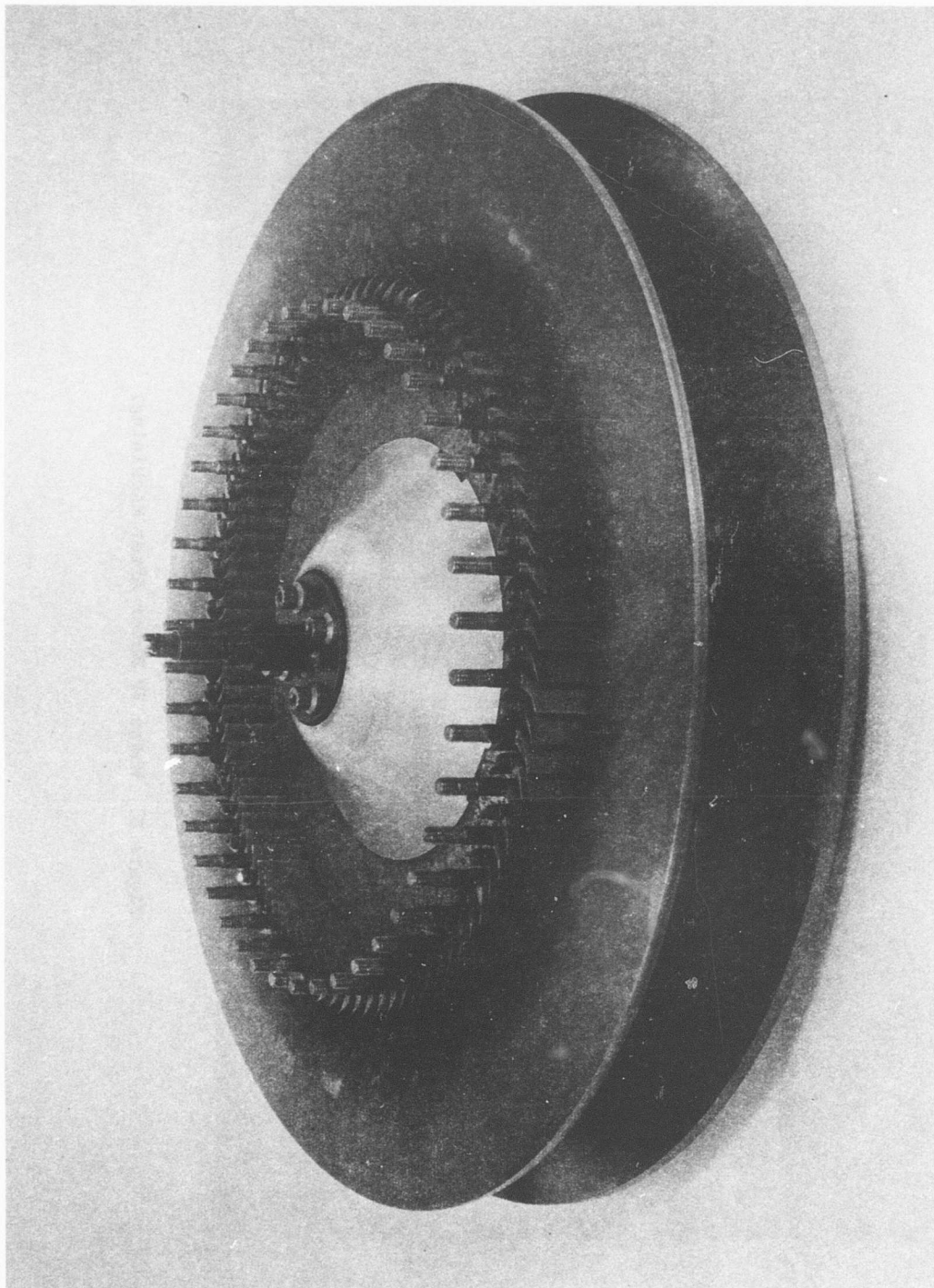
Figure 5. ROC Rotor Disc – No. 5 Contour with Blades in Place, Following Phase III Tests.

9
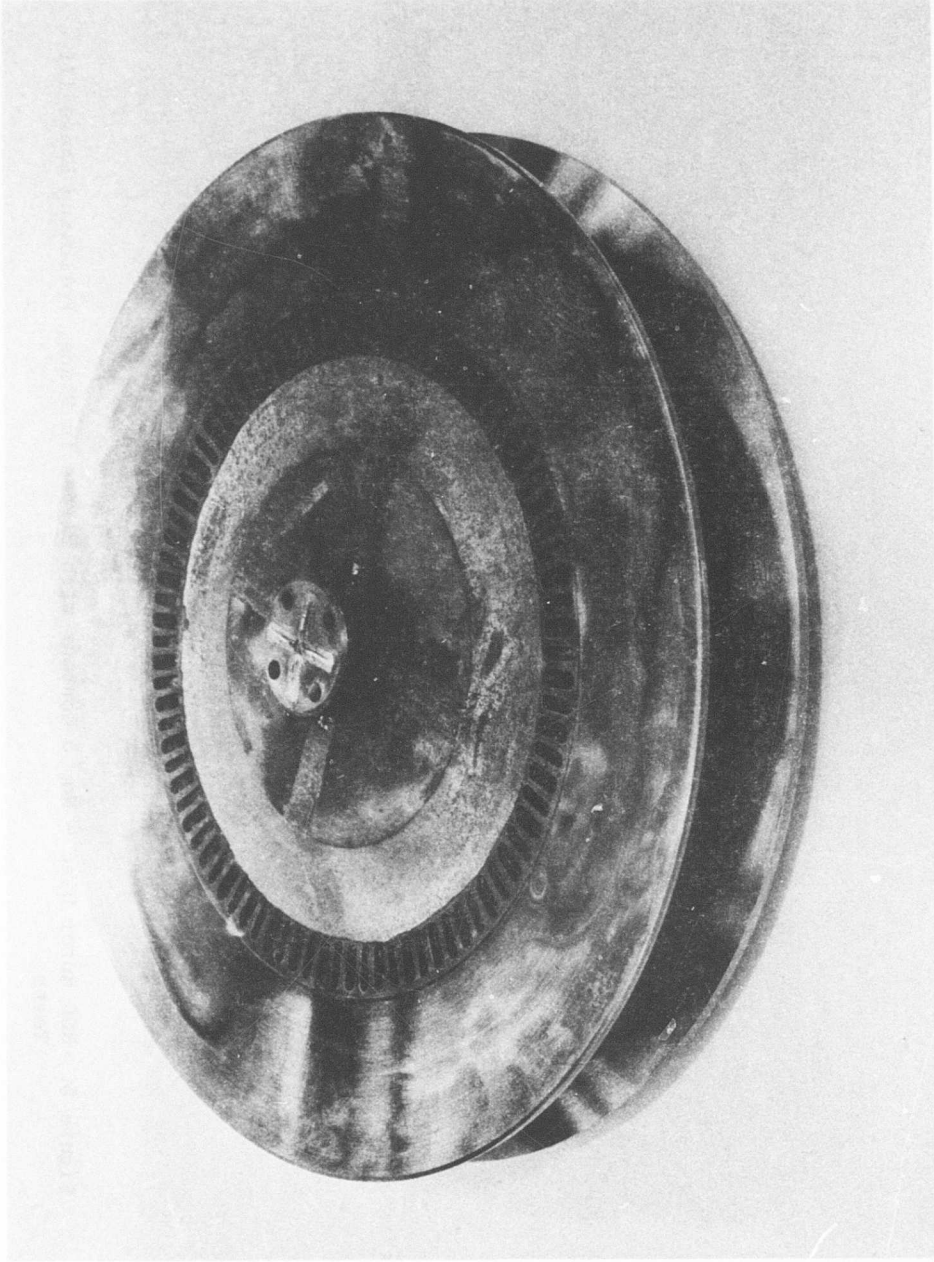
Figure 6. Phase IV Rotor After Machining.

10
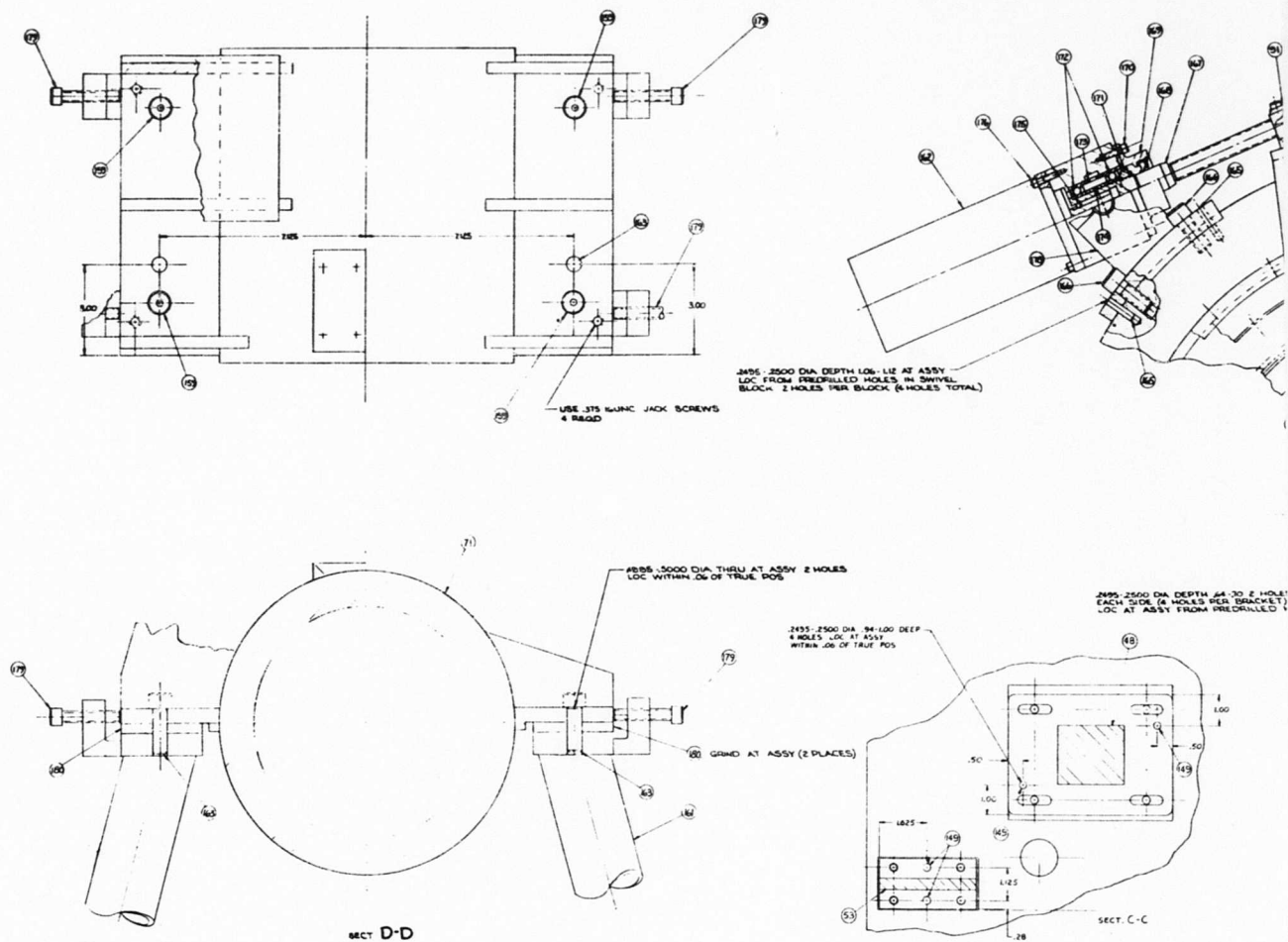
Figure 7. ROC Assembly for Phase III (Phase IV Is Same Assembly Except for Disc Contour).

12

SECT. H-H

SEE INSTALLATION DWG
40L22B7-88L

SECT. F-F

.4994-.4998 DIA THRU
BASE PLATE ASSY (40L22B7-807(60) &
PLATE ON SUPPORT STAND (40L22B7-U50-80)
2 HOLES LOC FROM PLUMB ON
(CENTER OF TORQUE ARM CLEVIS
(40L22B7-603 POS) TO CENTER OF
BASE PLATE CLEVIS (40L22B7-80LPOS)
WITHIN .010

.4995 .3000 DIA DEPTH AS SHOWN (FAR SIDE)
2 HOLES LOC AT ASSY FROM
PREDRILLED HOLES IN ITEM 151

TAP DRILL THRU
THD .500-13UNC-2B THRU
4 HOLES LOC FROM ITEM 15B

SECT. E-E

PARTIAL SECT. A-A

USE WITH LOCTITE

USE WITH LOCKTITE

GRIND AT ASSY

USE WITH LOCK TITE

A

Figure 7. (Concluded).

analysis of the Phase IV configuration led to the conclusion that operation to 100-percent speed should be possible if it is carefully executed. Although blade life might be compromised, it was unlikely that sudden failure would occur as a result of blade bending in the relatively short duration of the high-speed operation contemplated to be required to conduct the Phase IV tests, provided rotor vibration levels were minimized.

FORWARD BEARING TEMPERATURE CONTROL

A further modification was made to the ROC vehicle in an attempt to obtain reasonable life from the forward compressor thrust bearing. A means was provided for preventing leakage of air at compressor discharge temperature across the shaft seal from the PV6 cavity, Figure 8, into the bearing cavity. The interseal cavity was modified to incorporate an air pressure supply tube and a static pressure sensor. Undesirable hot air leakage into the bearing cavity was prevented by pressurizing the interseal cavity with shop air to 5 to 10 psi above the PV6 cavity pressure during test operations.

TEST FACILITY

The test facility was as used in Phase III testing except as noted below. In previous ROC testing, the compressor delivery air was discharged into the test tank, allowing closed-cycle operation. The discharge air, with temperatures as high as 700°F, was routed through the west and center tank coolers. To eliminate the heating of the gearbox and drive vehicle and to reduce the tank temperature, new piping and flexible hoses were installed, routing the compressor main air outside the test tank. A standard 5-inch orifice run was installed to measure compressor discharge airflow.

ASSEMBLING AND BALANCING THE ROTOR

In the initial attempt to assemble the Phase IV rotor, excessive clearance (0.005 inch) was observed between the end of the rotor blades and the rotating shroud after the blade retaining nuts had been torqued to the prescribed level. Removal of material from the shroud, by chamfering the holes, provided sufficient clearance over the radius on the blade stems to permit the blade to seat properly on the shroud. As a result of cleaning up the edges of the blade stem holes in the shroud, as well as a careful selection and matching of the rotor blades, rotor assembly with minimum runout was achieved, and a good balance of the rotor was facilitated. A comparison of the runouts of the rotor for Phase IV with those for Phase III Buildup C are given on Figure 9, illustrating the substantial reduction in runout obtained with the Phase IV rotor. The procedure followed for balancing the Phase IV rotor and shaft was the same as previously used in the Phase III program[3]. Using the balancing apparatus as shown in Figure 10, the Phase IV rotor had a 0.03-gram unbalance in Plane C and a 0.06-gram

15

Key to Auxiliary Air Systems:

① Through control valve to ejector

② Through control valve from 100-psi shop air supply

Ⓐ Interseal Cavity

PV2-out, for shroud cooling
PV6-out, for thrust balance and disc cooling
PV4-out, scavenge air seal leakage
PV2-in was set to equal PV2-out
PV6-in was set to equal PV6-out
All airflow measured except interseal cavity supply
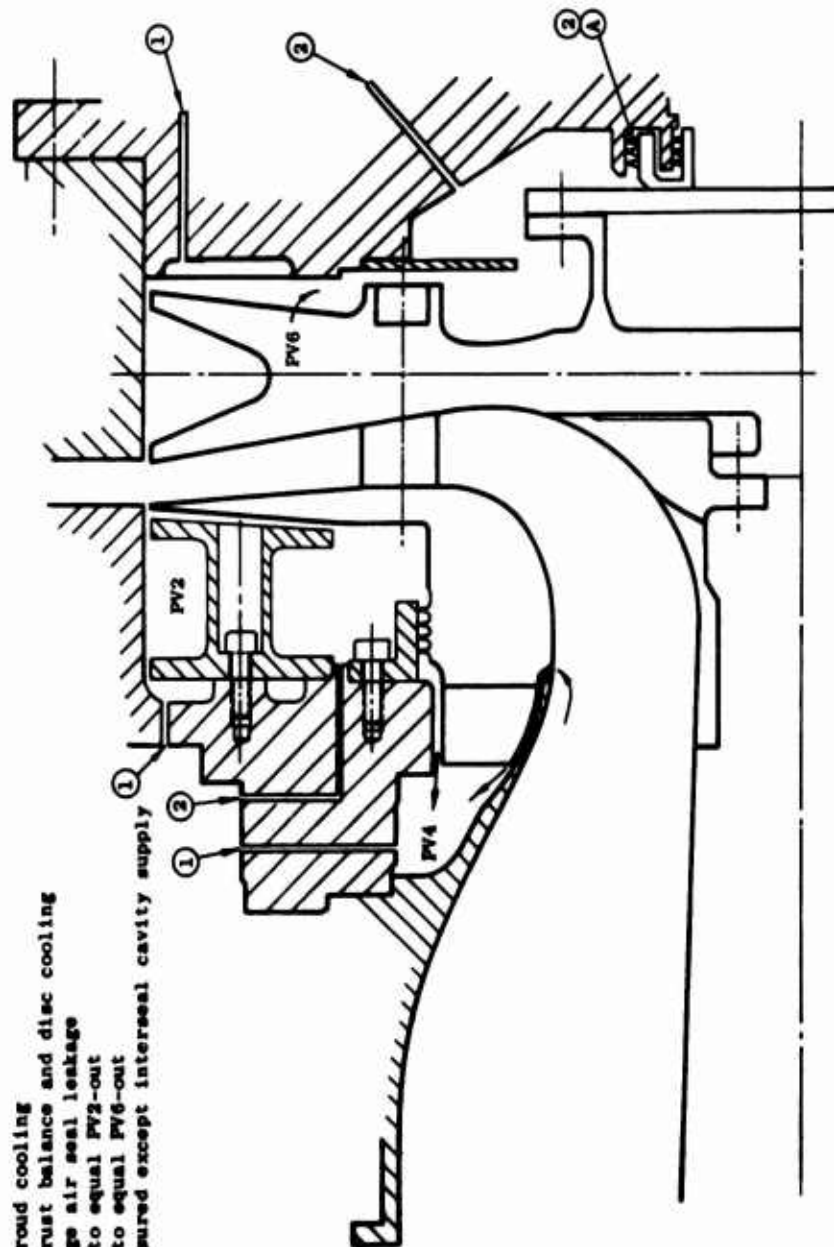
Figure 8. Schematic of ROC Auxiliary Air Systems.

16
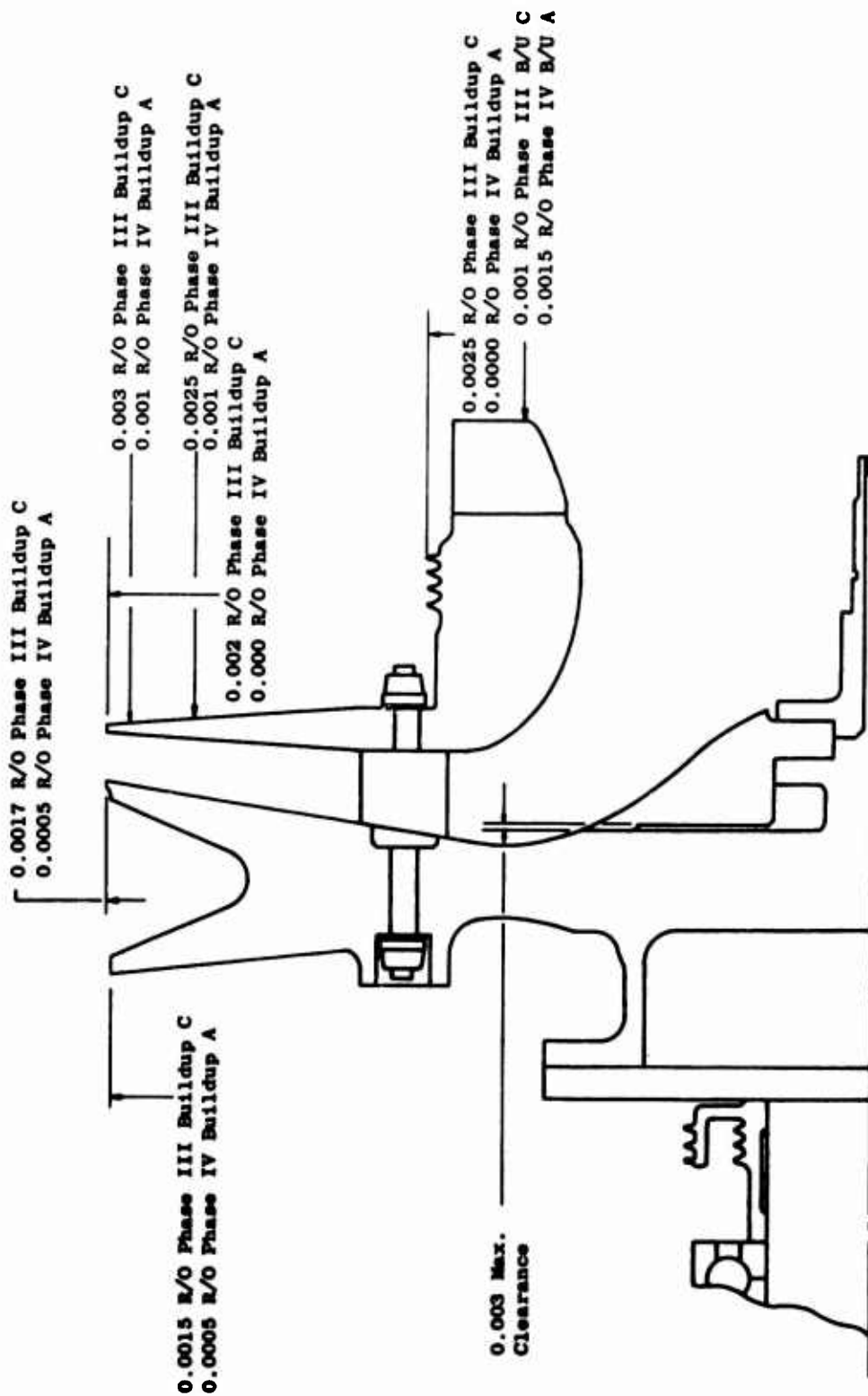
Figure 9. Comparison of Rotor Runout (R/O) for Phase III Buildup C with Phase IV Buildup A.

Shroud Balance
Plane D

Straight Belt
Drive

Disc Balance Plane C

Displacement Pickup

Disc-Shaft
Plane

B Right

A Left

Pedes-
tal

Pickup A Reads Balance Plane D (Right Plane)
Pickup B Reads Balance Plane C (Left Plane)
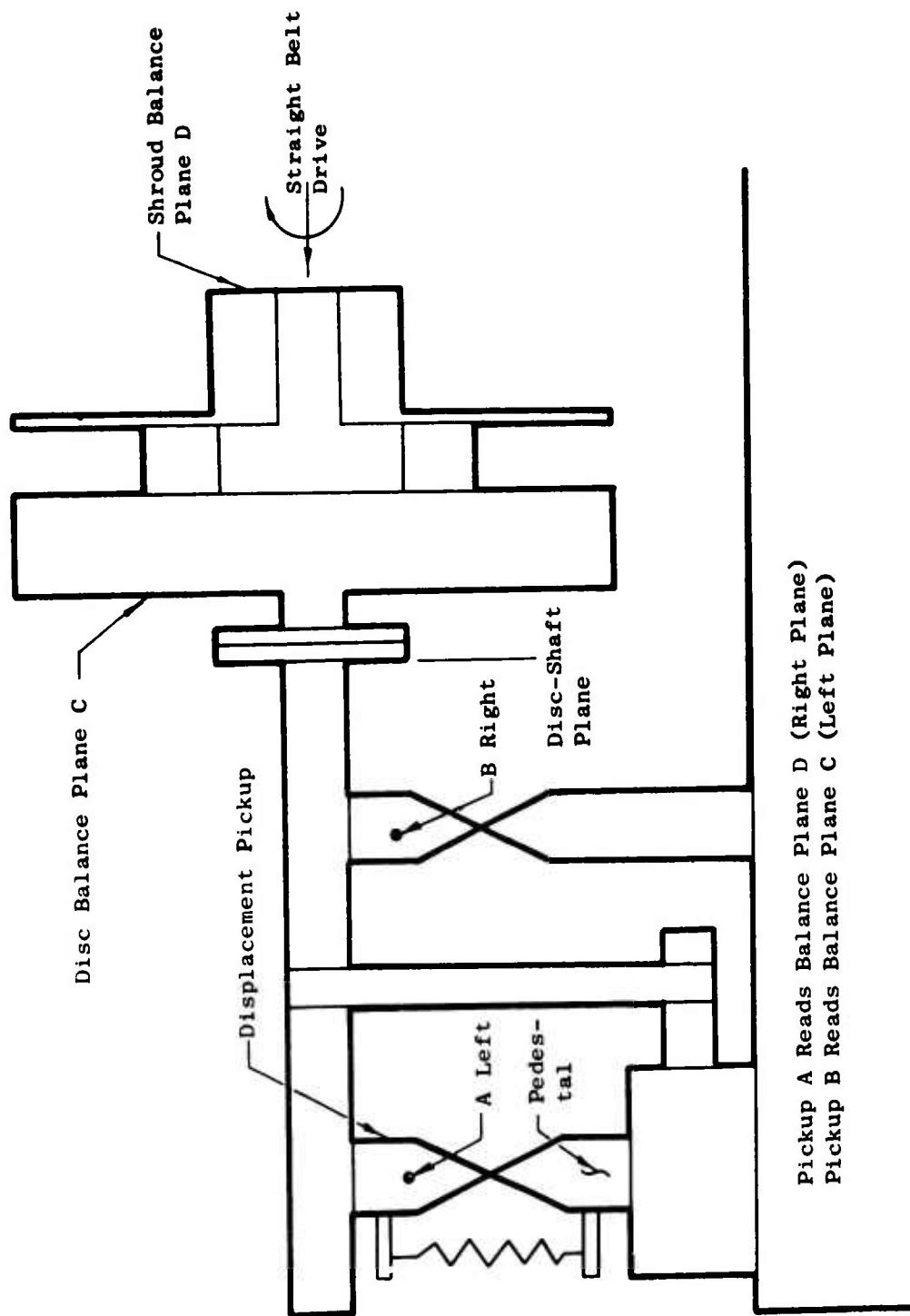
Figure 10. General Arrangement Used in Balancing Phase IV Rotor.

unbalance in Plane D. This is to be compared with the Phase-III Build-up-C unbalance of 0.1 and 0.2 gram for Planes C and D, respectively. The relatively lower unbalance levels for the Phase IV configuration were expected to result in vibration problems of reduced magnitude during the Phase IV testing.

STATOR SYSTEM

The array of supersonic and subsonic stator vanes installed in the forward stator casing is shown in Figure 11. A closeup of one of the rotor outlet (stator inlet) total head rakes is shown, mounted on a supersonic stator vane, in Figure 12. Each rake consisted of one pitot probe at the center of the passage with the two flanking pitot probes mounted close to the forward (rotor shroud side) and rear (rotor disc side) stator case walls.

INSTRUMENTATION

The instrumentation used in the ROC Phase IV testing was generally similar to that used in Phase III Buildup C testing. The compressor discharge traverse rake, containing 15 total pressure elements and 14 total temperature elements installed in the upper discharge duct for Phase III testing, was replaced with a single-element total pressure probe and two thermocouples providing identical instrumentation in the upper and lower discharge duct for the Phase IV testing. The number of Kistler (static) pressure sensors installed was reduced from seven to three - two located at stator outlet and one in the outlet scroll - for the Phase IV testing.

Compressor inlet total pressures were obtained from a single rake containing five total pressure sensing elements, and located in annular inlet ducting downstream of the inlet screen. Rotor outlet total pressures were sensed by a three-element rake located on each of two supersonic stator vanes (Figure 12). Rotor outlet static pressures were sensed by wall static pressure taps - twelve located on the front casing and six located on the rear casing, just upstream from the supersonic stator inlets. Rotor outlet total and static pressures were assumed to be identical to the stator system inlet total and static pressures.

Compressor inlet air temperature was obtained from the average of twelve thermocouple readings at the plane of the inlet screen in the compressor inlet duct. Compressor rotor discharge air temperature was assumed to be the same as compressor discharge temperature (Plane 8).
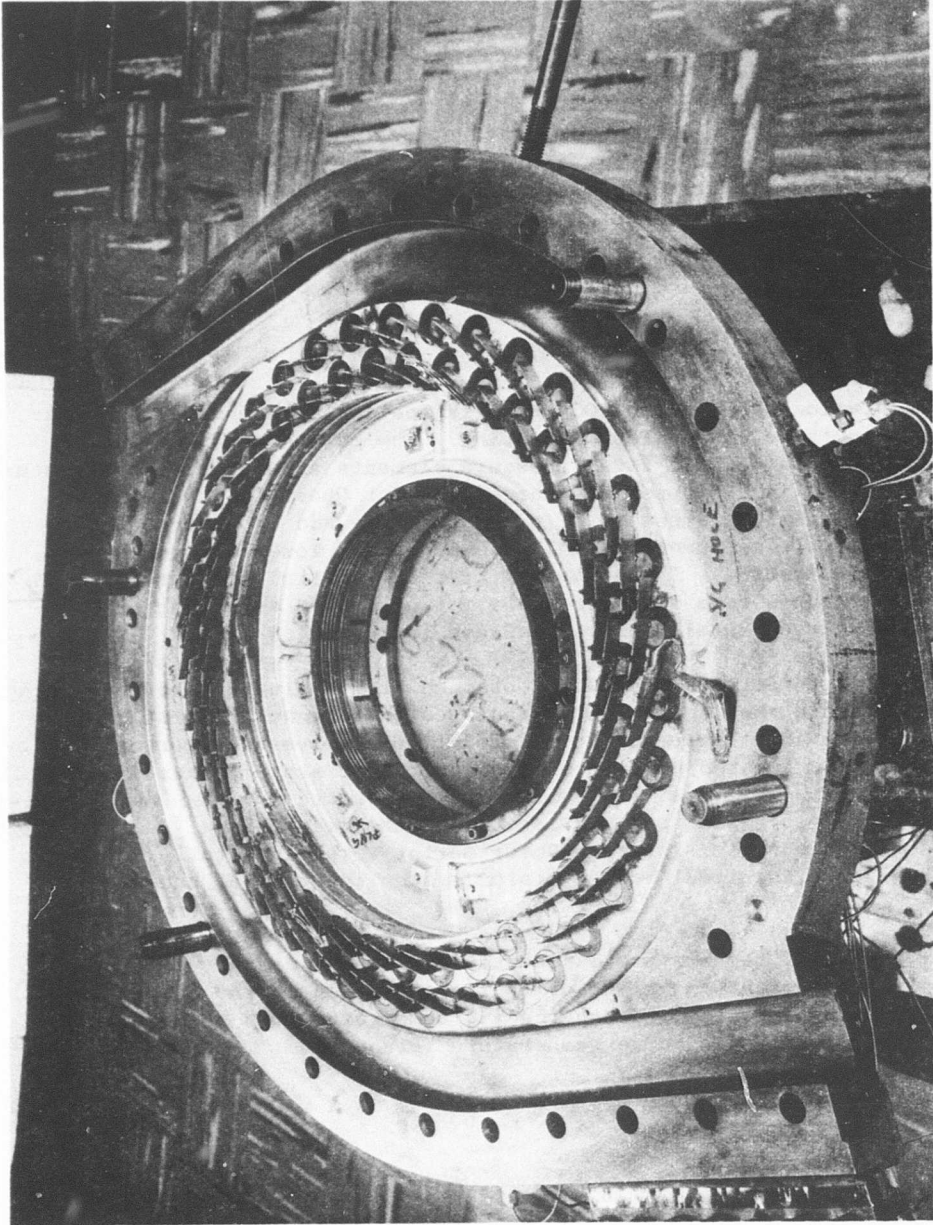
Figure 11. Stator Vane Array in Front Stator Casing – Aft Looking Forward.
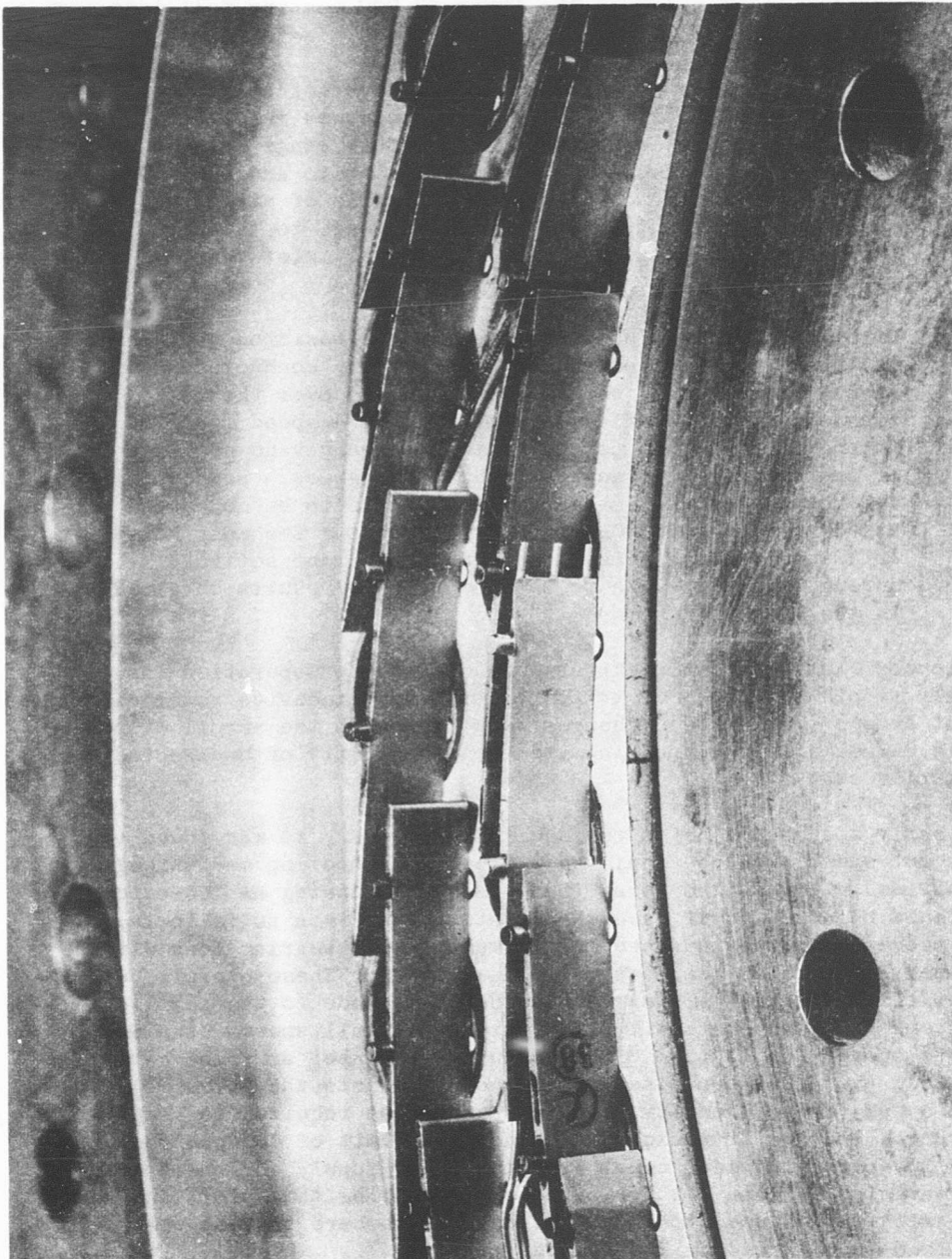
Figure 12. Total Pressure Rake Installed at Leading Edge of Supersonic Stator Vanes.

21

TEST PROGRAM

The requirements established for the Phase IV ROC testing fell into two categories:

(1) With the supersonic and subsonic stators set at a nominal position of approximately 82 and 76 degrees respectively, tests were to be conducted over the full range of speeds available (a minimum of 4 speed lines up to and including 80 percent, if the compressor was capable of attaining such speeds without risk of loss or damage to the compressor) at each of 3 different circular inlet vane positions.

(2) With the circular inlet vane set at the position yielding the best rotor performance during testing conducted under Item 1 above, tests were to be conducted over the full range of speeds available (a minimum of 4 speed lines up to and including 80 percent) at supersonic vane settings of approximately 79 degrees and 83.4 degrees. Based on the results of the foregoing, tests were to be conducted at 90-percent and 100-percent speeds using the most suitable supersonic vane setting. Subsonic vane settings during this step were to be based on the results obtained in the Phase III work.

Execution of Item 1 was straightforward. Compressor operation was generally smooth at speeds up to 80 percent, and excessive rotor vibrations were not encountered. Speed changes were made with the scroll discharge throttle valves wide open to minimize the probability of unexpectedly encountering stall.

In the early stages of the tests required by Item 2, it was found that 100-percent speed could be achieved without encountering mechanical difficulties. It was also found that sustained running at 100-percent speed could be achieved if careful attention was given to following a test procedure which maintained the forward thrust bearing load within limits and rotor metal temperatures below limits. These operational necessities were met by appropriate adjustments made to the auxiliary air systems shown schematically in Figure 8. At all speeds, the PV4 bleed was opened for maximum bleed, assuring that hot air from cavity PV2 leaking past the shroud seal would not leak into the inlet. At 80-percent speed, the PV6 cavity bleed was opened as required to keep rotor thrust loading from exceeding a nominal limit of 400 pounds. At 90- and 100-percent speed, equal amounts of air supply and bleed were set in cavities PV6 and PV2 for purposes of cooling the rotor, and the tank density was reduced to about one-half atmosphere to keep the rotor thrust load from exceeding 500 pounds.

22

Satisfactory mechanical operation of the ROC vehicle was obtained over the full speed range from the unstable flow region with wide-open discharge throttle valves, through the normal operating range, and into stall. The satisfactory experience with mechanical aspects of the compressor operation in the initial testing up to and including 100-percent speed at the 82-degree supersonic stator vane setting, along with the difficulties inherent in attempting to choose an optimum stator setting for higher speeds based on running up to only 80-percent speed, provided the motivation to attemp to run a full set of compressor characteristics at both the 79- and 83.4-degree supersonic stator settings. These two runs were successfully accomplished. Consideration of the Phase III results demonstrated that the subsonic stator angle had little effect on performance; therefore, the subsonic stator setting was set and held at 76 degrees during the Phase IV testing.

Of the total test operating time of 52.7 hours for the ROC in the Phase IV configuration, 19.8 hours (37.5 percent) were at or above 80-percent speed. The test operating time at or above 90-percent speed was 5.2 hours (9.9 percent). The test operating time at 100-percent speed was 2.9 hours (5.5 percent).

RESULTS OF TEST DATA ANALYSIS

THE EFFECT OF CIRCULAR INLET VANE POSITION ON ROTOR PERFORMANCE

Rotor characteristics were measured by a series of tests at speeds up to
80 percent for each of three axial positions of the circular inlet vane.
The three vane positions are shown schematically in Figure 13. The
forward and aft positions were at the physical limits available for
adjustment, and the nominal position was the same position used in the
earlier Phase III testing. Rotor total pressure ratios, as a function
of corrected airflow and for compressor operation at corrected speeds
of 50, 60, 70, and 80 percent, are shown in Figure 14. The circular
inlet vane position does not appear to have any significant effect on
rotor total pressure ratio. A similar presentation of rotor static
pressure ratio, Figure 15, shows no significant effect of circular inlet
vane position on rotor static pressure ratio. The rotor efficiency
characteristics shown in Figure 16 do not demonstrate any significant
sensitivity to circular inlet vane positions. As a result of these
somewhat surprising observations, when considered in the light of
allegations on the influence of the circular inlet vane on rotor per-
formance made in earlier work[1], the Phase IV test data were subjected
to further examination and analysis in an attempt to provide an improved
understanding of the apparent lack of influence of the circular inlet
vane position on rotor performance. Rotor discharge total pressure
distributions, as determined from measurements taken by the three-element
total pressure rake at the 195-degree location, were compared for each
significant data point for the three circular inlet vane settings. The
two total pressure distribution factors (as given in Table II) indicate
similar trends and levels for the three circular inlet vane positions at
each of the four speed levels tested.

THE EFFECT OF VARIATION OF SUPERSONIC STATOR SETTING ON ROC PERFORMANCE
CHARACTERISTICS (CIRCULAR INLET VANE FIXED AT THE NOMINAL POSITION)

Rotor Total Pressure Ratio

Supersonic Stator Setting, 82 Degrees

The rotor total pressure ratio characteristics for the 82-degree
supersonic stator angle setting are shown in Figure 17. The test
data points for corrected speeds of 50, 60, 70, 80, 90, and 100
percent are plotted together with the estimated compressor-
characteristic curves for the same speeds. At speeds of 80 percent
and lower, the rotor total pressure ratio tends to be higher than
the estimated levels for each speed, with the smaller differences
occurring for the lower speeds. For the 80-percent speed test
data, the airflows appear to be at approximately the same level

24
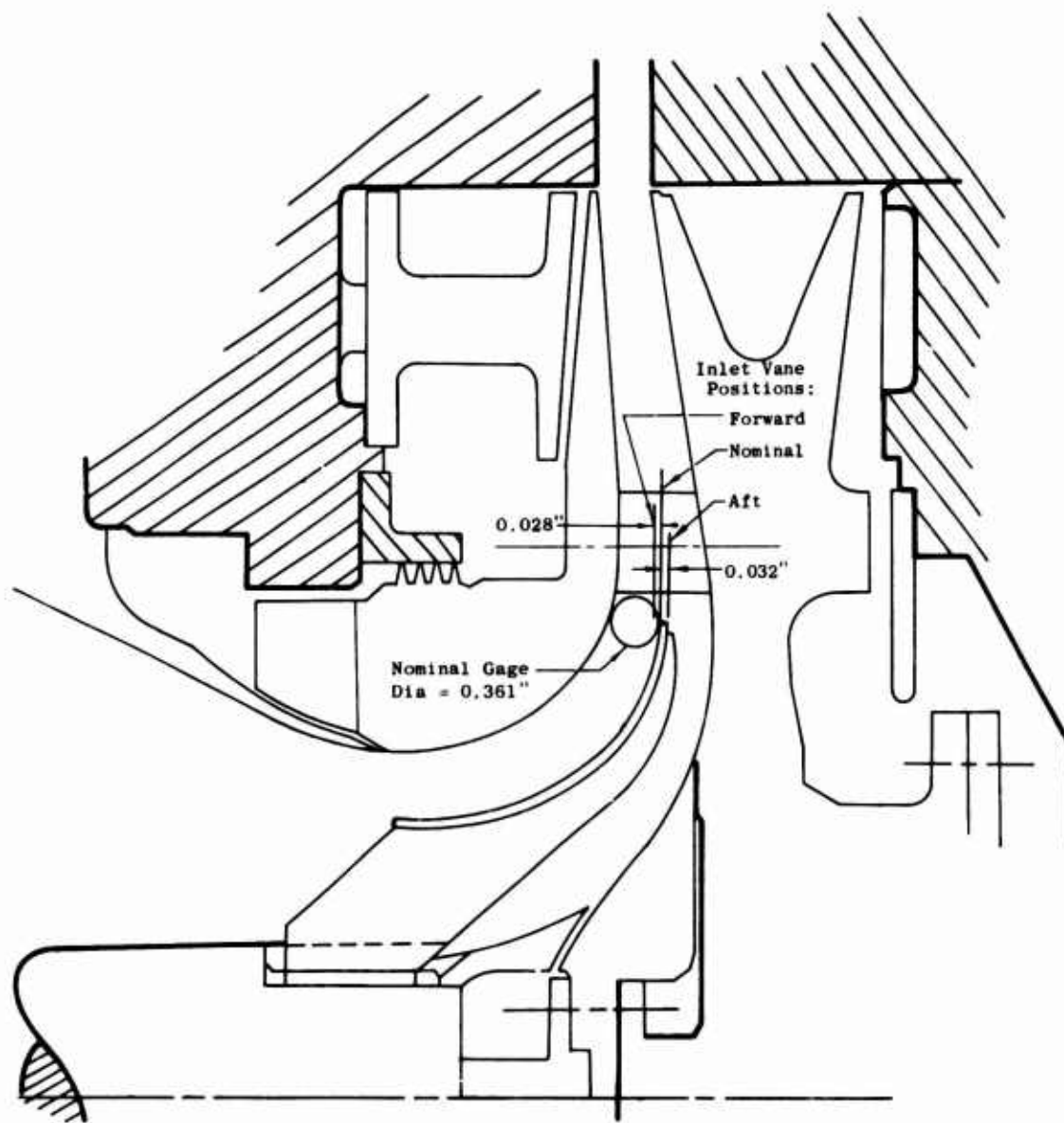
Figure 13. Circular Inlet Vane Positions.
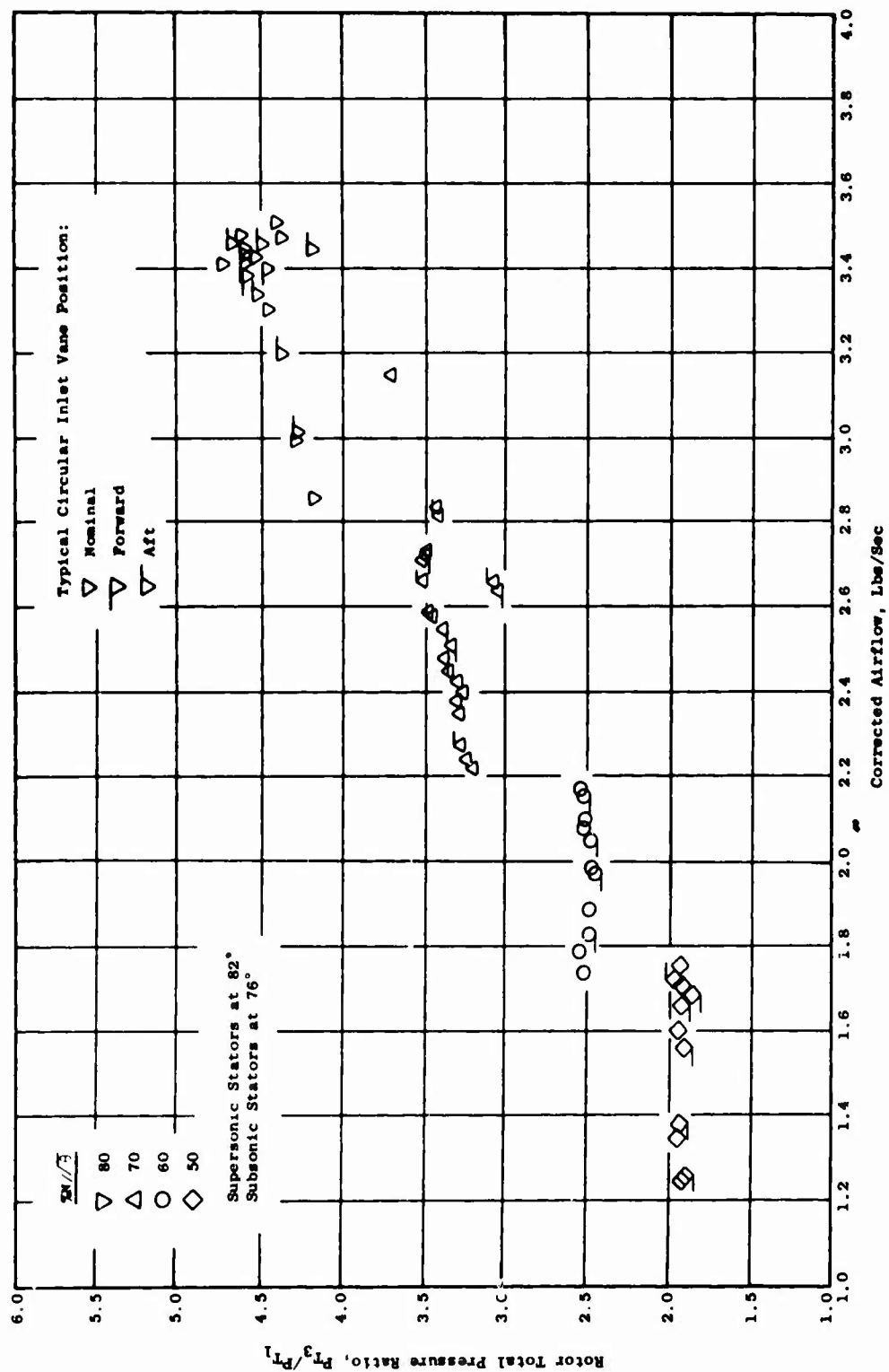
Figure 14. ROC Phase IV Test Data - Rotor Total Pressure Ratio Vs Airflow at Various Circular Inlet Vane Positions.
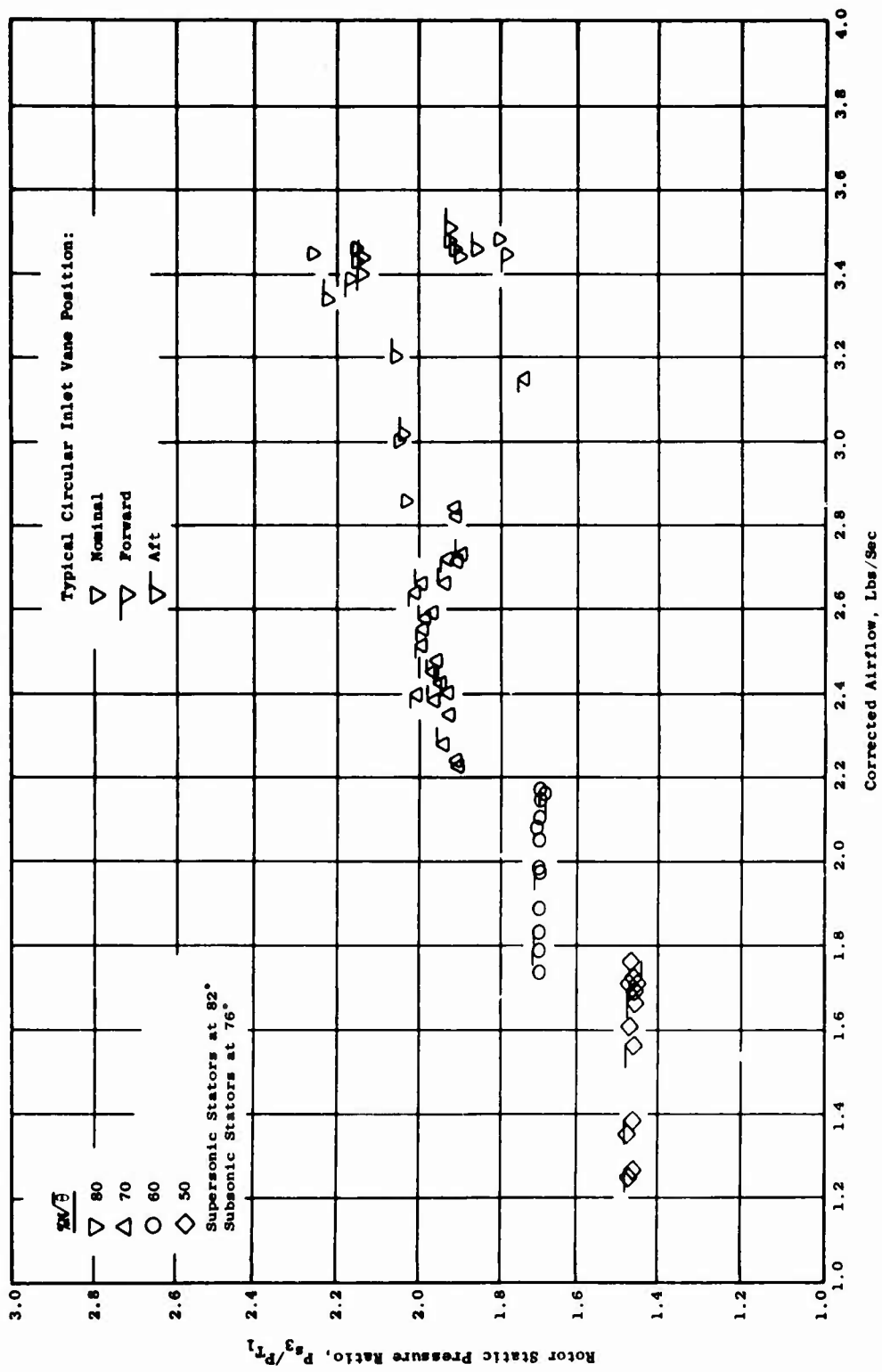
Figure 15. ROC Phase IV Test Data - Rotor Static Pressure Ratio Vs Airflow at Various Circular Inlet Vane Positions.
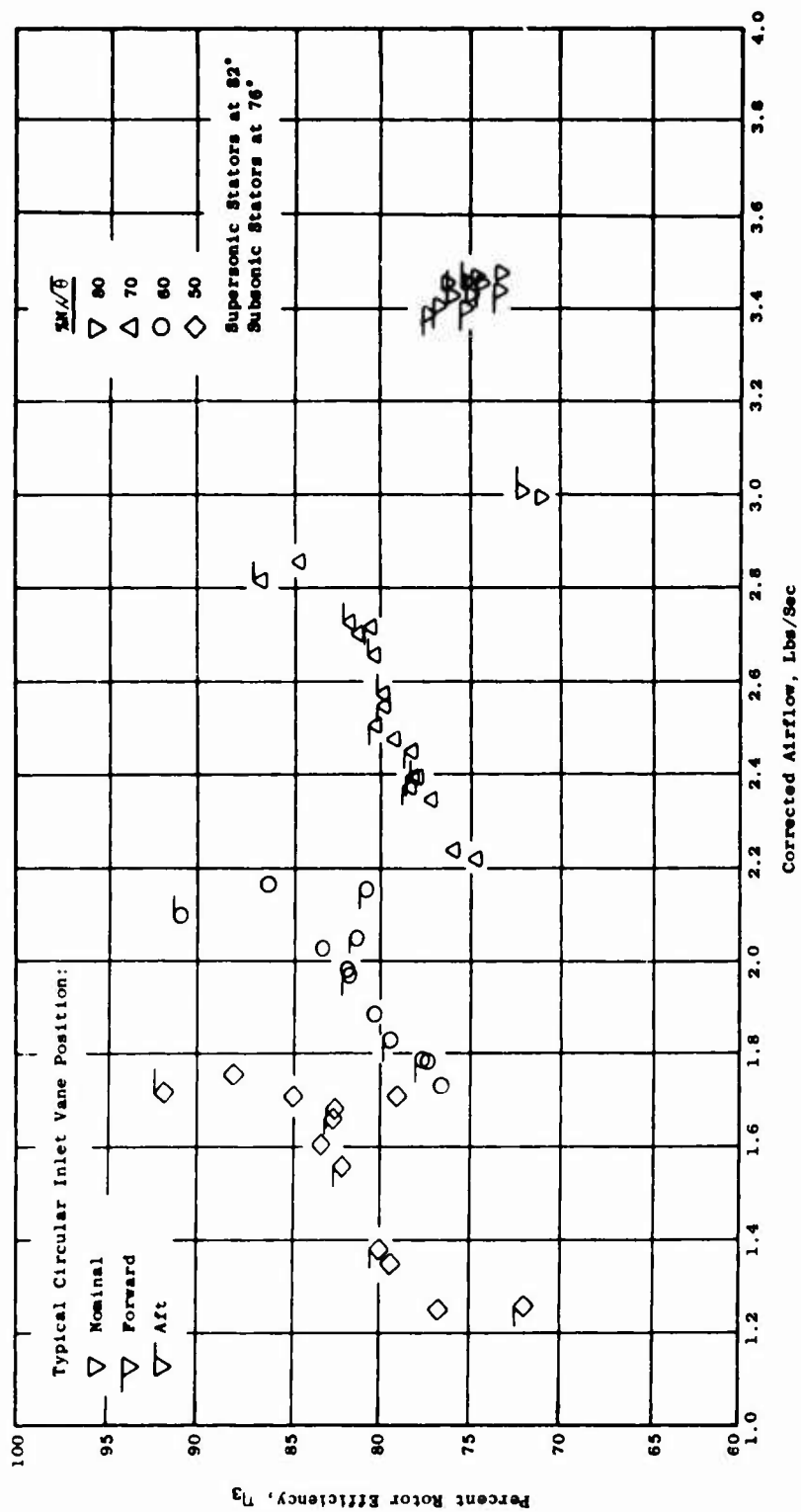
Figure 16. ROC Phase IV Test Data – Rotor Efficiency Vs Airflow at Various Circular Inlet Vane Positions.

All measurements taken fr(
Stator vane settings: sup(

PT$_{3C}$ = total pressure (rward
PT$_{3S}$ = total pressure $t$ator
PT$_{3D}$ = total pressure $t$asing

Distribution Factors

$$D_1 = \frac{PT_{3C} - PT_{3S}}{PT_{3Avg}*} \quad \text{(or P'}$$

$$*PT_{3Avg} = (PT_{3i}$$

$$D_2 = \frac{2(PT_{3S} - PT_{3D})}{(PT_{3S} + PT_{3D})} \times$$
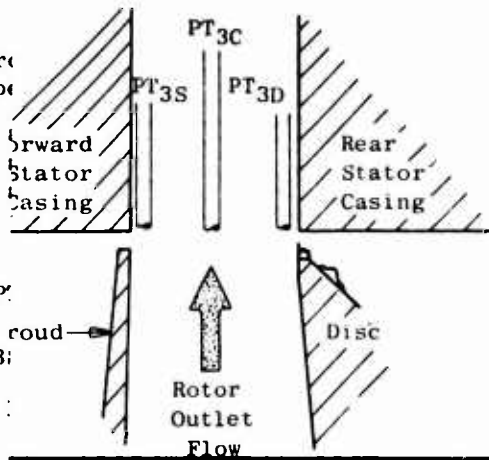
Aft

Percent Corrected Speed	Corrected Airflow (Lbs/Sec)	Rotor Pre Ra	Rotor Total Pressure Ratio	D$_1$ (%)	D$_2$ (%)	Rotor Outlet Mach No. (M$_3$)
80	3.46	4	4.50	11.9	-4.0	1.17
	3.44	4	4.54	22.0	-18.5	1.09
	3.41	4	4.31	20.7	-17.2	1.09
	3.39	4	4.59	21.4	-18.5	1.10
	3.40	4	-	-	-	-
70	2.72	3	3.43	4.1	-2.2	0.95
	2.55	3	3.51	4.5	-4.1	0.98
	2.51	3	3.53	5.7	-3.3	0.97
	2.46	3	3.46	6.2	-4.4	0.93
	2.39	3	3.31	5.2	-4.1	0.89
	-	3	3.28	9.0	-6.6	0.90
60	2.16	2	2.51	2.8	+0.6	0.77
	2.05	2	-	-	-	-
	1.98	2	-	-	-	-
	1.79	2	-	-	-	-
	1.77	2	-	-	-	-
50	1.71	1	1.99	3.6	+1.1	0.67
	1.69	1	-	-	-	-
	1.66	1	-	-	-	-
	1.56	1	-	-	-	-
	1.39	1	-	-	-	-
	1.26	1	-	-	-	-

TABLE II. ROTOR OUTLET CROSS-STREAM PRESSURE DISTRIBUT'

All measurements taken from rake at 195° position
Stator vane settings: supersonic = 82°, subsonic = 76°

PT_{3C} = total pressure at center
PT_{3S} = total pressure at shroud side
PT_{3D} = total pressure at disc side

Distribution Factors

D_1 = $\dfrac{PT_{3C} - PT_{3S}}{PT_{3Avg}^*}$ (or PT_{3D}, whichever is the lesser) x 100, maximum spread, percent

$^*PT_{3Avg}$ = $(PT_{3S} + PT_{3C} + PT_{3D})/3$

D_2 = $\dfrac{2(PT_{3S} - PT_{3D})}{(PT_{3S} + PT_{3D})}$ x 100, wall-to-wall spread, percent

Circular Inlet V

			Forward					Nomin
Percent Corrected Speed	Corrected Airflow (Lbs/Sec)	Rotor Total Pressure Ratio	D_1 (%)	D_2 (%)	Rotor Outlet Mach No. (M_3)	Percent Corrected Speed	Corrected Airflow (Lbs/Sec)	Rotor Total Pressure Ratio
80	3.46	4.35	12.8	-4.9	1.16	80	3.48	4.37
	3.44	4.57	12.1	-4.8	1.24		3.48	4.62
	3.41	4.59	16.4	-14.2	1.10		3.46	4.69
	3.39	4.57	17.8	-16.4	1.09		3.46	4.69
	3.40	4.46	21.6	-20.8	1.08		3.00	4.30
70	2.72	3.50	4.5	-3.1	0.96	70	2.84	3.43
	2.55	3.39	6.4	-4.0	0.90		2.71	3.53
	2.51	3.35	6.1	-3.8	0.89		2.48	3.38
	2.46	3.36	12.8	-12.0	0.90		2.35	3.29
	2.39	3.31	15.0	-14.2	0.88		2.24	3.25
	-	-	-	-	-		2.22	3.19
60	2.16	2.52	3.5	+2.3	0.77	60	2.17	2.54
	2.05	2.49	2.9	+2.0	0.75		2.08	2.51
	1.98	2.46	2.4	+1.4	0.74		1.99	2.47
	1.79	2.55	8.4	-1.1	0.78		1.89	2.50
	1.77	2.53	8.4	-1.2	0.77		1.79	2.54
50	1.71	1.92	2.6	+1.1	0.64	50	1.76	1.95
	1.69	1.91	2.8	+1.4	0.63		1.71	1.94
	1.66	1.95	3.4	+1.2	0.65		1.60	1.96
	1.56	1.93	3.0	+1.2	0.64		1.35	1.96
	1.39	1.95	5.2	+1.2	0.65		1.25	1.94
	1.26	1.93	7.7	-1.8	0.64		-	-

29

ent

cular Inlet Vane Position

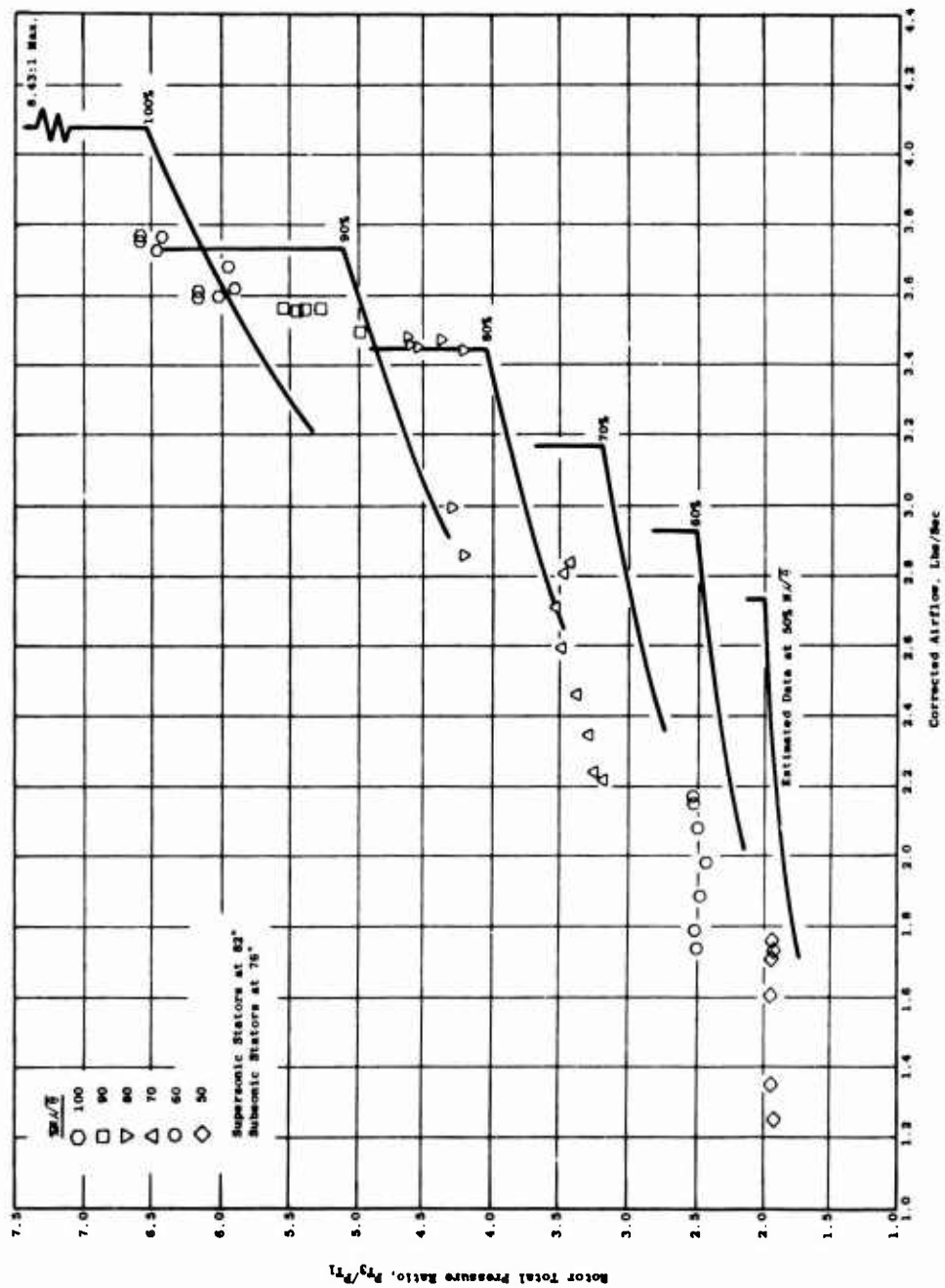| Nominal					Aft				
Rotor Total Pressure Ratio	D_1 (%)	D_2 (%)	Rotor Outlet Mach No. (M_3)	Percent Corrected Speed	Corrected Airflow (Lbs/Sec)	Rotor Total Pressure Ratio	D_1 (%)	D_2 (%)	Rotor Outlet Mach No. (M_3)
4.37	12.1	-5.6	1.15		3.47	4.50	11.9	-4.0	1.17
4.62	10.5	-3.5	1.24		3.44	4.54	22.0	-18.5	1.09
4.69	18.3	-14.7	1.11	80	3.01	4.31	20.7	-17.2	1.09
4.69	31.9	-29.9	1.08		3.43	4.59	21.4	-18.5	1.10
4.30	22.6	-20.0	1.08		-	-	-	-	-
3.43	4.4	-2.8	0.95		2.82	3.43	4.1	-2.2	0.95
3.53	4.4	-3.2	0.98		2.73	3.51	4.5	-4.1	0.98
3.38	6.9	-5.8	0.92	70	2.66	3.53	5.7	-3.3	0.97
3.29	8.1	-6.0	0.91		2.56	3.46	6.2	-4.4	0.93
3.25	8.6	-5.7	0.91		2.38	3.31	5.2	-4.1	0.89
3.19	7.6	-5.1	0.89		2.40	3.28	9.0	-6.6	0.90
2.54	3.1	+0.45	0.78		2.10	2.51	2.8	+0.6	0.77
2.51	2.5	+0.11	0.76		-	-	-	-	-
2.47	2.3	-0.20	0.75	60	-	-	-	-	-
2.50	4.4	-0.80	0.76		-	-	-	-	-
2.54	9.5	-2.0	0.78		-	-	-	-	-
1.95	2.7	+0.62	0.64		1.72	1.99	3.6	+1.1	0.67
1.94	2.8	+0.99	0.64		-	-	-	-	-
1.96	2.7	+0.51	0.65	50	-	-	-	-	-
1.96	5.2	-0.07	0.65		-	-	-	-	-
1.94	8.2	-1.69	0.64		-	-	-	-	-
-	-	-	-		-	-	-	-	-

BLANK PAGE

Figure 17. ROC Phase IV Test Data – Rotor Total Pressure Ratio Vs Airflow.

31

as the estimates. Airflow is progressively much lower than the
estimated levels for 70-percent speed and lower. The test data
for speeds of 70-percent and below demonstrate a reduction in
flow as expected as the compressor discharge is throttled. The
test data at 80-percent speed indicate a similar rollback in
airflow as the compressor discharge is throttled, but of less
range. The test data for 90-percent speed do not show any indi-
cation of flow rollback as the compressor discharge is throttled.
Airflow remains relatively constant with increasing pressure ratio,
an opposite trend from that expected from the estimated data.
The increment in flow for the 90-percent speed test data over
that for the 80-percent speed test data is smaller than would
be expected from the estimated data.

The test data for 100-percent speed exhibit trends similar to
those for 90-percent speed. Flow and total pressure ratio are
substantially less than estimated levels, with highest total pres-
sure ratio occurring with maximum compressor discharge throttling,
as contrasted to that occurring at minimum throttling implicit in
the estimated data. The maximum total pressure ratio of 6.6 was
close to stall pressure ratio.

Supersonic Stator Setting, 83.4 Degrees

The rotor total pressure ratio characteristics for the 83.4-degree
supersonic stator setting are shown on Figure 18. The test data
points for corrected speeds of 50, 60, 70, 80, 90, and 100 percent
are plotted together with the estimated compressor characteristics
for the same speeds. The test data for speeds below 80 percent
exhibit the higher total pressure ratios and lower airflows relative
to the estimated characteristics, as was encountered with the 82-
degree stator setting. At 80-percent speed, the test data indicate
that maximum airflows are substantially less than the estimated
levels; at 90-percent speed, they are about the same as at 80-percent
speed. At 100-percent speed, the measured flows are low relative to
the estimated levels, but are not nearly so low as those for the 90-
percent speed airflows. For the 83.4-degree stator setting, airflow
reduction with compressor discharge throttling occurred for all speeds
but with only minor rollback of airflow occurring at 90- and 100-percent
speeds. As with the 82-degree stator setting data, there is no indi-
cation that the shape of the test data pattern approaches the shape of
the estimated total pressure ratio/airflow characteristics as a function
of throttling the compressor discharge. The comparable Phase III
high-speed test data, displayed by the distinctive symbols on Figure
18, indicate that the rotor total pressure ratios were generally lower
than those for Phase IV, and the airflow increments between the test
data groups for the speed characteristics were more evenly spaced than
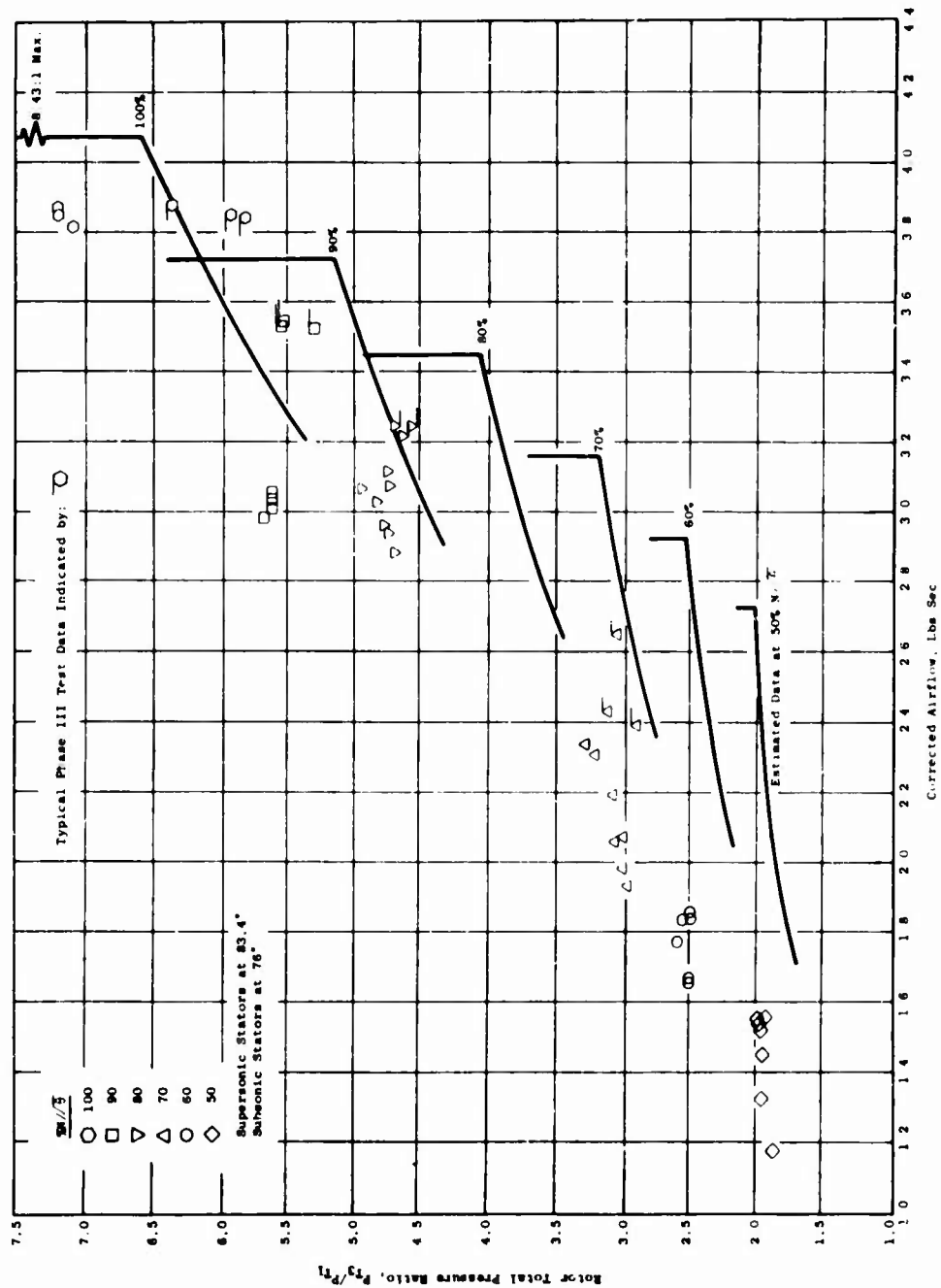for the Phase IV test data.

32

Figure 18. ROC Phase IV Test Data – Rotor Total Pressure Ratio Vs Airflow.

Supersonic Stator Setting, 79 Degrees

The rotor total pressure ratio characteristics for the 79-degree supersonic stator setting are shown in Figure 19. The test data for corrected speeds of 50, 60, 70, 80, 90, and 100 percent are plotted together with the estimated compressor characteristics for the same speeds. The test data for 50- and 60-percent speeds indicate that the rotor total pressure ratio was about the same or slightly higher than the estimated characteristics, similar to that apparent for the other two stator settings. However, the airflow levels closely approximate those for the estimated compressor characteristics up through 70-percent speed. At 80-percent speed, the test data are grouped around the corresponding vertical portion of the estimated total pressure ratio characteristic, but the total pressure ratio level is generally below the estimated levels. The 90- and 100-percent speed test data display some rollback in airflow as the compressor discharge is throttled, but total pressure ratio and airflow levels are substantially below those for the estimated characteristics.

Rotor Static Pressure Ratio

Supersonic Stator Setting, 82 Degrees

The rotor static pressure ratio characteristics for the 82-degree supersonic stator angle setting are shown in Figure 20. The test data for corrected speeds of 50, 60, 70, 80, 90, and 100 percent are plotted together with the estimated rotor characteristic curves for the same speeds. The test data for 50-percent speed locate the rotor static pressure ratios at the same levels as the estimated static pressure ratios. For higher speeds, the measured rotor static pressure ratios are below the estimated static pressure ratio levels. This discrepancy increases with increasing speed. The differences between measured and estimated airflow for each speed characteristic are the same as described previously for the rotor total pressure ratio characteristics. The measured rotor static pressure ratio characteristic at 80-percent speed has a shape similar to that of the estimated characteristic.

Supersonic Stator Setting, 83.4 Degrees

The rotor static pressure ratio characteristics for the 83.4-degree supersonic stator angle setting are shown in Figure 21. The test data for corrected speeds of 50, 60, 70, 80, 90, and 100 percent are plotted together with the estimated rotor characteristic curves for the same speeds. At the 50-percent speed level, the measured rotor static pressure ratio is about the same level as
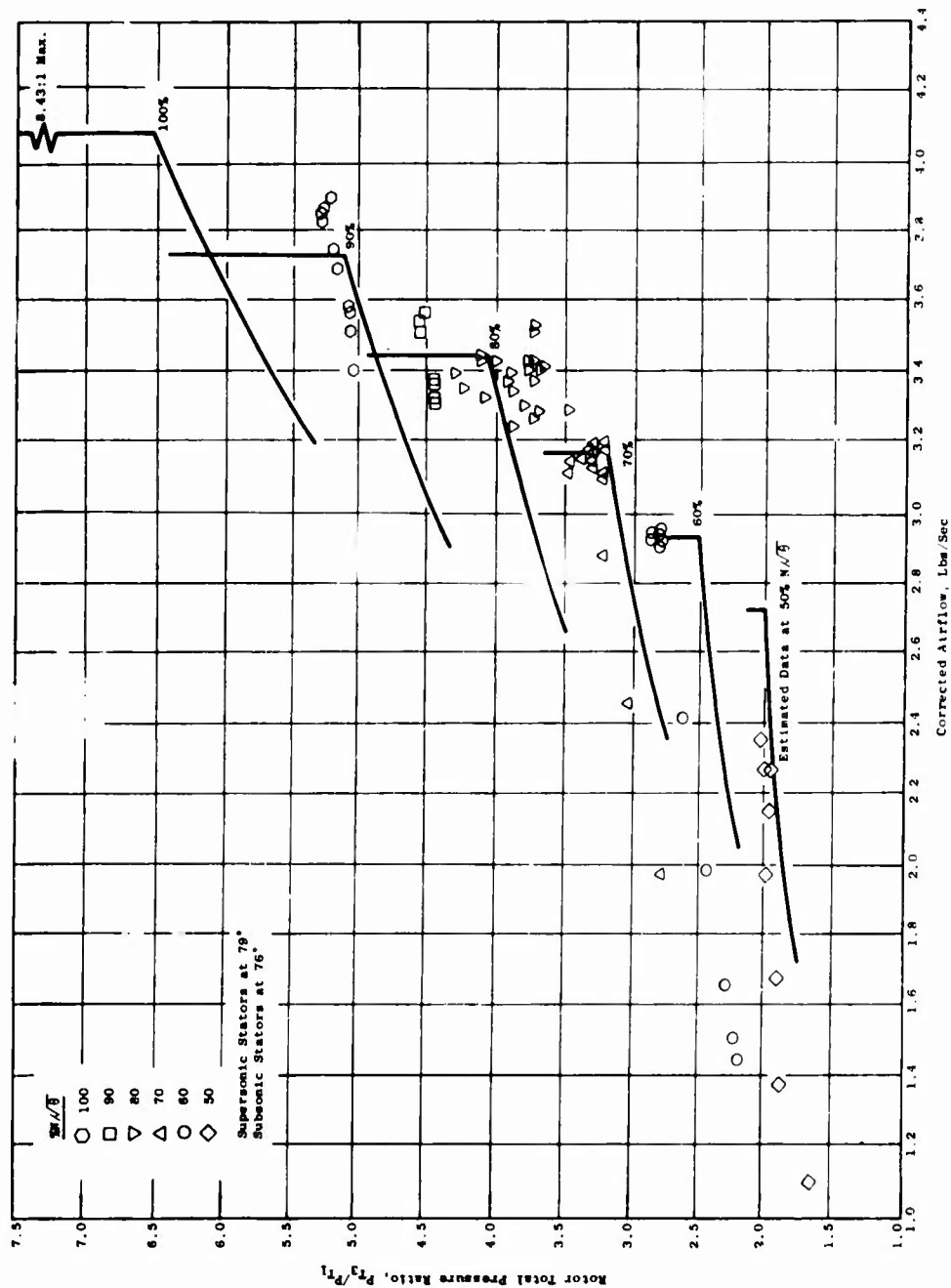
Figure 19. ROC Phase IV Test Data – Rotor Total Pressure Ratio Vs Airflow.
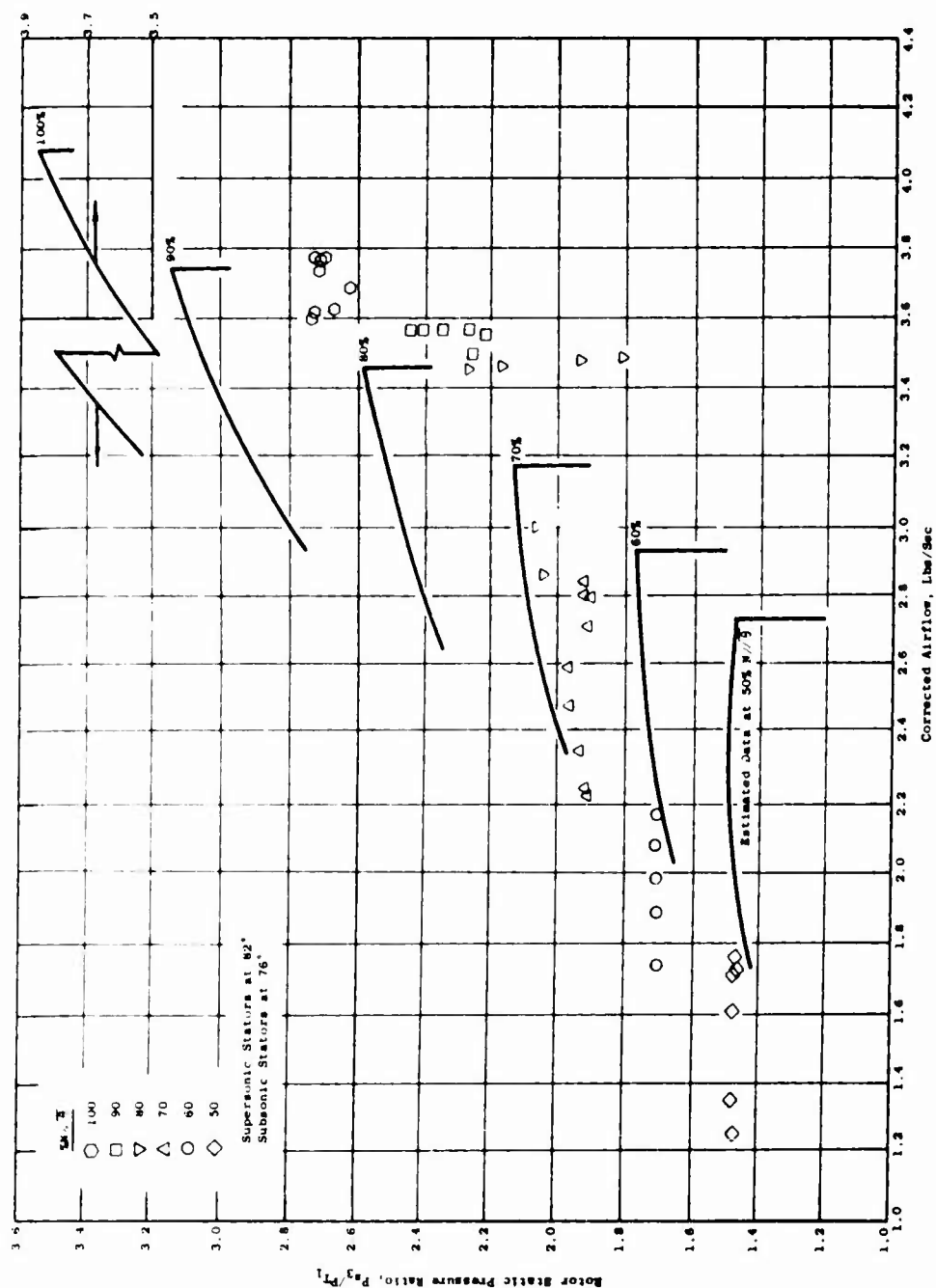
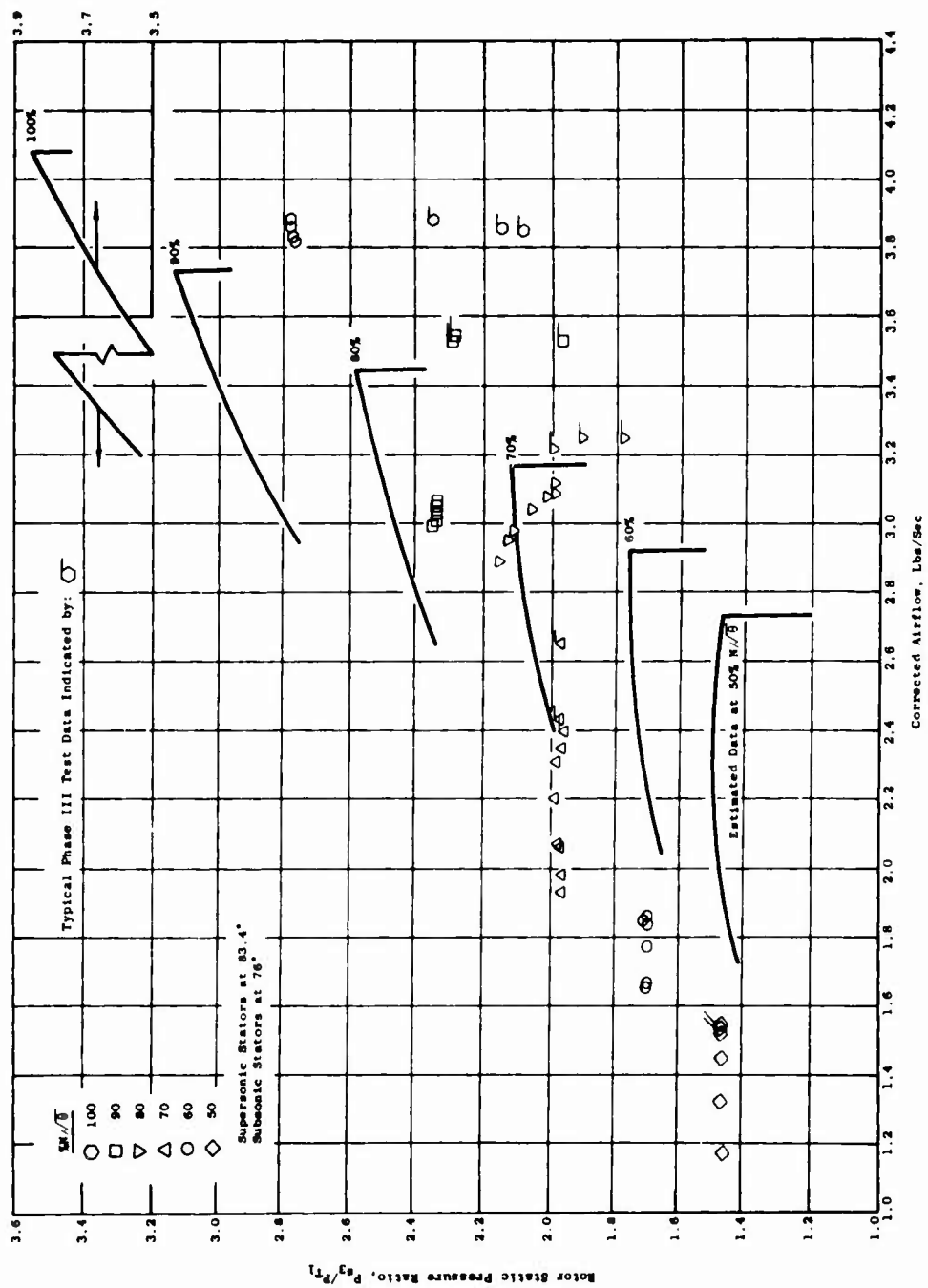Figure 20. ROC Phase IV Test Data – Rotor Static Pressure Ratio Vs Airflow.

Figure 21. ROC Phase IV Test Data – Rotor Static Pressure Ratio Vs Airflow.

the estimated data, but the measured airflows are substantially
lower than the corresponding estimated airflows. At speeds from
60 to 100 percent, the measured rotor static pressure ratios are
substantially lower than the estimated data, and the discrepancy
between measured and estimated airflow persists through this range
of speeds. None of the measured data provide a speed characteris-
tic shape approaching that expected when the compressor would be
operating in a manner implied by the shape of the estimated rotor
static pressure ratio characteristics. Available Phase III
measured rotor static pressure ratio data have been plotted on
Figure 21 and identified by distinctive symbols. Trends similar
to those for the Phase IV data are observed, with the rotor static
pressure ratios all being lower than the corresponding Phase IV
pressure ratios for corrected speeds of 70, 80, 90, and 100
percent.

Supersonic Stator Setting, 79 Degrees

The rotor static pressure ratio characteristics for the 79-degree
supersonic stator angle setting are shown in Figure 22. The test
data for corrected speeds of 50, 60, 70, 80, 90, and 100 percent
are plotted together with the estimated rotor characteristic
curves for the same speeds. The test data for the 50-percent
speed case indicate rotor static pressure levels very close to
those of the estimated characteristic, but the maximum flow
obtained is substantially less than that expected from the
estimated data. The test data for the 60- and 70-percent speed
cases display a pattern which closely resembles the estimated
static presure ratio characteristics, with the measured and
estimated maximum flows nearly equal. The measured rotor static
pressure ratio levels for these two speeds, however, are sub-
stantially lower than the corresponding estimated values. At
the 80-percent speed level, the measured rotor static pressure
ratios are well below the estimated levels, and no airflow roll-
back is observed. Maximum measured airflows are about the same
as the predicted values. At 90- and 100-percent speeds, the
measured rotor static pressure ratios are very much below
estimated levels. The measured airflow rolls back, and the
static pressure ratio rises without displaying the anticipated
constant airflow characteristic during the compressor discharge
throttling.

Rotor Discharge Mach Number

Supersonic Stator Setting, 82 Degrees

The rotor discharge Mach number characteristics for the 82-degree
supersonic stator setting are shown in Figure 23. The test data
points for corrected speeds of 50, 60, 70, 80, 90, and 100 percent
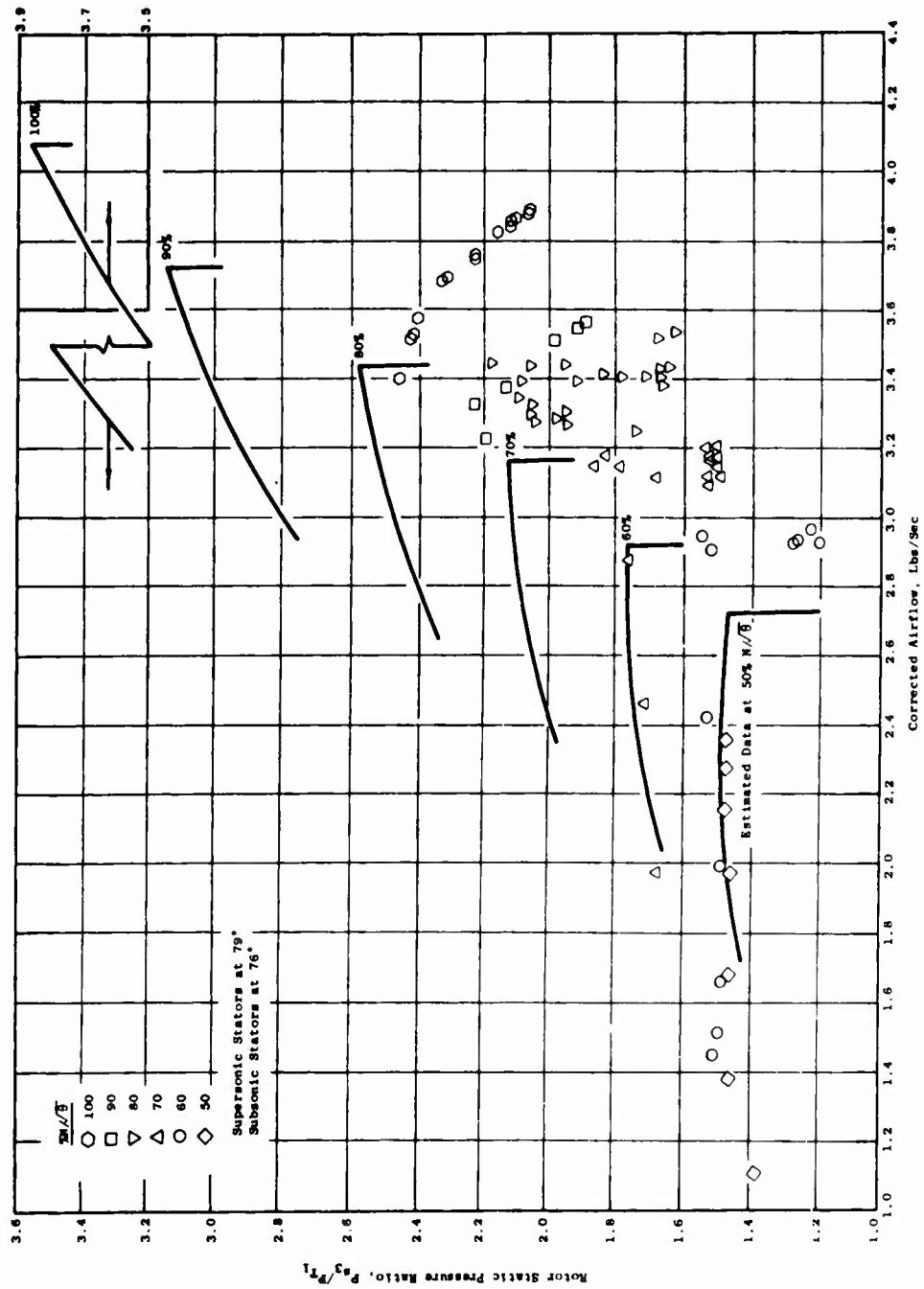
38

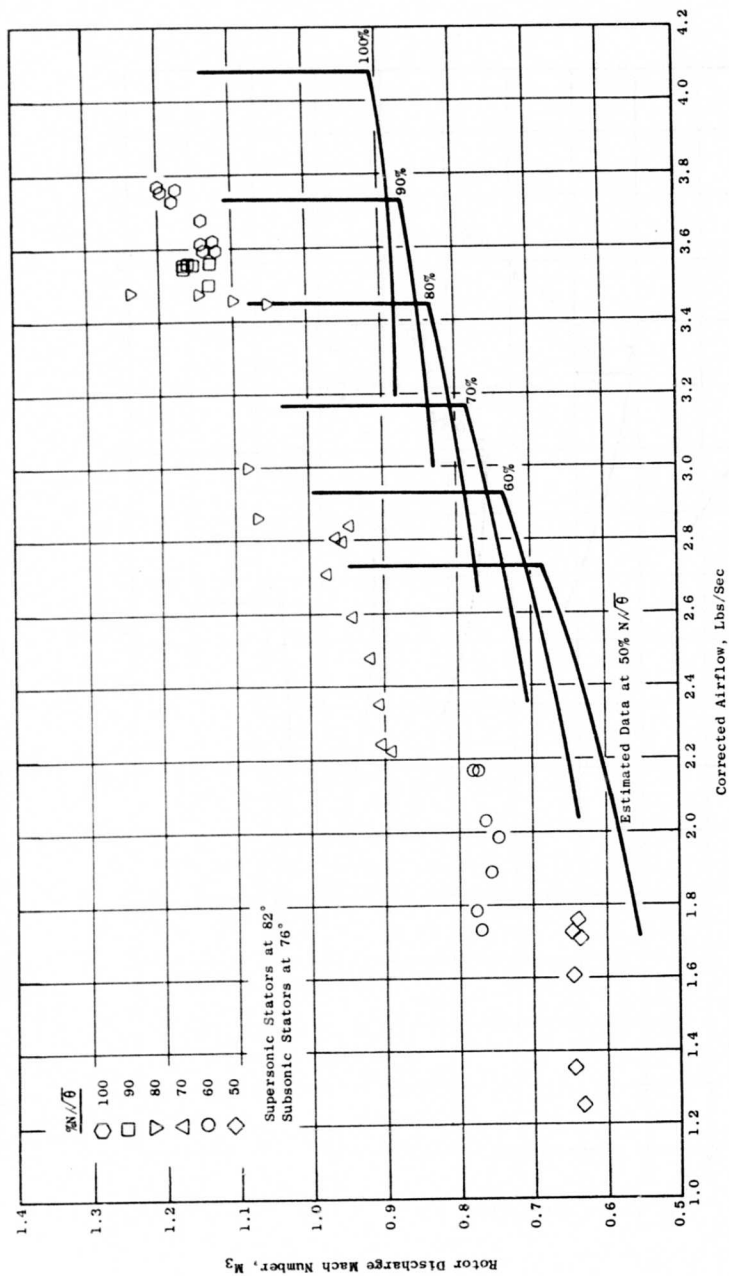Figure 22. ROC Phase IV Test Data – Rotor Static Pressure Ratio Vs Airflow.

Figure 23. ROC Phase IV Test Data – Rotor Discharge Mach Number Vs Airflow.

are plotted together with the estimated rotor discharge Mach number
characteristic curves for the same speeds. As would be expected
from consideration of the rotor total and static pressure ratio
test data, previously described, the test data show rotor discharge
Mach numbers to be substantially higher at all speeds than the
corresponding estimated values. The measured airflow discrepancies,
below estimated levels, are as described previously.

Supersonic Stator Setting, 83.4 Degrees

The rotor discharge Mach number characteristics for the 83.4-degree
supersonic stator setting are shown in Figure 24. The test data
points for corrected speeds of 50, 60, 70, 80, 90, and 100 percent
are plotted together with the estimated rotor discharge Mach
number characteristic curves for the same speeds. At all speeds
from 50 through 100 percent, the rotor discharge Mach number test
data are substantially and progressively higher than the estimated
characteristics.

Comparable Phase III test data for corrected speeds of 70, 80, 90,
and 100 percent are plotted in Figure 24 and identified by the dis-
tinctive symbols. These data indicate that the rotor discharge Mach
number for each Phase III configuration data point was somewhat higher
than the Phase IV configuration test data.

Supersonic Stator Setting, 79 Degrees

The rotor discharge Mach number characteristics for the 79-degree
supersonic stator setting are shown in Figure 25. The test data
points for corrected speeds of 50, 60, 70, 80, 90, and 100 percent
are plotted together with the estimated rotor discharge Mach
number characteristics curves for the same speed. As with the
other two sets of test data for the other supersonic stator set-
tings, rotor discharge Mach numbers are substantially in excess
of the estimated values except at 50-percent speed, where they
are nearly equal.

Rotor Efficiency

Supersonic Stator Angle, 82 Degrees

The rotor efficiency characteristics for the 82-degree supersonic
stator angle setting are shown in Figure 26. The test data points
for corrected speeds of 50, 60, 70, 80, 90, and 100 percent are
plotted together with the estimated rotor efficiency character-
istic curves for the same speeds.

41
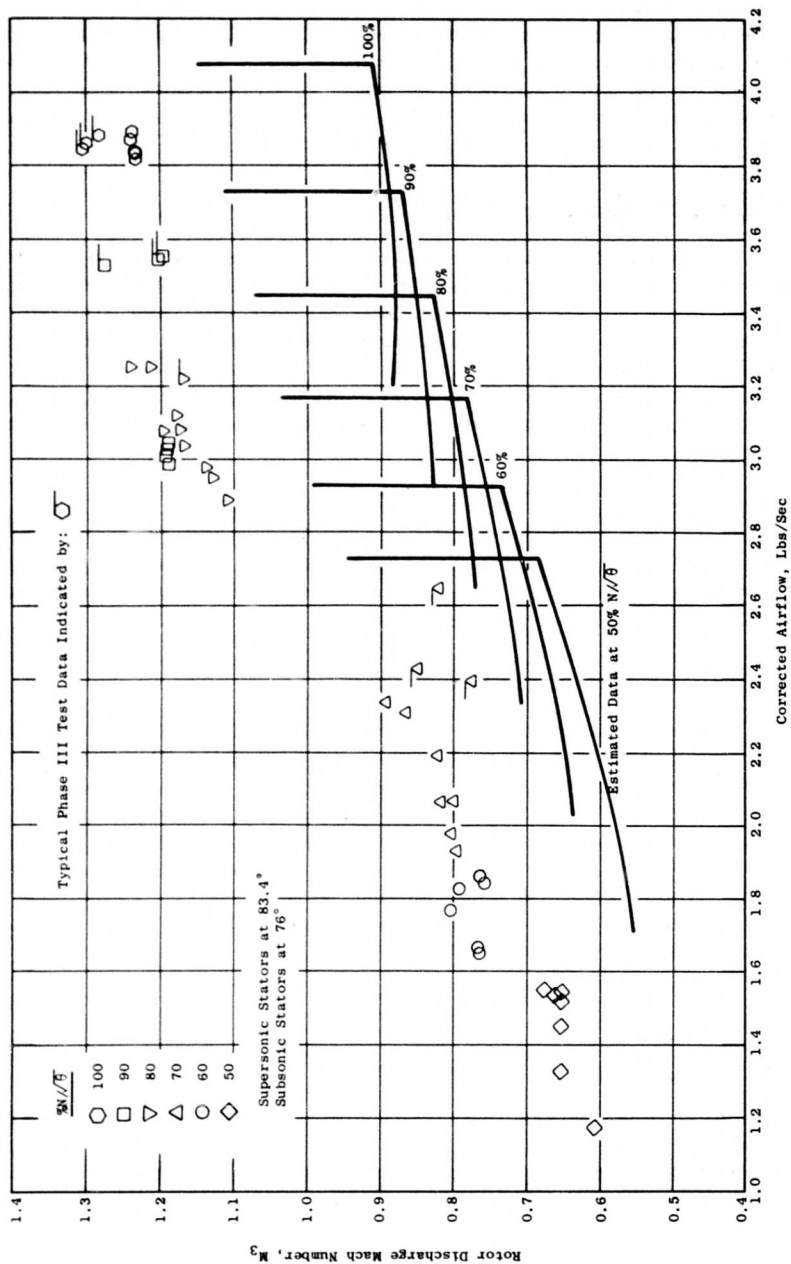
Figure 24. ROC Phase IV Test Data – Rotor Discharge Mach Number Vs Airflow.

42
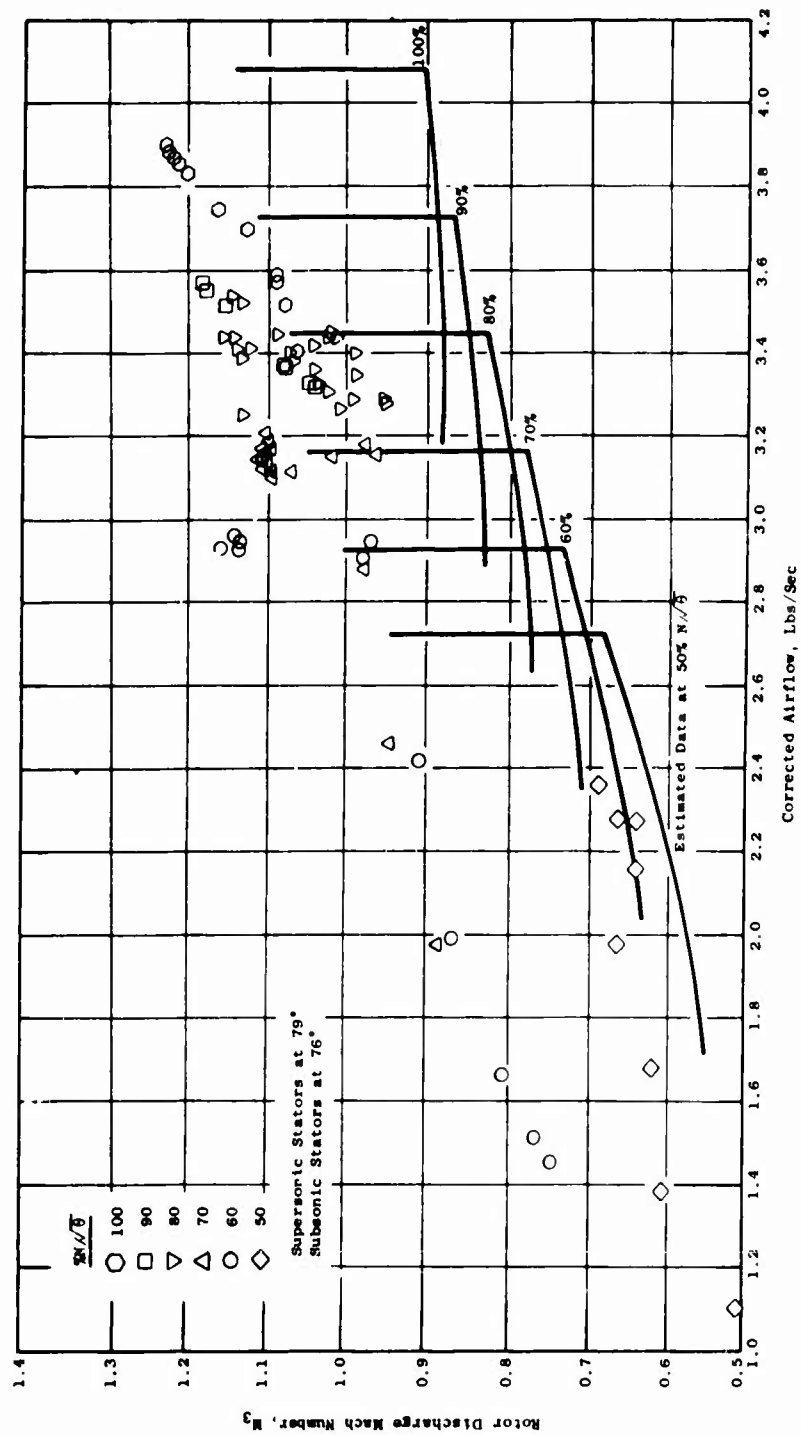
Figure 25. ROC Phase IV Test Data – Rotor Discharge Mach Number Vs Airflow.
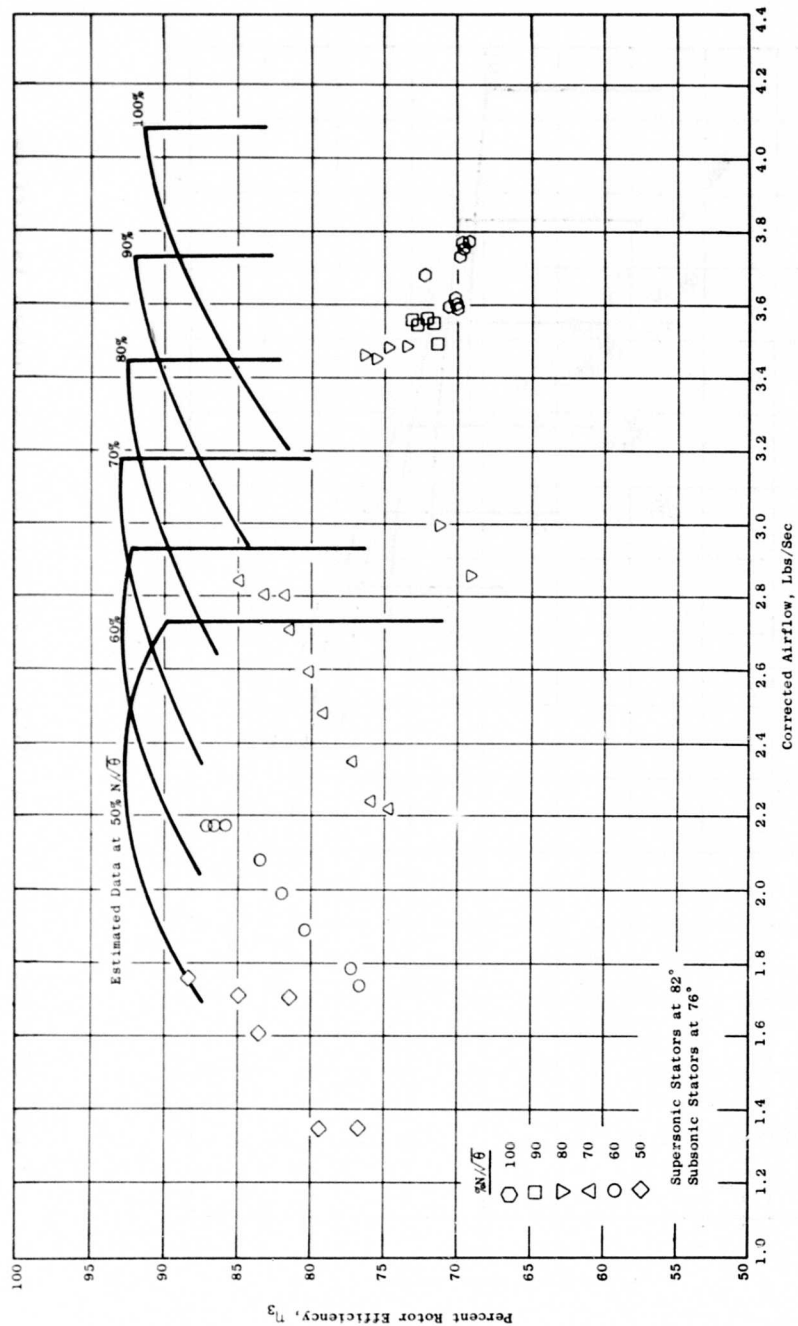
Figure 26. ROC Phase IV Test Data - Rotor Efficiency Vs Airflow.

44

At the 50-percent speed level, the higher rotor efficiencies from the test data approach the estimated levels but at lower airflows as previously observed. The test data efficiency for speeds from 60 through 100 percent are progressively lower than the estimated characteristic at each corresponding speed level.

The test data pattern for 80-percent speed resembles the estimated characteristic in shape with the maximum measured and estimated airflows equal. Efficiency levels are 14 points or more below the estimated efficiency characteristic. The rotor efficiency test data for the 90- and 100-percent speeds are clustered between 69 and 73 percent, up to 22 points below the estimated levels.

Supersonic Stator Angle, 83.4 Degrees

The rotor efficiency characteristics for the 83.4-degree supersonic stator angle setting are shown in Figure 27. The test data points for corrected speeds of 50, 60, 70, 80, 90, and 100 percent are plotted together with the estimated rotor efficiency characteristic curves for the same speeds. With increasing speeds, the rotor efficiency test data progressively fall below the estimated level and, at 100-percent corrected speed, by as much as 18 points. Test data for Phase III corrected speeds of 70, 80, 90, and 100 percent are also plotted on Figure 27 for comparative purposes. The Phase III rotor efficiency test data are about the same level as the Phase IV test data at 70-percent speed but are progressively lower with increasing speed. At 100-percent corrected speed, the Phase IV rotor efficiency test data are 9 or more points higher than the corresponding Phase III rotor efficiency data.

Supersonic Stator Angle, 79 Degrees

The rotor efficiency characteristics for the 79-degree supersonic stator angle setting are shown in Figure 28. The test data points for corrected speeds of 50, 60, 70, 80, 90, and 100 percent are plotted together with the estimated rotor efficiency characteristics for the same speeds.

At all speed levels, with the exception of 50 percent, the test data rotor efficiency levels are well below the estimated rotor efficiency characteristics, ranging from 14 points at 60-percent speed to 30 points at 100-percent speed. As for the other rotor performance characteristics obtained from the test data, only rotor efficiencies from 60- and 70-percent speed resemble the shape of the estimated characteristics, suggesting that the intended flow-pressure relationships for the rotor were being approached.
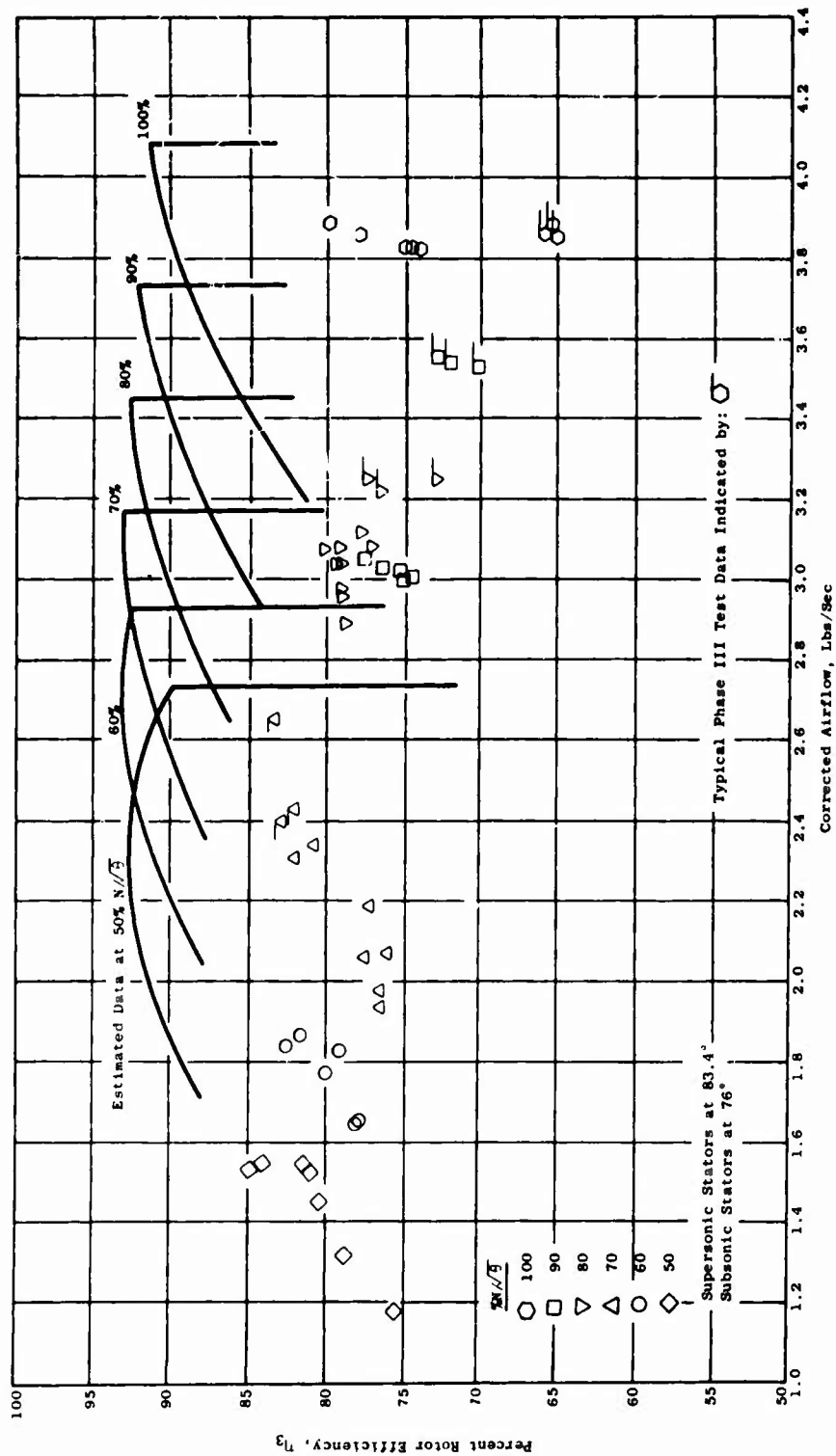
45

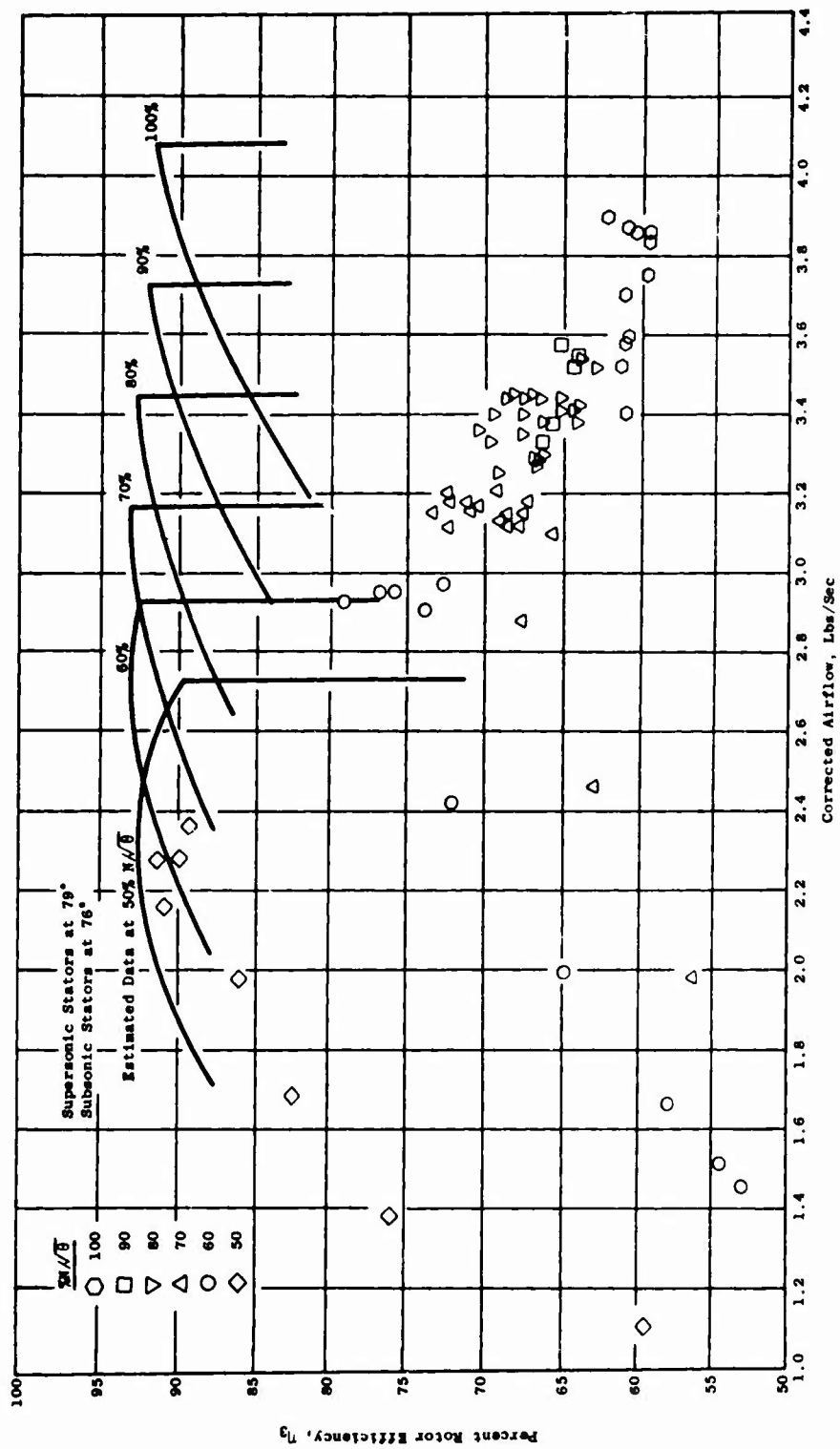Figure 27. ROC Phase IV Test Data - Rotor Efficiency Vs Airflow.

Figure 28. ROC Phase IV Test Data – Rotor Efficiency Vs Airflow.

47

Rotor Total Temperature Ratio

The rotor total temperature ratio characterisitcs for the 82-, 83.4-, and 79-degree supersonic stator angles are shown in Figures 29, 30, and 31, respectively. For each supersonic stator angle, the test data points for corrected speeds of 50, 60, 70, 80, 90, and 100 percent are plotted together with the estimated rotor total temperature ratio for the same speeds. The rotor discharge total temperature was assumed to be the same as scroll outlet total temperature.

Stage Pressure Ratio

The compressor overall pressure ratio, the ratio of the average total pressure in the discharge ducting downstream of the scroll to the average total pressure in the inlet ducting is shown in Figures 32, 33, and 34 for supersonic stator angle settings of 82, 83.5, and 79 degrees, respectively. The test data points for corrected speeds of 50, 60, 70, 80, 90, and 100 percent are plotted together with the estimated stage pressure ratio characteristic curves for the same speeds.

Supersonic Stator Setting, 82 Degrees

The stage pressure ratio test data, plotted in Figure 32 for corrected speeds from 50 through 80 percent, are higher than the estimated pressure ratio characteristics; the corresponding airflows are generally lower except at 80-percent speed, where the maximum measured airflows closely match the estimated maximum airflows. The test data stage pressure ratio trends are opposite to the trends of the estimated pressure ratio. As the compressor discharge is throttled, it would be expected that the stage pressure ratio would decrease at constant airflow; then, with further throttling toward stall, a further decrease in pressure ratio would occur, accompanied by decreasing airflow. The test data indicate at 80-percent speed that, with the closing of the discharge throttle valve, pressure ratios increase at essentially constant flow; then the pressure ratio decreases with decreasing flow as further throttling takes place. At 90- to 100-percent speeds, the airflow remains approximately constant, and the stage pressure ratio increases toward stall as the compressor discharge is throttled. The airflow increments (in going from 80- to 90- and 100-percent speed) are much smaller than expected, with some overlap of the airflows (at these speeds) as observed previously.

48

Figure 29. ROC Phase IV Test Data – Rotor Total Temperature Ratio Vs Airflow.
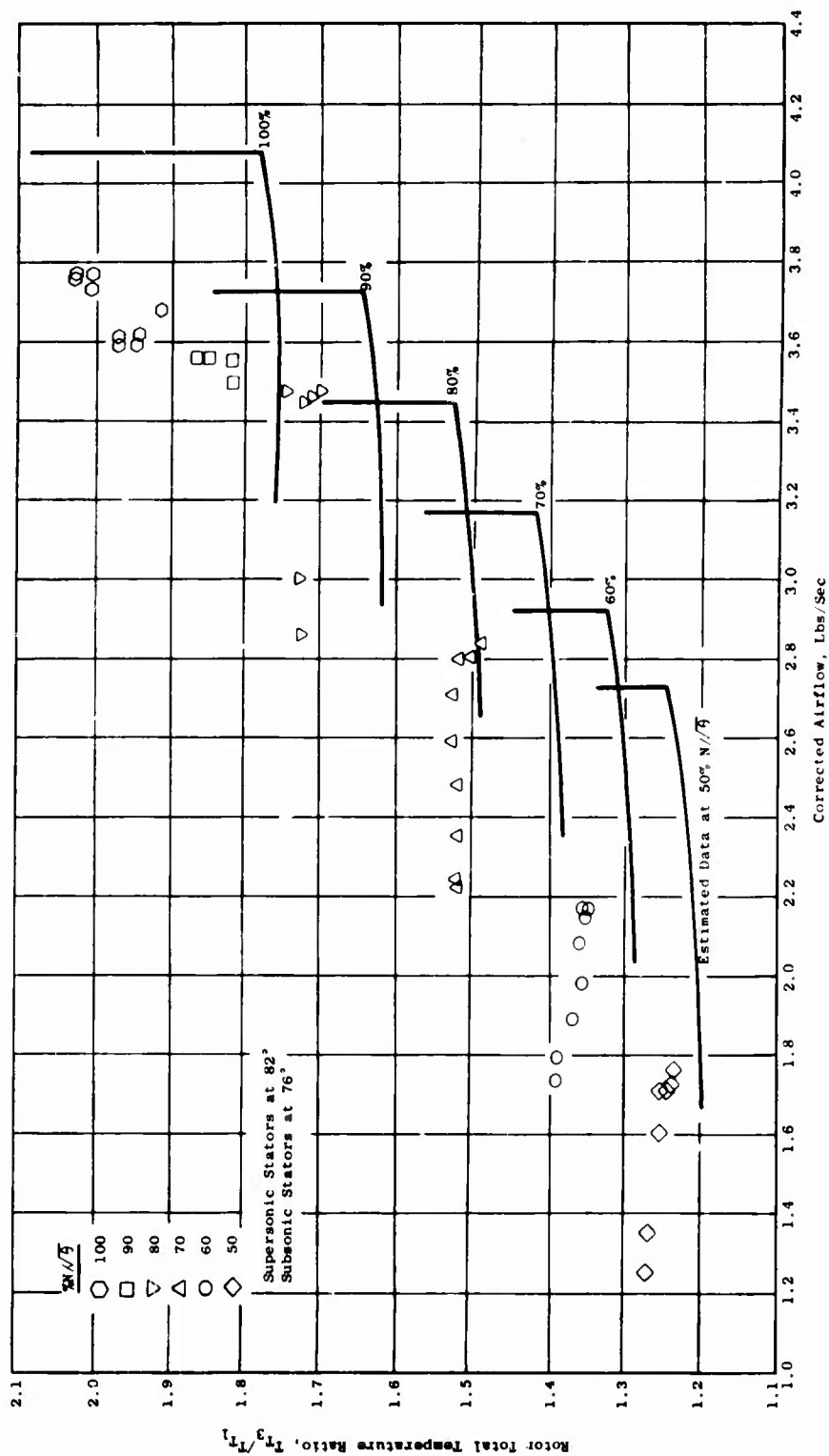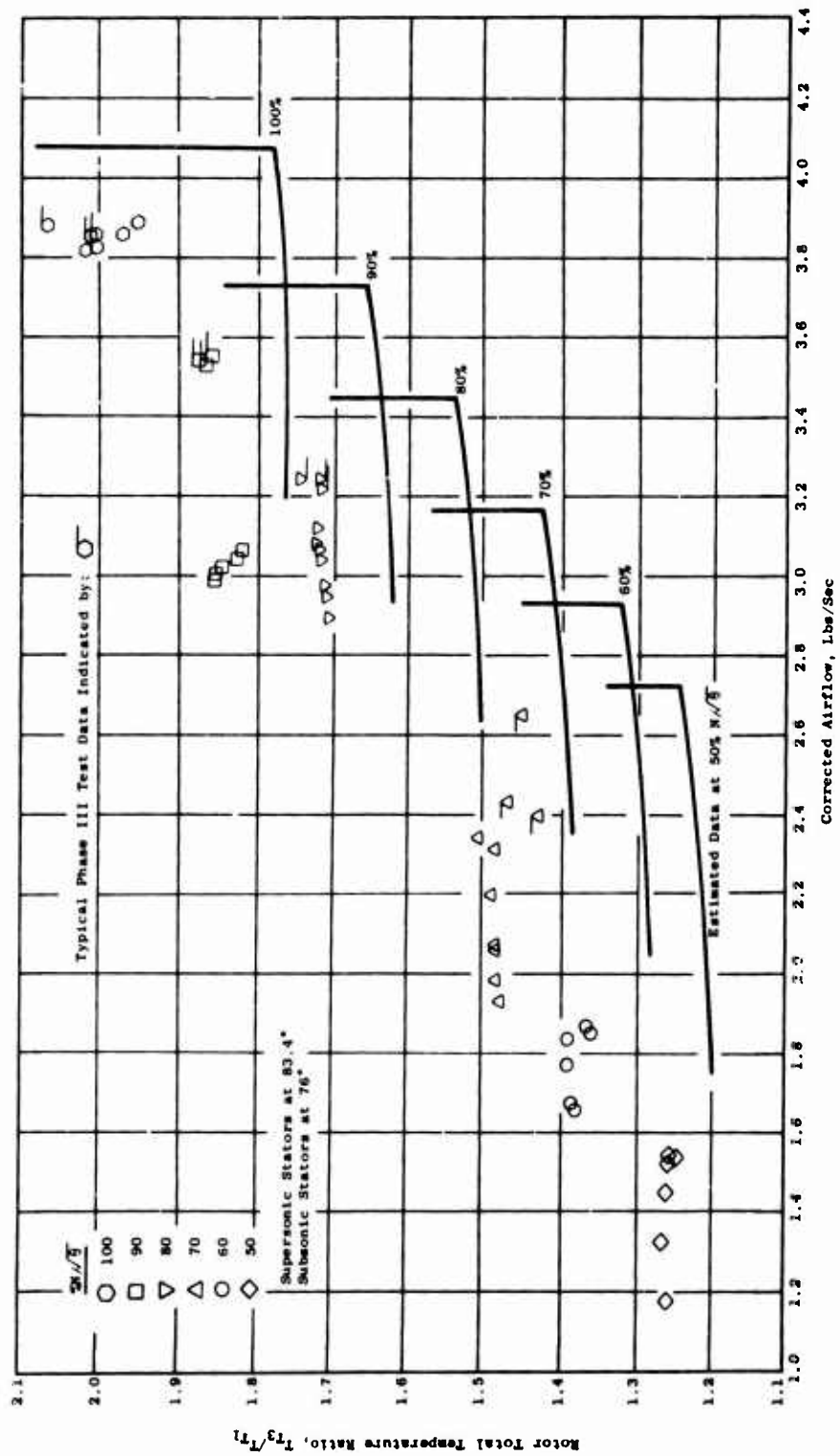
49

Figure 30. ROC Phase IV Test Data – Rotor Total Temperature Ratio Vs Airflow.
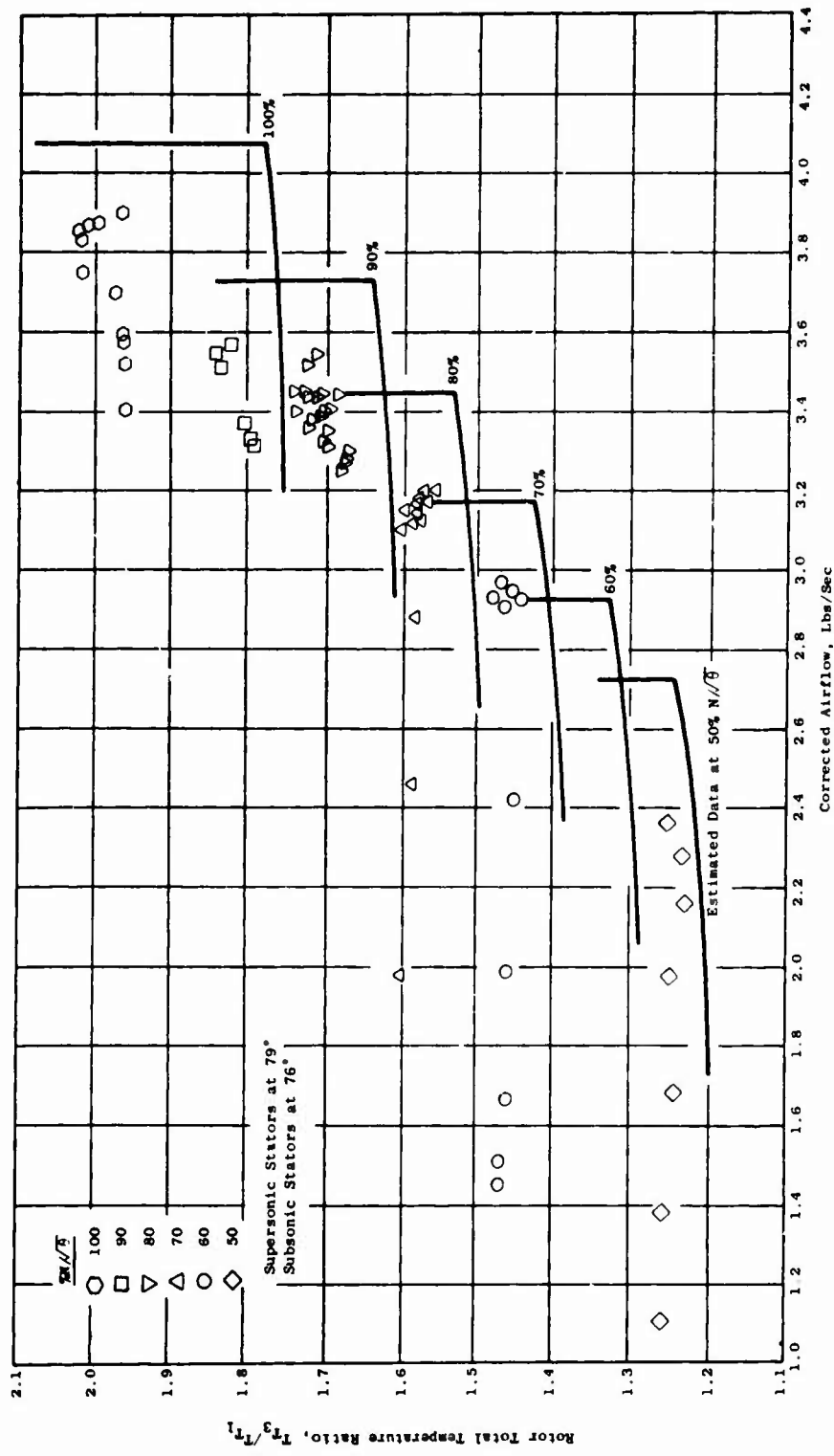
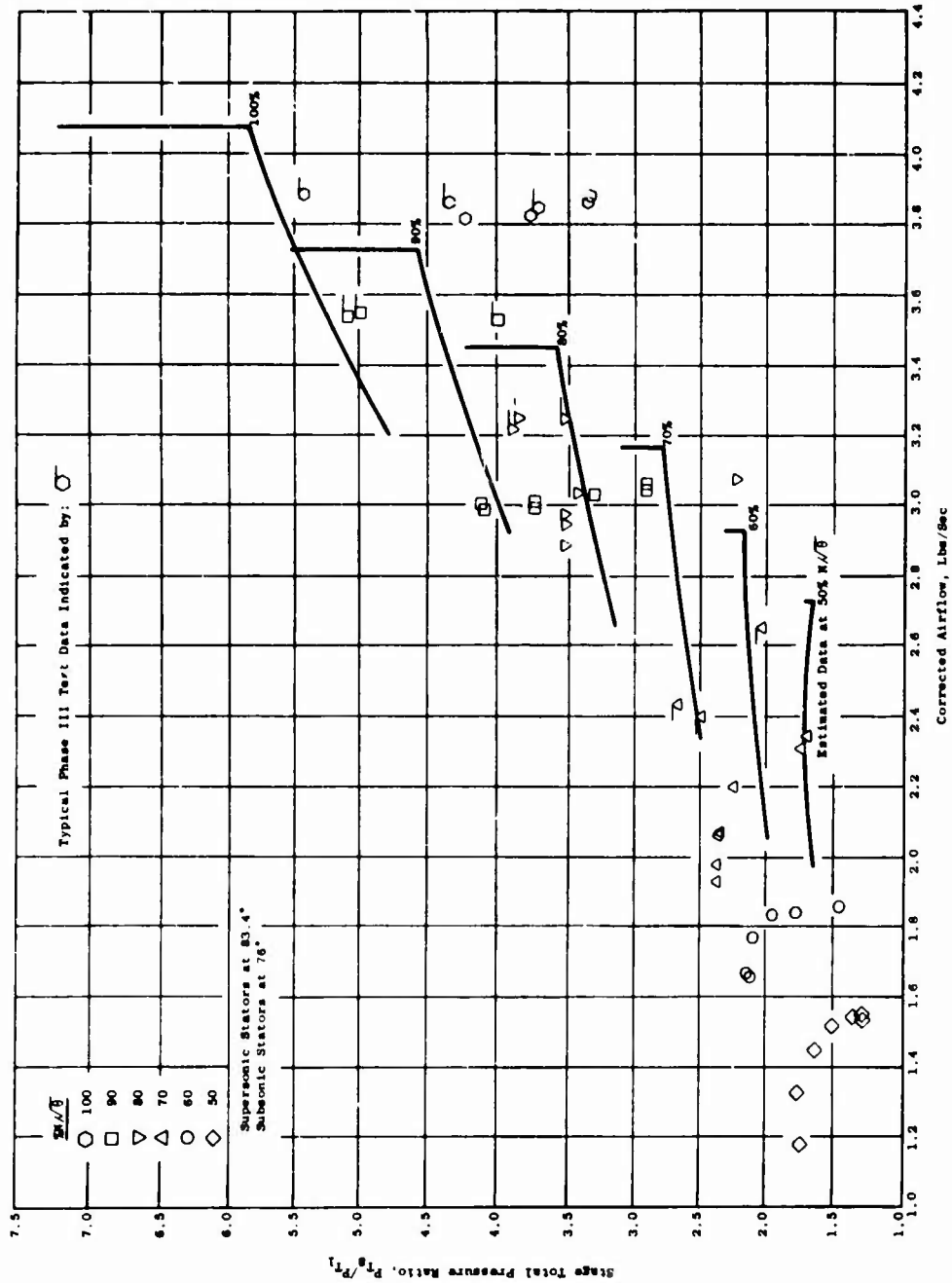Figure 31. ROC Phase IV Test Data - Rotor Total Temperature Ratio Vs Airflow.

51

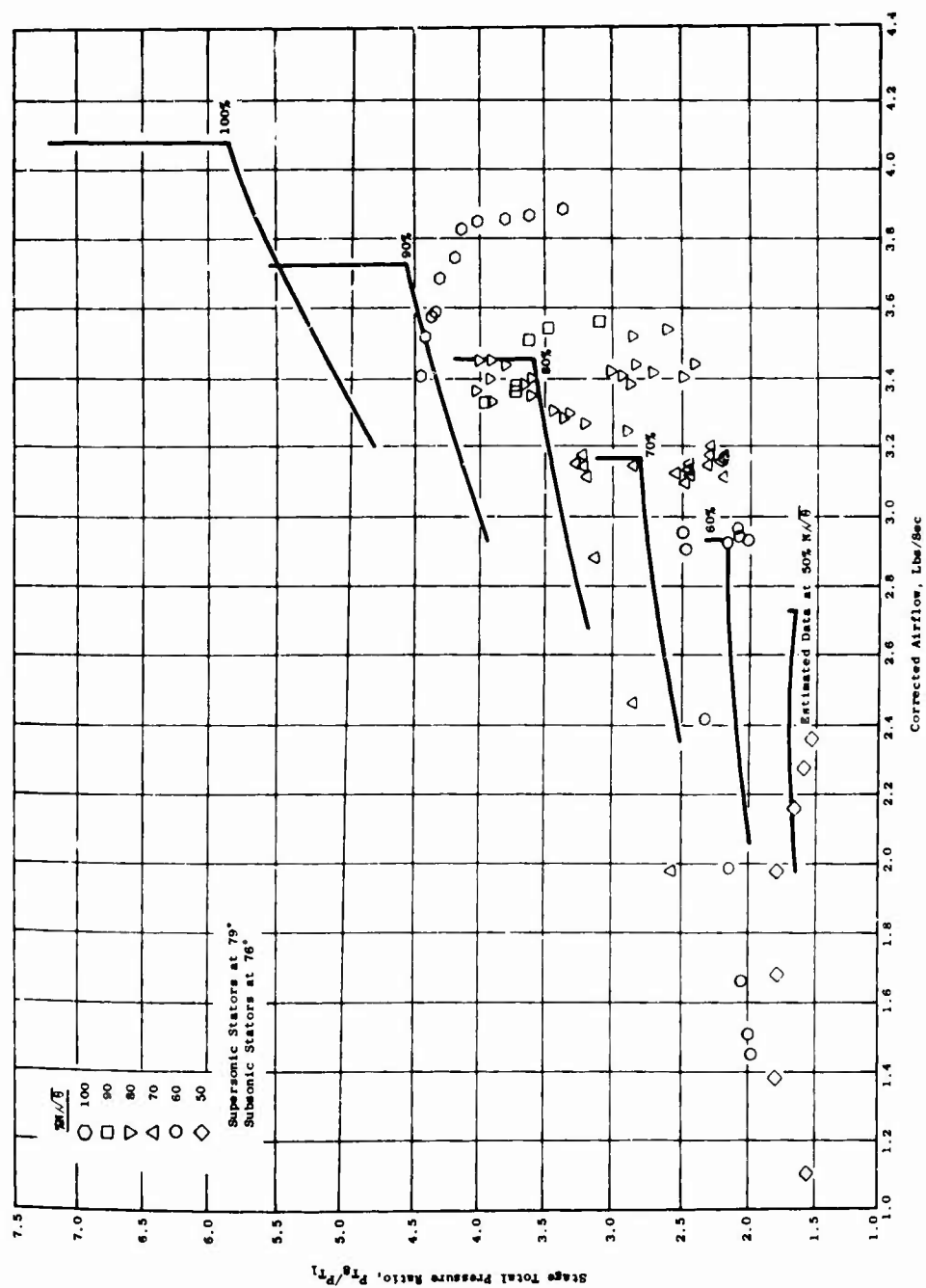Figure 33. ROC Phase IV Test Data - Stage Pressure Ratio Vs Airflow.

Figure 34. ROC Phase IV Test Data – Stage Pressure Ratio Vs Airflow.

Stage Efficiency

The overall compressor stage efficiency is the measure of the adiabatic
efficiency of the compression process from the level of the total pres-
sure in the inlet ducting to the level of total pressure at Plane 8 in
the outlet ducting. The Mach number in the outlet ducting, calculated
from the total and static pressure measurements at Plane 8, ranged from
0.25 to 0.30 over the speed range from 50 to 100 percent with compressor
operation at the higher pressure ratios at the more closed settings of
the discharge throttle valves. When the compressor was operated with
more open discharge throttle valve settings, the indicated Mach number at
Plane 8 ranged up to 0.60. The stage efficiency test data are shown in
Figures 35, 36, and 37, for supersonic stator angles of 82, 83.4, and 79
degrees, respectively. For each stator setting, test data are given for
corrected speeds of 50, 60, 70, 80, 90, and 100 percent, and estimated
stage efficiency characteristics are also given for the same speeds. The
test data for the 82-degree stator setting, Figure 35, show that the
highest measured stage efficiencies fall in the range from 70 percent
down to 65 percent for corrected speeds from 50 to 100 percent. These
efficiencies are down from the estimated data peak efficiencies by 6 to
18 percentage points for the corresponding speed range.

The test data for the 83.4-degree stator setting, Figure 36, show that
the highest measured stage efficiencies range from about 60 percent
(at 80-percent corrected speed) down to about 50 percent (at 100-percent
corrected speed). These efficiencies are down from the estimated data
peak efficiencies by 10 to 34 percentage points for the same speed range.

Comparable Phase III test data are shown in Figure 36. The highest
measured stage efficiencies range from 70 percent (at 70-percent corrected
speed) down to 58.5 percent (at 100-percent corrected speed) and are
higher than the corresponding Phase IV data by 11 to 8 percentage points
for the same corrected speed range.

The test data for the 79-degree stator setting, Figure 37, show the
highest measured stage efficiencies, ranging from about 73 percent (at
80-percent corrected speed) down to about 55 percent (at 100-percent
corrected speed). These efficiencies are down from the estimated data
peak efficiencies by 3 to 30 percentage points for the same speed range.

Stator System Loss Coefficient

The stator system loss coefficient, $\overline{\omega}$, is defined as the ratio of the aver-
age loss in total pressure through the stator system to the difference
between the average total pressure and the average static pressure at the
entry to the stator system. The stator system total pressure loss coeffi-
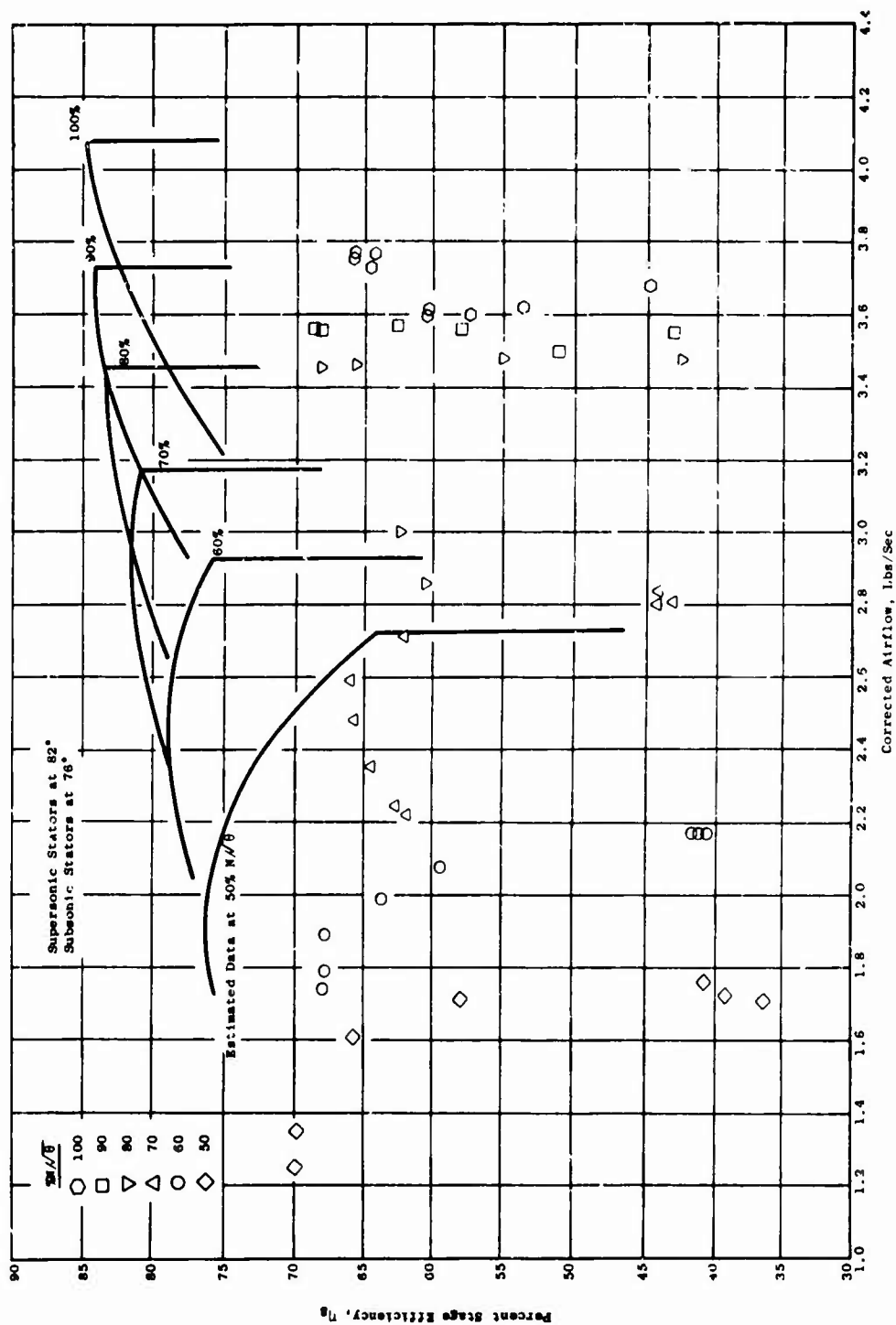cients were determined by the same methods that were used on the Phase III

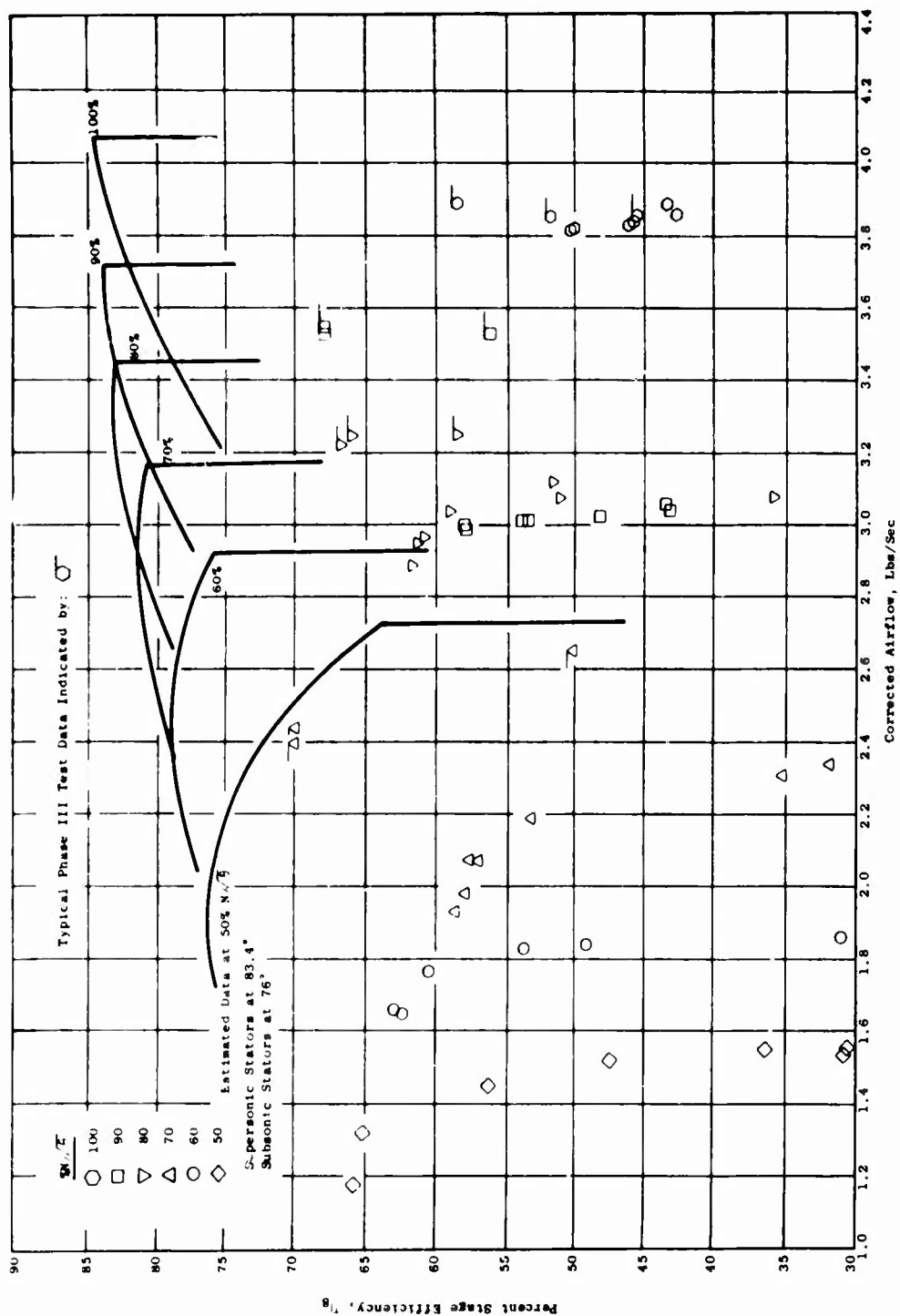Figure 35. ROC Phase IV Test Data – Stage Efficiency Vs Airflow.

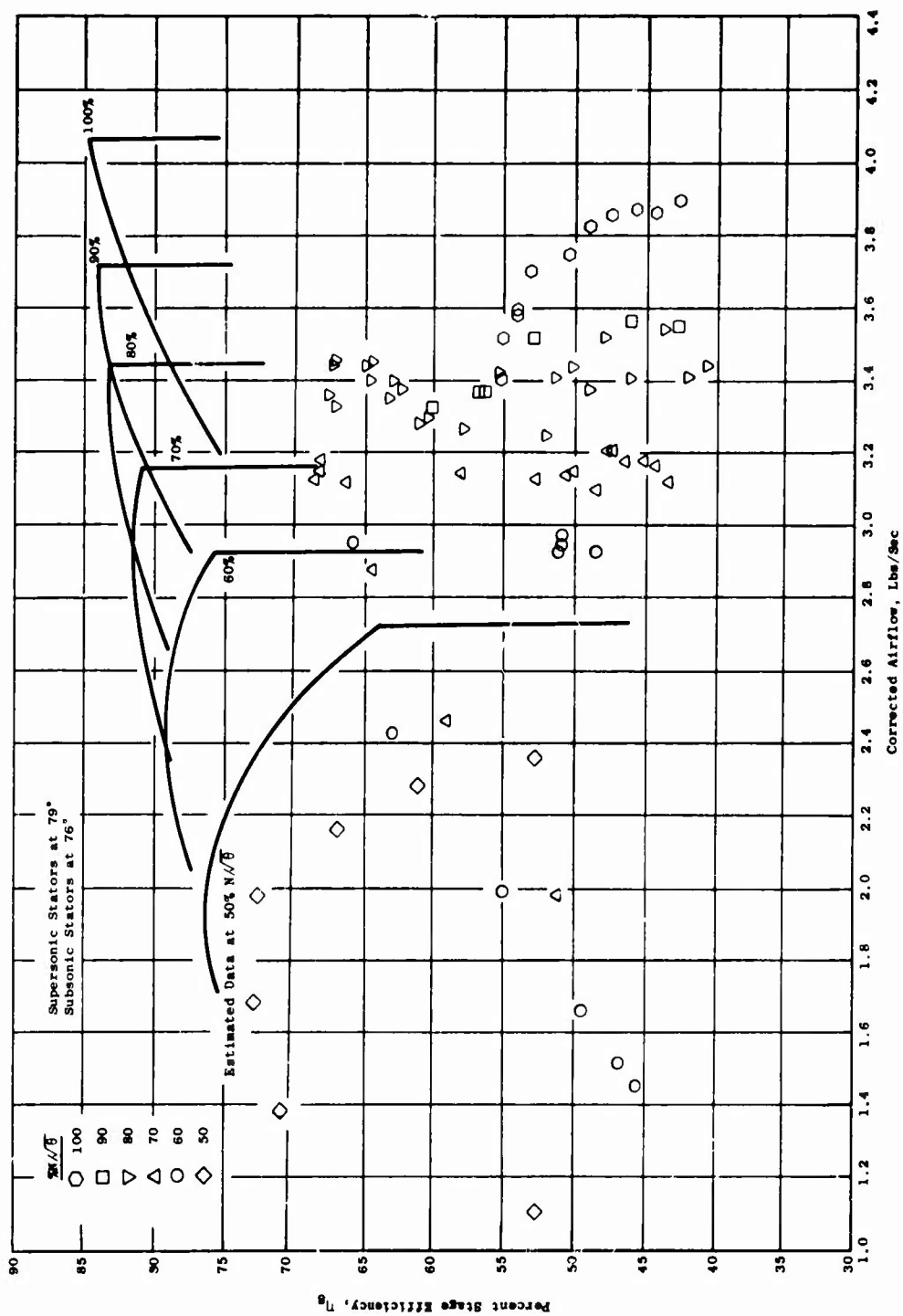Figure 36. ROC Phase IV Test Data - Stage Efficiency Vs Airflow.

Figure 37. ROC Phase IV Test Data - Stage Efficiency Vs Airflow.

59

work. Stator inlet total pressure was obtained by averaging the readings from the center element on each of the two total head rakes attached to the leading edge of the supersonic stators. This was done because it was found in the Phase III work that when an arithmetic average of all six stator leading edge readings was used, excessively high values of static pressure coefficient and excessively low values of loss coefficient were obtained. The pressure loss coefficients determined from this average inlet total pressure are designated by the symbol $\overline{\omega}'$. Corrections for the total pressure loss (assuming a normal shock) were made for $M_3 > 1$. Total pressure at the subsonic stator exit was obtained by an arithmetic average of the readings from the 9-element total pressure rake located midway between the front and rear stator casing walls (Figure 11, foreground).

The average static pressure at the inlet to the stator system was determined by averaging static pressures obtained from wall static pressure taps circumferentially distributed on the front and rear stator casings in the rotor-outlet/stator-inlet region.

The stator system total pressure loss test data are plotted in Figures 38, 39, and 40 for supersonic stator angles of 82, 83.4, and 79 degrees, respectively. The test data are shown for corrected speeds of 50, 60, 70, 80, 90, and 100 percent along with estimated loss coefficients for the same speeds.

An additional presentation of test data loss coefficients is given in Figures 41, 42, and 43 for supersonic stator angles of 82, 83.4 and 79 degrees, respectively. In these figures, loss coefficient is plotted against the Mach number at the stator system inlet. In addition to the test data, estimates of the stator system loss coefficient are shown as a function of inlet Mach number, based on tandem cascade test data[3] as in Figure 1. Comparable high-speed test data from Phase III are shown in Figures 39 and 42 for comparative purposes.

Stator System Static Pressure Coefficient

The stator system static pressure coefficient is defined as the ratio of the average rise in static pressure through the stator system to the difference between the average total pressure and the average static pressure at entry to the stator system. The stator system inlet total and static pressure measurements were as described for the stator system loss coefficients.

The static pressure coefficient determined from the use of the average of the two centerline inlet total pressures is designated by C_p'.

The stator system average outlet static pressure was determined from measurements made by wall static pressure taps, circumferentially distributed on both the front and rear stator casings, in the region of the stator system outlet.

Figure 38. ROC Phase IV Test Data – Pressure Loss Coefficient Vs Airflow.

61
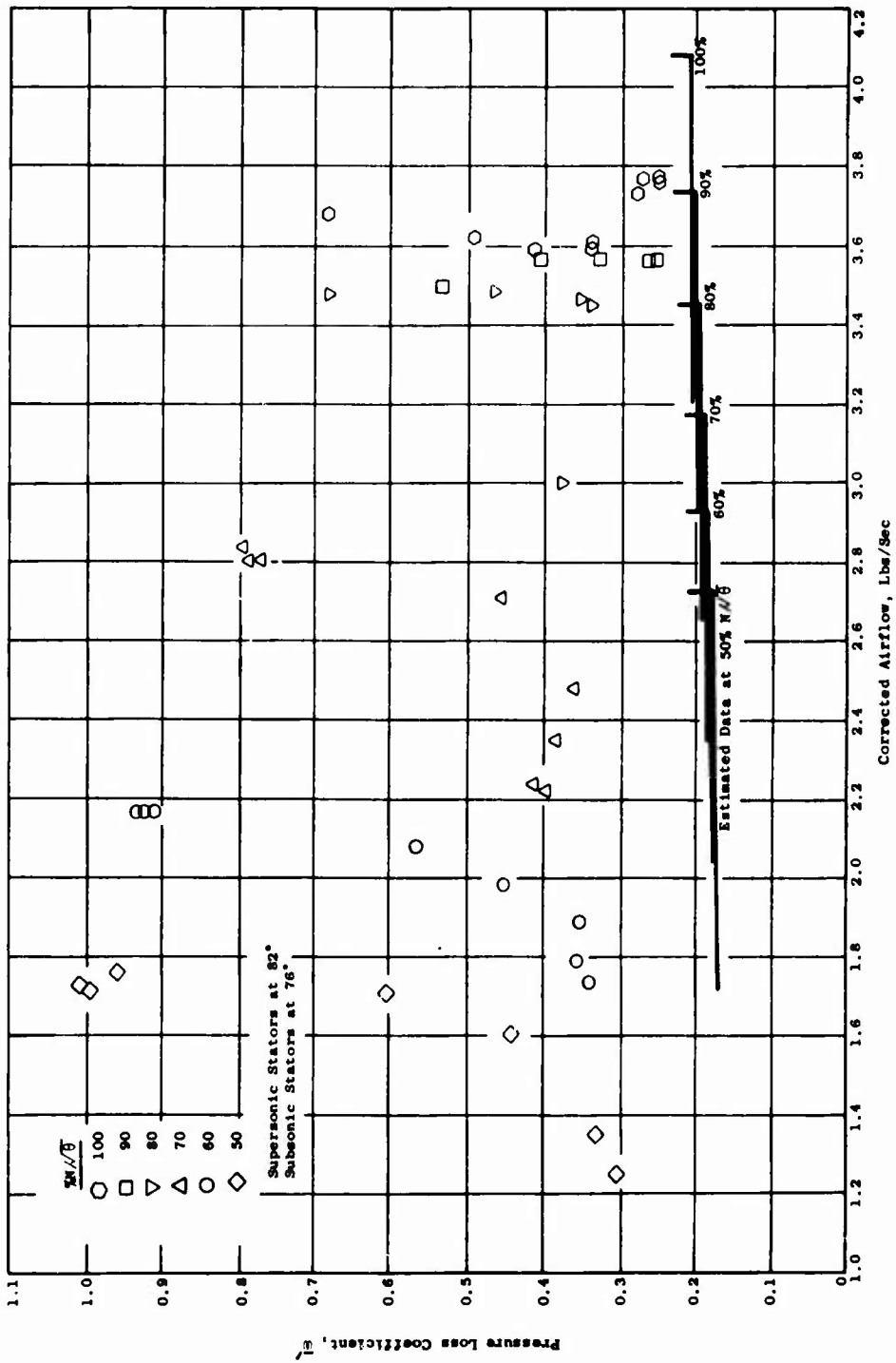
Figure 39. ROC Phase IV Test Data – Pressure Loss Coefficient Vs Airflow.

Figure 40. ROC Phase IV Test Data – Pressure Loss Coefficient Vs Airflow.

63

Figure 41. ROC Phase IV Test Data - Stator System Total Pressure Loss Coefficient Vs Stator Inlet Mach Number.

64
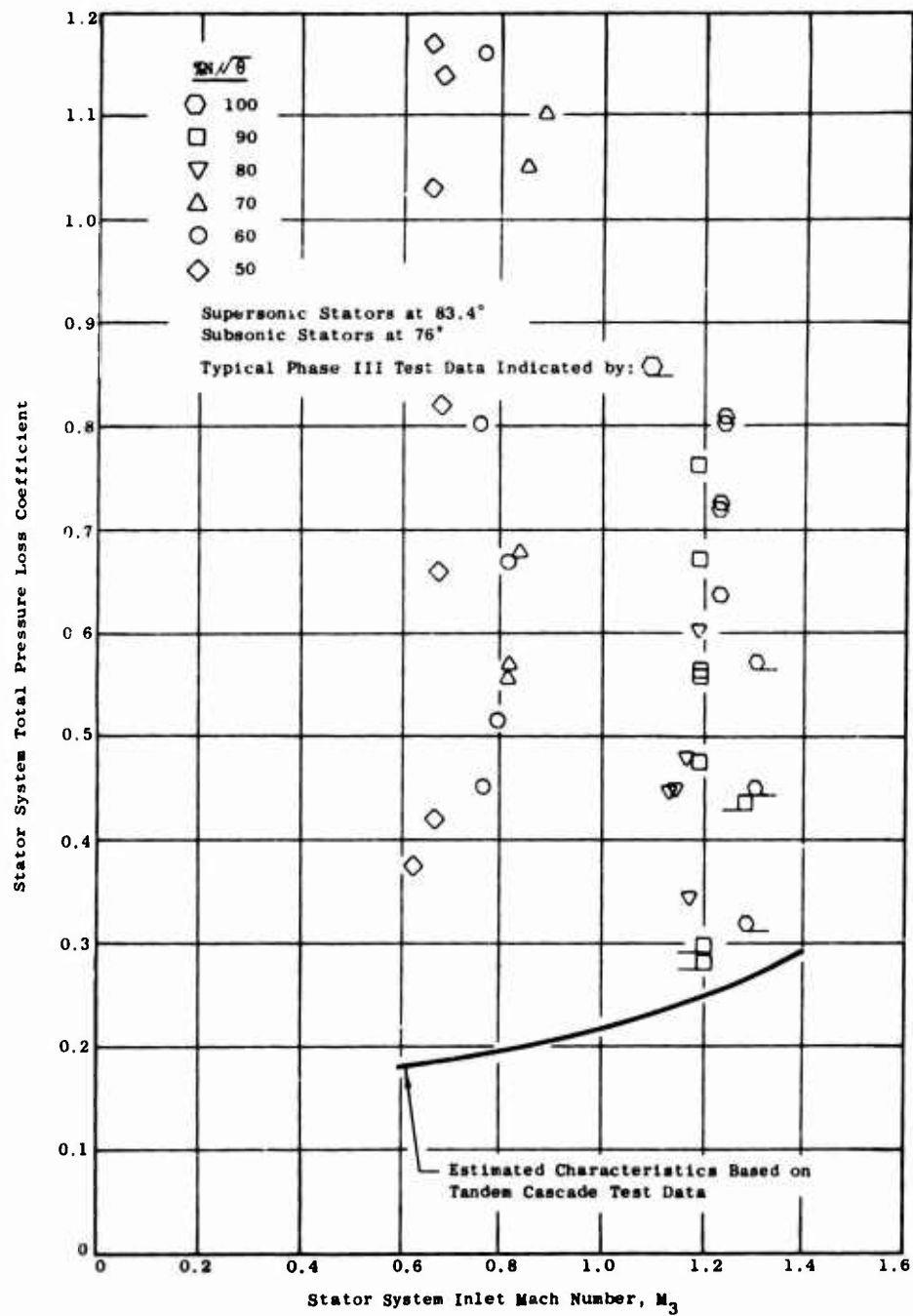
Figure 42. ROC Phase IV Test Data - Stator System Total Pressure
Loss Coefficient Vs Stator Inlet Mach Number.
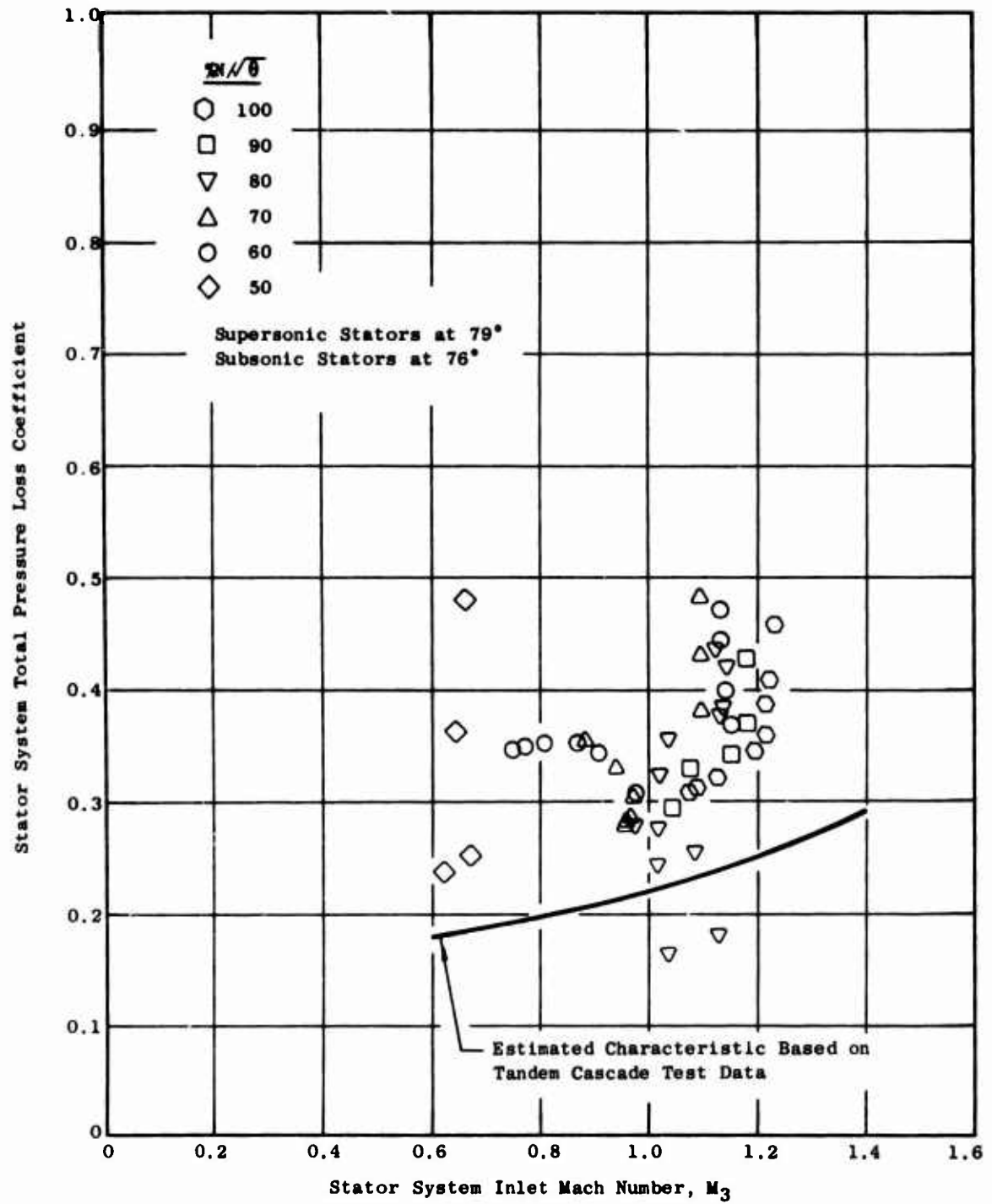
Figure 43. ROC Phase IV Test Data - Stator System Total Pressure Loss Coefficient Vs Stator Inlet Mach Number.

The stator system static pressure coefficients obtained from the test
data are shown in Figures 44, 45, and 46 for stator settings of 82, 83.4,
and 79 degrees, respectively, for corrected speeds of 50, 70, 80, 90, and
100 percent. Also shown in these plots are the static pressure coeffi-
cients implicit in the estimated performance data.

High-speed test data from Phase III are shown in Figure 45 for comparative
purposes.

67

The stator system static pressure coefficients plotted from the test data are shown in Figures 44, 45, and 69 for stator vane angles of 82, 76, and 70 degrees, respectively, for corrected speeds of 50, 60, 70, 80, 90, and 100 percent. Also shown in these plots are the static pressure coefficients for the 1% cascade performance data.

High-speed performance data will not allow a stator to reach maximum purposes.

Figure 44. ROC Phase IV Test Data – Static Pressure Coefficient Vs Airflow.

Static Pressure Coefficient, C_p

Corrected Airflow, Lbs/Sec

$\frac{W\sqrt{\theta}}{\delta}$

○ 100
□ 90
▷ 80
△ 70
○ 60
◇ 50

Supersonic Stators at 82°
Subsonic Stators at 76°

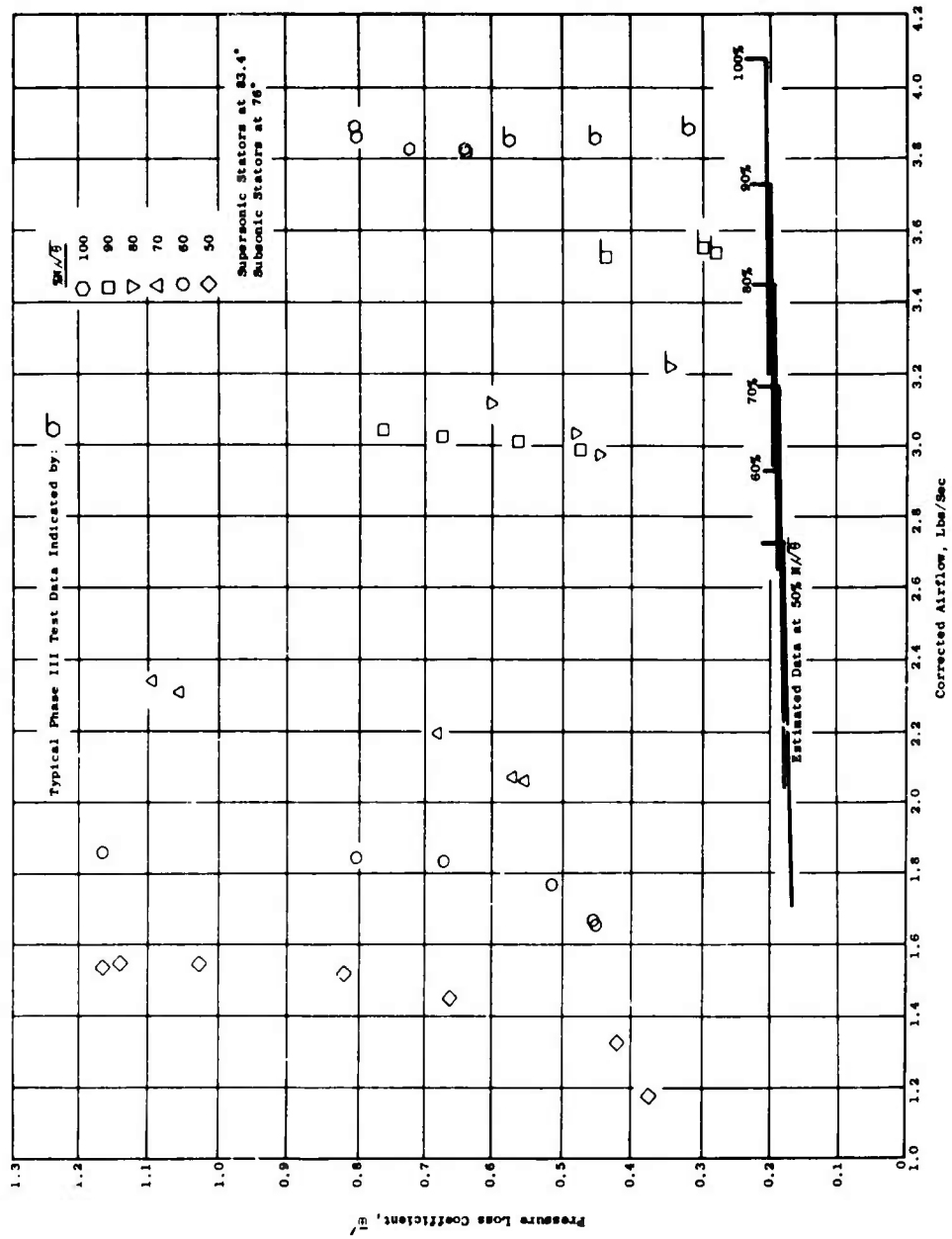Estimated Data at 50% N/√θ

100%
90%
80%
70%
60%

Figure 45. ROC Phase IV Test Data – Static Pressure Coefficient Vs Airflow.

69

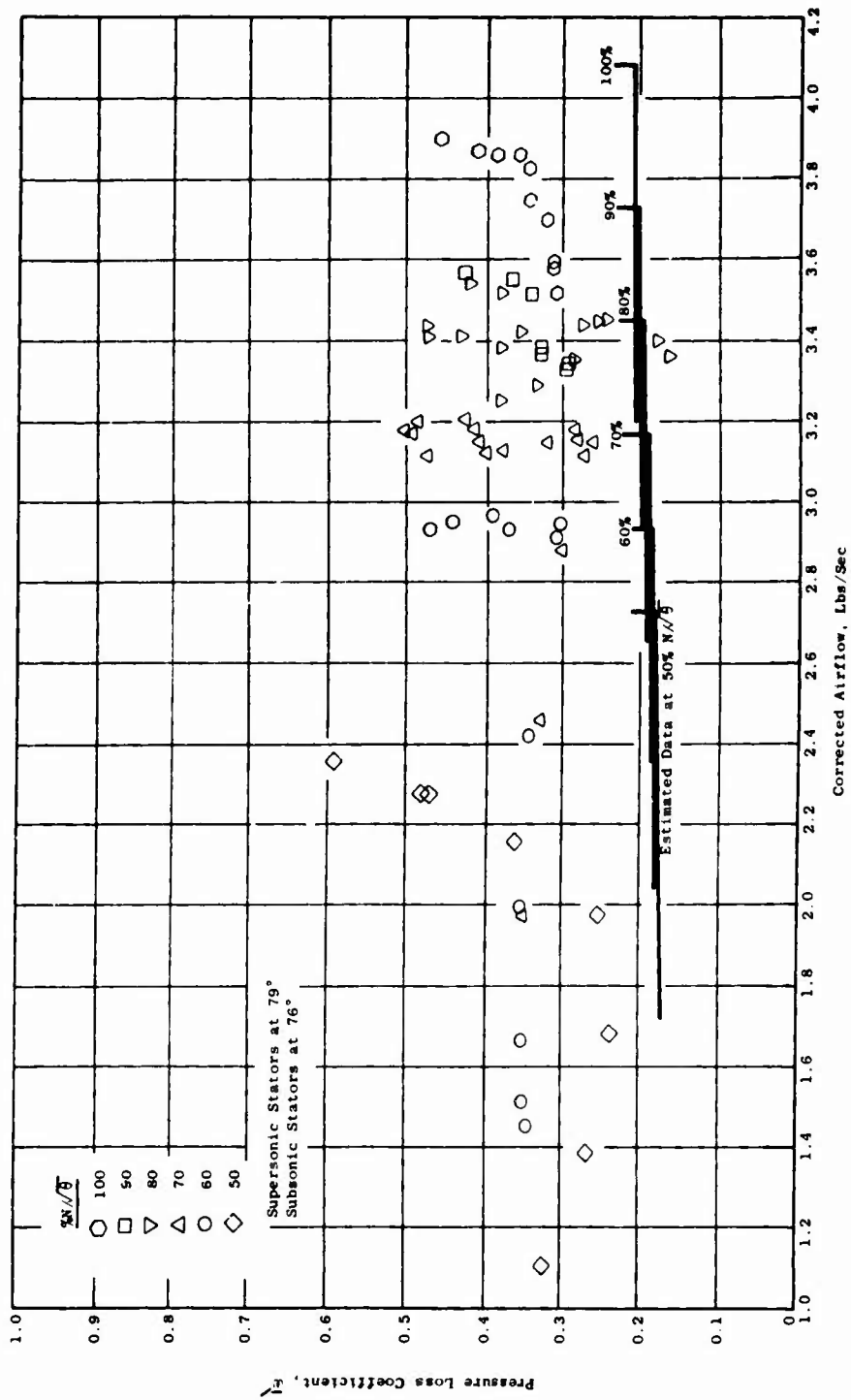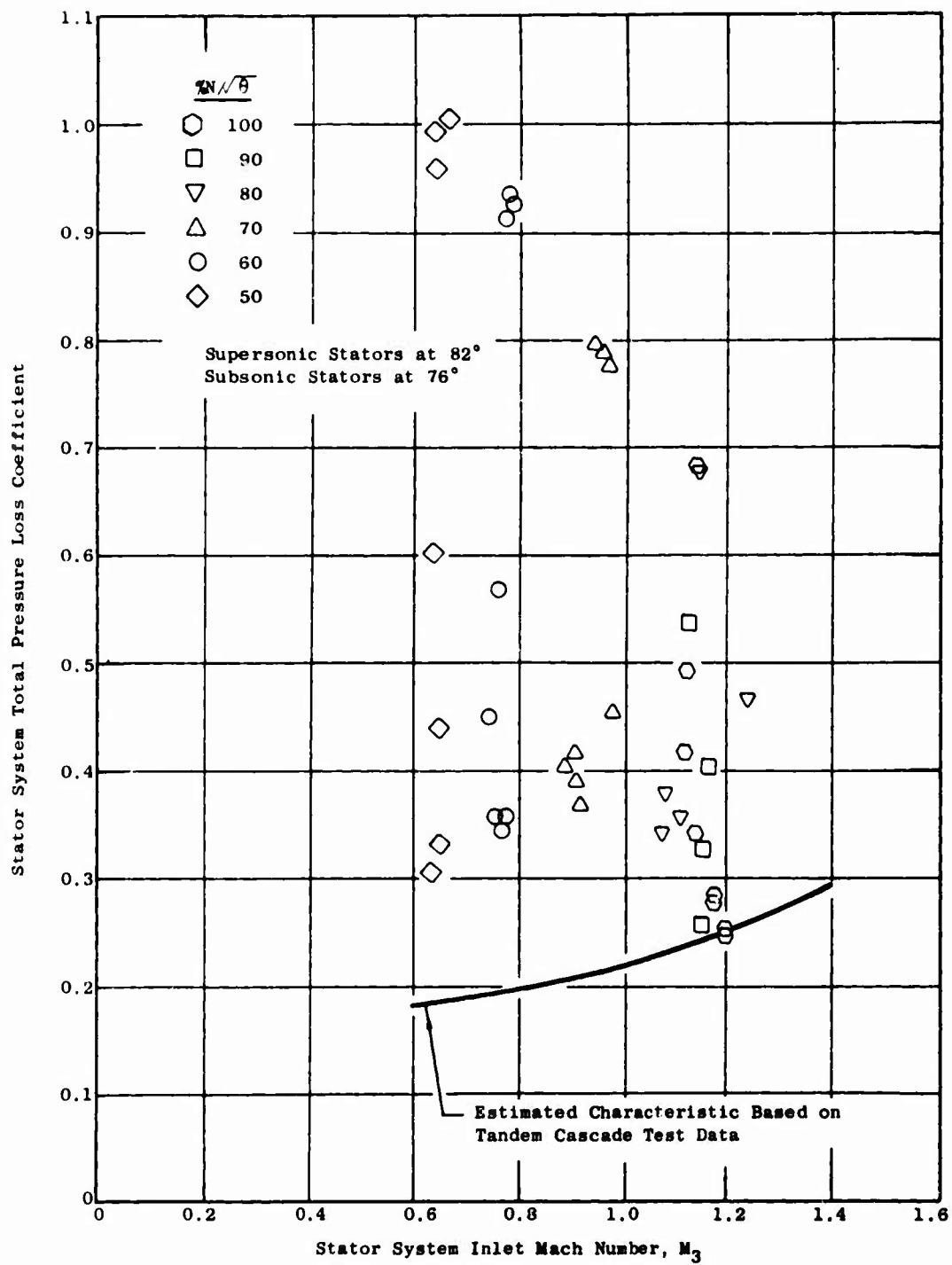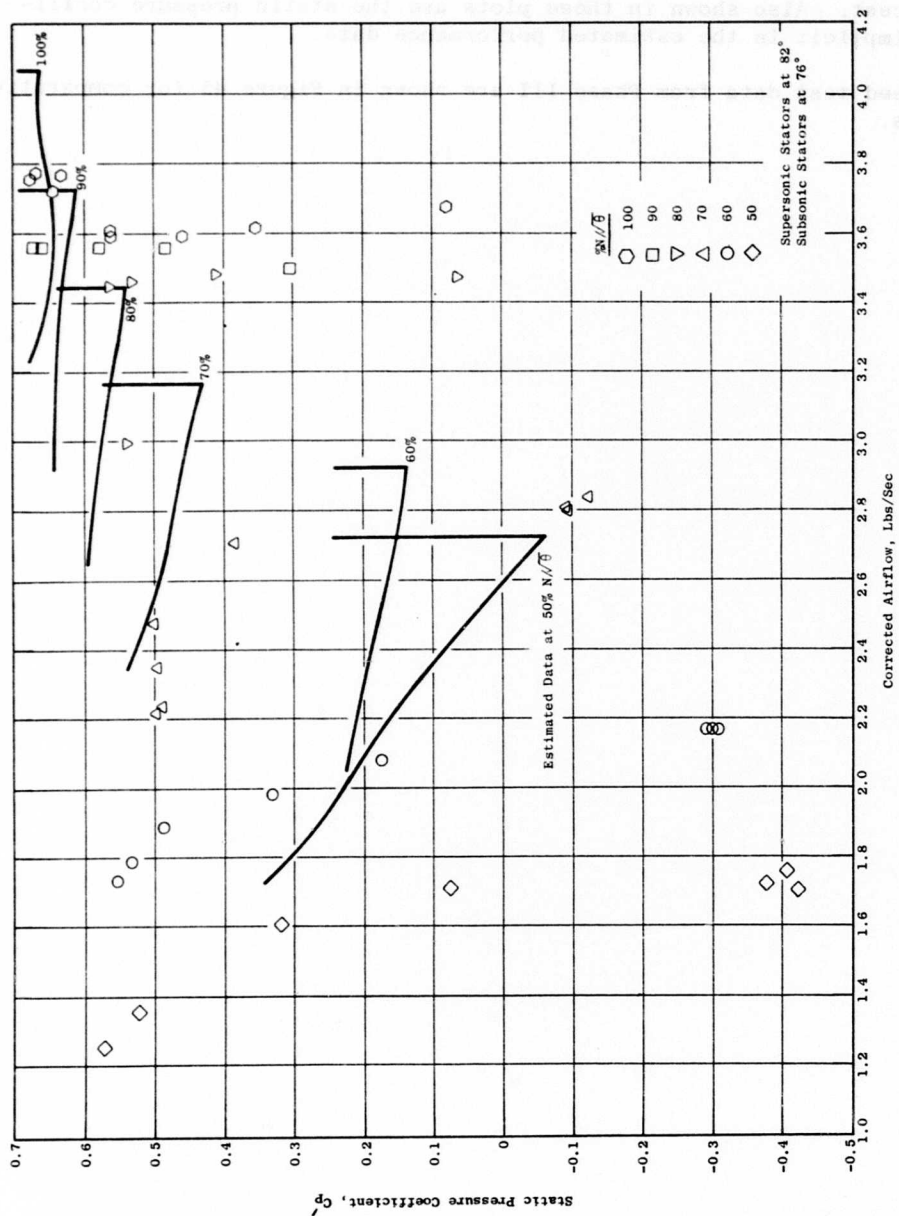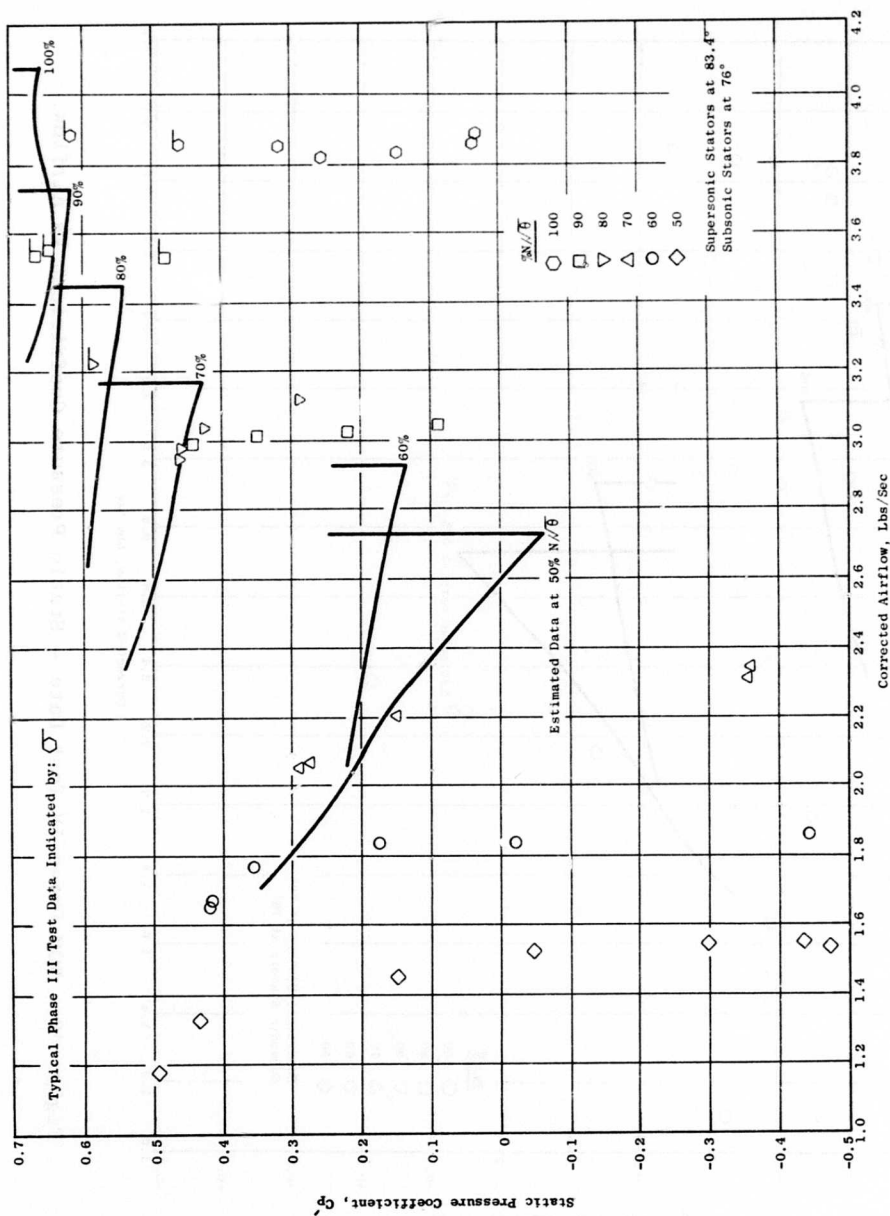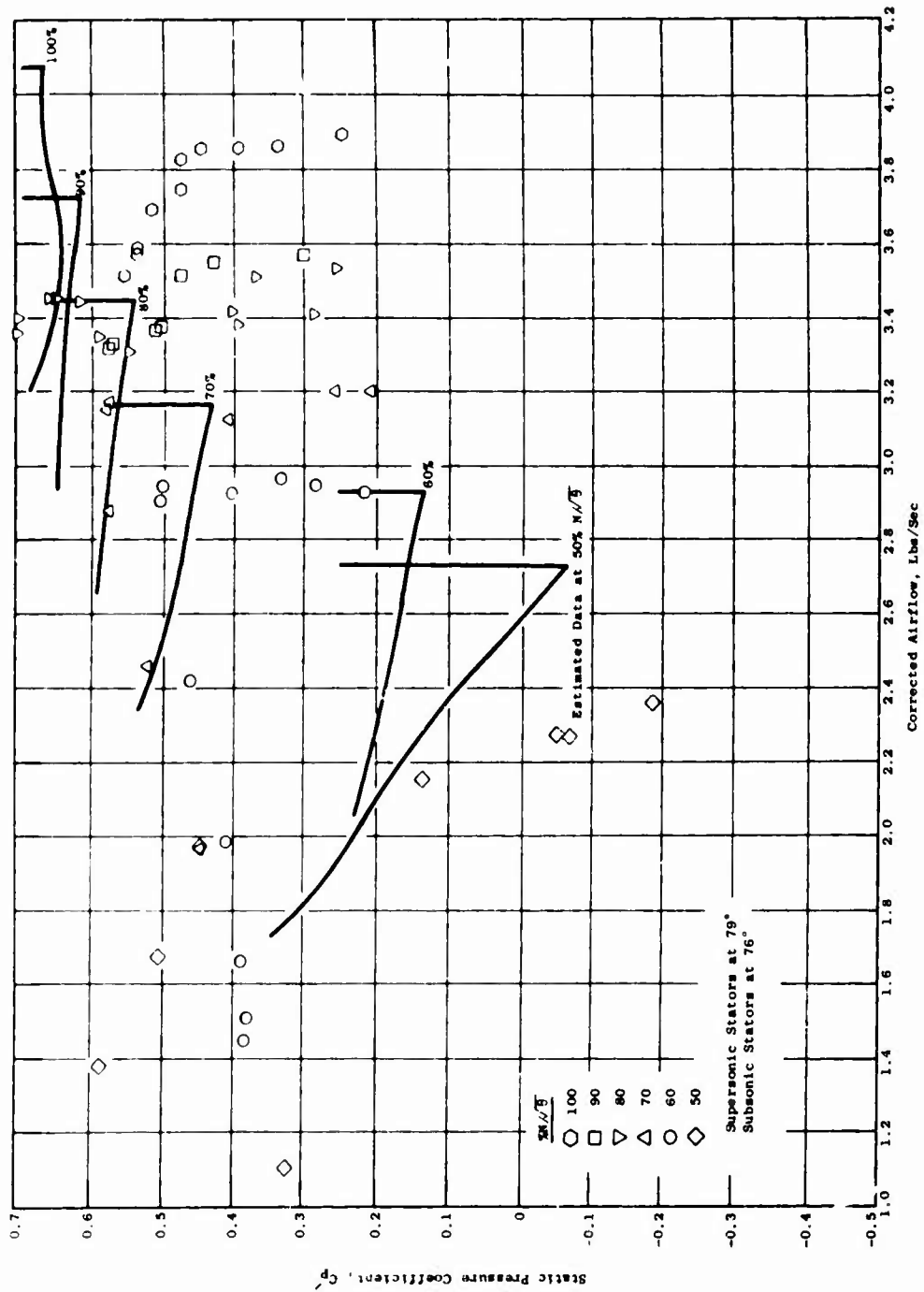Figure 46. ROC Phase IV Test Data - Static Pressure Coefficient Vs Airflow.

CONCLUSIONS

(1) Inlet vane position did not have a significant effect on rotor performance in the speed range tested from 50- through 80-percent corrected speed.

(2) The highest levels of measured rotor performance were obtained at the 83.4-degree suspersonic stator setting. A maximum rotor pressure ratio of 7.2 was measured with a rotor efficiency of 80 percent at 100-percent corrected speed. The total pressure ratio is of the expected order of magnitude at design speed; however, the static pressure rise is lower than expected, resulting in high rotor discharge Mach numbers. Total pressure ratio distribution at rotor outlet is relatively uniform. At the other two supersonic stator settings, the rotor outlet pressure distribution is skewed, changing, and more peaked and variable, indicating the possibility of upstream flow separation. The Phase IV rotating diffuser area distribution, similar to that of the original Phase II diffuser, appeared to be responsible for small improvements in measured rotor performance parameters when compared with corresponding Phase III test data.

(3) The stator system demonstrated loss levels that approached the tandem cascade test data for some conditions of operation.

(4) The highest level of stage performance was obtained with the intermediate supersonic stator setting of 82 degrees, where a maximum stage total pressure ratio of 6.1 was obtained with a stage efficiency of 66 percent at 100-percent corrected speed.

(5) The rotor and stator system are mismatched. The rotor achieves peak performance with the supersonic stators in the closed (83.4-degree) position, while the stator system achieves peak performance in the open (79-degree) position.

(6) Substantial inconsistency in corrected airflow is observed. There appear to be several distinctively different modes of operation of the ROC as characterized by different patterns of the test data (for corrected speeds of 70 percent and below, at 80 percent, and at 90 and 100 percent). For each of these speeds, or speed ranges, specific and different adjustments were made to the compressor or the facility to maintain bearing thrust load and disc temperature below limits. A substantial difference in corrected airflow was observed to occur, when, other things being apparently similar, a change was made in the auxiliary airflows and when the compressor inlet density was reduced. In the latter case, the change in airflow cannot be accounted for by Reynolds number effects alone.

71

RECOMMENDATIONS

The Phase IV Radial Outflow Compressor (ROC) program provided a significant quantity of high-speed performance data for the first time in the overall program. The performance characteristics obtained during the tests and the differences between actual data and earlier estimates pose several questions. Answers are needed to develop a better understanding and perspective of the ROC concept relative to other types of radial compressors.

The questions and the means for providing answers served as the basis for the following recommendations:

1. The test data acquired in the Phase IV program should receive analysis and evaluation extended beyond the minimal level specified for producing this report. For an example, interpretation of the pressure distributions at rotor outlet and in the stator passages should be undertaken as a step toward developing a better understanding of the matching of the rotor and stator.

2. A series of short ROC tests should be carried out in the manner and for the purposes described below:

   a. Determine the high-speed characteristics of the ROC uninfluenced by secondary airflow, pressure distributions, or rotor deflections induced by the auxiliary air system. A change in the forward thrust bearing is required.

   b. Determine the change in air angle leaving the rotor and entering the stator system as a function of both speed and back-pressure level to develop an improved understanding of the requirements for achieving the matching between the rotor and stator systems. Vane incidence angle measurements are required.

   c. Determine the high-speed characteristics of the ROC uninfluenced by whirl at blade entry as caused by the rotating walls of the inlet. The application of stationary shrouds in the inlet passage or inlet guide vanes is required.

3. A study should be conducted to determine the paths for developing and exploiting the ultimate performance potential of the ROC concept. This segment of the work should be implemented by the extension of earlier studies of the ROC rotor using larger-chord

blades with a modified area distribution through the blade
row and resulting in near-sonic flow velocity at rotor exit
(3). Identification of design modifications of stator sys-
tems and scrolls compatible with this rotor design is required.

LITERATURE CITED

(1) Erwin, J.R., and Vitale, N.G., RADIAL OUTFLOW COMPRESSOR COMPONENT DEVELOPMENT, Volume II, Phase II - Design, Fabrication, and Test of an Experimental Compressor, USAAVLABS Technical Report 68-38B, U.S. Army Aviation Materiel Laboratories, Fort Eustis, Virginia, March 1969.

(2) Erwin, J.R., and Vitale, N.G., RADIAL OUTFLOW COMPRESSOR COMPONENT DEVELOPMENT PROGRAM, Volume I, Phase I - Aerodynamic and Mechanical Design Analysis and Diffuser Tests, USAAVLABS Technical Report 68-38A, U.S. Army Aviation Materiel Laboratories, Fort Eustis, Virginia, May 1969.

(3) Erwin, J.R., RADIAL OUTFLOW COMPRESSOR COMPONENT DEVELOPMENT, Volume III, Phase III - Mechanical Design and Experimental Investigation Using Modified Rotor, USAAVLABS Technical Report 68-38C, U.S. Army Aviation Materiel Laboratories, Fort Eustis, Virginia, August 1969.

DOCUMENT CONTROL DATA - R & D

(Security classification of title, body of abstract and indexing annotation must be entered when the overall report is classified)

1. ORIGINATING ACTIVITY *(Corporate author)*	2a. REPORT SECURITY CLASSIFICATION
ADVANCED TECHNOLOGY PROGRAMS DEPT., AEG GENERAL ELECTRIC COMPANY CINCINNATI, OHIO 45215	Unclassified
	2b. GROUP

3. REPORT TITLE

RADIAL OUTFLOW COMPRESSOR COMPONENT DEVELOPMENT - Phase IV, Test Results

4. DESCRIPTIVE NOTES *(Type of report and inclusive dates)*
Final Report

5. AUTHOR(S) *(First name, middle initial, last name)*

D. E. Morrison

6. REPORT DATE	7a. TOTAL NO. OF PAGES	7b. NO. OF REFS
September 1970	84	3

8a. CONTRACT OR GRANT NO	9a. ORIGINATOR'S REPORT NUMBER(S)
DAAJ02-69-C-0070	USAAVLABS Technical Report 70-40
b. PROJECT NO	
Task 1G162203D14413	
c.	9b. OTHER REPORT NO(S) *(Any other numbers that may be assigned this report)*
d.	R70AEG211

10. DISTRIBUTION STATEMENT

This document is subject to special export controls, and each transmittal to foreign governments or foreign nationals may be made only with prior approval of U.S. Army Aviation Materiel Laboratories, Fort Eustis, Virginia 23604.

11. SUPPLEMENTARY NOTES	12. SPONSORING MILITARY ACTIVITY
	U.S. Army Aviation Materiel Laboratories Fort Eustis, Virginia 23604

13. ABSTRACT

The purpose of the Phase IV program was to obtain high-speed performance data for the optimum circular inlet vane position and stator vane settings. The only difference from the Phase III configuration was a change made to the rotating diffuser area schedule. The circular inlet vane position had little effect on rotor performance. The recontoured rotating diffuser provided some improvement in rotor pressure ratio and efficiency relative to Phase III data. Maximum rotor performance was obtained with a supersonic stator setting of 83.4 degrees. Best stator system performance was obtained with a supersonic stator setting of 79 degrees. Maximum stage performance was obtained with a supersonic stator setting of 82 degrees.

DD FORM 1 NOV 65 1473

KEY WORDS	LINK A		LINK B		LINK C	
	ROLE	WT	ROLE	WT	ROLE	WT
Compressor						
High-Pressure-Ratio Compressor						
Radial Outflow Compressor						
Variable Geometry						
Rotating Diffuser						

7433-70